UNIVERSIDADE FEDERAL DE SANTA CATARINA
CENTRO DE CIÊNCIAS BIOLÓGICAS
PROGRAMA DE PÓS-GRADUAÇÃO EM BIOTECNOLOGIA E BIOCIÊNCIAS

Thaís Fávero Massocato

Biofiltração de efluentes de aquicultura com *Ulva* spp. (Chlorophyta): ecofisiologia e valorização da biomassa

Florianópolis
2022

Thaís Fávero Massocato

Biofiltração de efluentes de aquicultura com *Ulva* spp. (Chlorophyta): ecofisiologia e valorização da biomassa

Tese submetida ao Programa de Pós-Graduação em Bioctenologia e Biociências da Universidade Federal de Santa Catarina para a obtenção do título de Doutor em Biotecnologia e Biociências
Orientador: Prof. Dr. Leonardo Rubi Rörig
Coorientador: Prof. Dr. Félix Diego López Figueroa

Florianópolis
2022

Ficha de identificação da obra

Massocato, Thais Fávero
Biofiltração de efluentes de aquicultura com Ulva spp. (Chlorophyta): : ecofisiologia e valorização da biomassa / Thais Fávero Massocato ; orientador, Leonardo Rubi Rörig, coorientador, Félix Diego López Figueroa, 2022.
159 p.

Tese (doutorado) - Universidade Federal de Santa Catarina, Centro de Ciências Biológicas, Programa de Pós Graduação em Biotecnologia e Biociências, Florianópolis, 2022.

Inclui referências.

1. Biotecnologia e Biociências. 2. Biofiltração. 3. Biomassa algal. 4. Fotossintese. 5. Ulva spp.. I. Rörig, Leonardo Rubi. II. Figueroa, Félix Diego López. III. Universidade Federal de Santa Catarina. Programa de Pós Graduação em Biotecnologia e Biociências. IV. Título.

Thaís Fávero Massocato

Biofiltração de efluentes de aquicultura com *Ulva* spp. (Chlorophyta): ecofisiologia e valorização da biomassa

O presente trabalho em nível de doutorado foi avaliado e aprovado por banca examinadora composta pelos seguintes membros:

Prof. Dr. Rubens Tadeu Delgado Duarte,
Universidade Federal de Santa Catarina

Dr.Caio Cesar França Magnotti,
Universidade Federal de Santa Catarina

Prof. Dr. Fábio de Farias Neves,
Universidade do Estado de Santa Catarina

Certificamos que esta é a **versão original e final** do trabalho de conclusão que foi julgado adequado para obtenção do título de doutora em biotecnologia e biociências pelo Programa de Pós-Graduação em Biotecnologia e Biociências.

Documento assinado digitalmente
Glauber Wagner
Data: 21/11/2022 13:04:16-0300
CPF: ***.019.139-**
Verifique as assinaturas em https://v.ufsc.br

_____

Prof. Dr, Glauber Wagner
Coordenação do Programa de Pós-Graduação

Documento assinado digitalmente
Leonardo Rubi Rorig
Data: 22/11/2022 11:31:00-0300
CPF: ***.737.740-**
Verifique as assinaturas em https://v.ufsc.br

_____

Prof. Dr, Leonardo Rubi Rörig
Orientador

Florianópolis, 2022.

Dedico essa tese a cinco eternas e importantes pessoas Martim H. Massocato, Caetano H. Massocato, Daniel André Fávero (*in memorian*), Luzia Fantini Fávero (*in memorian*) e João Antônio Fávero.

“Se as coisas são inatingíveis... ora!
Não é motivo para não querê-las...
Que tristes os caminhos, se não fora
A presença distante das estrelas!”

Mario Quintana

AGRADECIMENTOS

Ao começar esse trabalho não imaginava o turbilhão de acontecimentos, experiências, sentimentos, pessoas e amizades que viriam a surgir ao longo desses últimos quatro anos. Como disse uma amiga em uma conversa "por detrás de uma tese existe a pessoa que a está executando". Pois, sem a participação de uma rede de pessoas que me apoiaram e me motivaram de pertinho, e de longe, o presente trabalho jamais teria sido realizado e concluído.

Primeiramente agradeço as quatro mais importantes pessoas da minha vida: meus pais (Laércio e Cleusa) e meus irmãos (Fá e Gabri). Vocês são o meu esteio e os meus maiores exemplos. O amor de vocês nutre a minha busca em ser uma pessoa cada vez melhor.

Agradeço de toda minha alma ao meu namorado Kai, que surgiu (quase que do céu) quando eu menos esperava e acompanhou, de longe e de perto, o desdobramento dos últimos dois anos desse trabalho.

Serei eternamente grata aos meus amigos e companheiros de trabalho do Laboratório de Ficologia (Lafic-UFSC). Lá foi minha segunda casa e onde eu pude ser quem eu realmente sou. Um ambiente alegre em que as pessoas buscam trabalhar em equipe e dão o melhor de si para compreender esse lindo universo das algas, bem como, as múltiplas maneiras que podemos usá-las para contornar os desastres que a sociedade humana vem causando no planeta.

Agradeço ao meu orientador Prof. Leonardo R. Rörig que aceitou embarcar comigo nesse projeto. Acredito que a busca pelo conhecimento e transformações que visem reduzir os impactos humanos no meio ambiente nos une e nos motiva, mesmo em momentos de dificuldades e desafios. Sob sua orientação consegui expandir minha bagagem pessoal e profissional e levarei comigo seus ensinamentos e sua forma de conectar ideias.

Meus sinceros agradecimentos ao meu segundo orientador, Prof. Félix D. L. Figueroa. Agradeço por todo o aporte em conhecimento, e por me ensinar a ver a ciência de forma mais holística. Acredito que sempre iremos nos recordar da minha chegada à Espanha apenas quatro dias antes de toda a loucura pandêmica começar.

Também não poderia deixar de agradecer especialmente ao Prof. José Bonomi Barufi, quem acompanhou minha jornada acadêmica desde 2014. Zé, suas palavras de força e motivação me deram suporte em momentos cruciais. Seus conhecimentos ampliaram minha visão e me ajudaram a construir cada vez mais essa tese.

Agradeço também aos meus primos e primas, familiares, colegas do pólo aquático, aos amigos e amigas do Rio Tavares, e as minhas amigas e amigo: Ellie, Meli, Mari Wagner,

VanVan, Bru, Taís Téo e Wagner, e aos antigos colegas do mestrado com quem cruzei em corredores e aulas.

Gostaria de ressaltar que este trabalho foi fruto da participação e colaboração de grupos de pesquisa e instituições. Meu sinceros agradecimentos à Universidade Federal de Santa Catarina (UFSC) e à Universidade de Málaga (UMA), em especial aos docentes e técnicos do Laboratório de Ficologia (LAFIC - UFSC), Laboratório de Fotobiología e Biotecnología de Organismos acuáticos (FYBOA - UMA), centro de pesquisa Grice Hutchinson (UMA) e aos Servicios Centrales de Apoyo a la Investigación (SCAI - UMA), por ceder espaço e recursos para este trabalho. Agradeço também à Julia Vega, Marta G. Sanchez, Fabian Lopez, David Paniagua, Prof. Roberto Abdala, Profª Nathalie K. Peinado, Prof. Paulo Horta, Eduardo Bastos, Prof. Antonio Avilles, Lorena Pinheiro-Silva, Willian da Silva Oliveira, e Cristina Gonzáles Fernández pelo apoio e assistência na realização de experimentos, coleta de dados e colaborações para a escrita dos artigos que compõe este trabalho. Agradeço fortemente a Pablo Varela e Bruna Moreira pela colaboração através dos ensaios de citotoxicidade celular, a Victor Robles-Carnero por ter sido meu braço direito nos experimentos realizados na Espanha e à Ingrid Palica pela elaboração dos cosméticos com biomassa e extrato algal.

Por fim, agradeço às instituições de fomento que me forneceram suporte financeiro para execução dessa pesquisa. À Coordenação de Aperfeiçoamento de Pessoal de Nível Superior (CAPES), pela bolsa de doutorado sanduíche (edital/ PRINT nº 88887.470102 / 2019-00), e à Fundação de Amparo à Pesquisa e Inovação do Estado de Santa Catarina (FAPESC), pela bolsa vigente no Brasil.

A todxs quiridx dessa ilha linda chamada Florianópolis, meus sinceros agradecimentos.

RESUMO

O incremento descontrolado de resíduos poluentes não tratados decorrente de atividades antropogênicas é um problema mundial que põe em risco ecossistemas continentais e costeiros. A descarga excessiva de nutrientes nos corpos d'água, principalmente na forma de compostos nitrogenados e fosforados, leva ao fenômeno de eutrofização, o qual compromete os ecossistemas aquáticos em termos químicos e biológicos. A aquicultura é uma prática que vem crescendo ao longo dos últimos anos, gerando efluentes ricos em nutrientes que, se não tratados, podem contribuir com o processo de eutrofização. Sistemas de aquicultura multitróficos integrados consistem no cultivo interligado de organismos de diferentes níveis tróficos, permitindo o reuso dos efluentes ricos em nutrientes para o cultivo de organismos filtradores, como algas marinhas. Nesse sentido, algas do gênero *Ulva* têm sido exploradas como biofiltradoras de efluentes de maricultura. Além de atuarem como biofiltros, os cultivos de *Ulva* sp. podem ser fonte de biomassa para obtenção de compostos de interesse biotecnológico, como polissacarídeos denominados ulvanos. Nesse cenário, o presente trabalho buscou, através de experimentos em escala piloto, a perspectiva de utilização de cultivo de duas espécies de *Ulva*: *U. pseudorotudata* e *U. rigida* para biofiltração de efluentes advindos de cultivos de peixes. Além da redução no teor da concentração de compostos nitrogenados, decorrente do processo de remoção dos nutrientes pelas algas no meio, também foram avaliados aspectos fisiológicos obtidos por parâmetros fotossintéticos, crescimento e composição da biomassa. No âmbito relacionado ao uso da biomassa algal, realizou-se a extração e caracterização de polissacarídeos da biomassa obtida nos cultivos de ambas as espécies. Posteriormente foram avaliadas a atividade antioxidante e de citotoxicidade dos polissacarídeos em ensaios *in vitro* de 4 linhagens celulares: câncer de cólon (HCT-116), leucemia (U-937), queratinócitos (HACAT) e melanoma (G361). Tais resultados visaram avaliar o potencial dos polissacarídeos ulvanos, para aplicação na indústria farmacêutica. Para tal, a presente tese está estruturada em três capítulos. Os resultados obtidos no capítulo 1 mostram que cultivos de *U. pseudorotundata* foram eficientes na remoção de NH_4^+ e NO_3^- nas 3 concentrações iniciais testadas de nutrientes (150, 300 e 500 μmol L^{-1}) garantindo a biofiltração completa da água em um período de 24 h, embora tenham sido observadas diferenças na eficiência e velocidade de remoção dos nutrientes dependendo da densidade inicial da biomassa algal e do tipo de fonte de nitrogênio. No capítulo 2, ao comparar aspectos de biofiltração e performance fotossintética dos cultivos de *U. pseudorotundata* e *U. rigida* em 50% e 100% de efluente de *Chelon labrosus* verificou-se que ambas as espécies possuem capacidades semelhantes para remover nutrientes inorgânicos de efluentes de peixes. Também foi observado que os cultivos apresentaram desempenho fotossintético e composição de biomassa equivalentes. Com os dados obtidos foi gerado um modelo de regressão linear entre a eficiência de remoção de NO_3^- e a eficiência fotossintética (αETR), este último obtido através de curvas rápidas de luz. O terceiro e último capítulo apresenta que polissacarídeos, constituídos majoritariamente por ulvanos, obtidos de *U. pseudorotundata* e *U. rigida* revelam composição química e estrutural semelhante. Também se constatou que ambos polissacarídeos apresentaram capacidade antioxidante em função do incremento das concentrações testadas. Foi verificado que os polissacarídeos obtidos das duas espécies exibiram toxicidade moderada contra as linhagens celulares HCT-116 e índice de seletividade >3, demonstrando ser um potencial composto isolado para o desenvolvimento de produtos farmacêuticos. De forma geral, esta tese contribui com o entendimento sobre biofiltração de nutrientes presentes nos efluentes de aquicultura utilizando cultivos de duas espécies de *Ulva* através da performance fisiológica das algas e posterior utilização da biomassa para aplicações biotecnológicas.

Palavras-chave: Aquicultura, Biofiltração, Biomassa algal, Fotossíntese, Nitrogênio, *Ulva* spp., Ulvanos.

ABSTRACT

The increased discharge of wastewater from anthropogenic activities is a worldwide problem which compromises continental and coastal ecosystems. Nutrient discharge into water bodies, mainly as nitrogen and phosphorus compounds, leads to the phenomenon of eutrophication, which can alter chemical and biological composition of aquatic ecosystems. Aquaculture is an activity that has grown over the last few years, generating effluents with a high nutrient content, which, if not treated, can contribute to the eutrophication process. Integrated multi-trophic aquaculture systems (IMTA) consist in the connected cultivation of organisms from different trophic levels, allowing the reuse of nutrient-rich effluents for cultivation by filtering organisms, such as seaweed. In this sense, seaweed from the genus *Ulva* have been explored as biofilters of mariculture effluents. In addition to its role as biofilters, *Ulva* sp. biomass can be a source of compounds with biotechnological interest, such as ulvans polysaccharides. In this scenario, the present work sought, through pilot scale experiments, the perspective of using the cultivation of two Ulva species: *U. pseudorotudata* and *U. rigida* as biofilters of fish ponds effluents. Besides the reduction in the concentration of nitrogen compounds, physiological aspects obtained by photosynthetic parameters, growth and biomass composition were also evaluated. Regarding the use of algal biomass, the extraction and characterization of polysaccharides from the biomass obtained in the cultures of both species were carried out. Subsequently, the antioxidant capacity and cytotoxicity activity of the polysaccharides were evaluated in vitro assays of 4 cell lines: colon cancer (HCT-116), leukemia (U-937), keratinocytes (HACAT) and melanoma (G361). These analyses aimed to evaluate the potential of ulvan polysaccharides for application in the pharmaceutical industry. To access the objectives mentioned above this thesis is presented in three chapters. The results obtained in Chapter 1 show that *U. peudorotundata* cultures were efficient in removing NH_4^+ and NO_3^- in the 3 initial concentrations of nutrients tested (150, 300 and 500 μmol L^{-1}) ensuring complete water remediation in a period of 24 h, although differences were observed depending on the initial biomass stocking density and type of nitrogen source. In chapter 2, when comparing aspects of biofiltration and photosynthetic performance of *U. pseudorotundata* and *U. rigida* cultures in 50% and 100% of *Chelon labrosus* effluent, it was found that both species possess similar capabilities of removing inorganic nutrients from fish effluents. Additionally, both seaweed species presented equivalent photosynthetic performance and biomass composition. A linear regression model between NO_3^- uptake efficiency and photosynthetic efficiency (α_{ETR}), obtained from Rapid Light Curves, is presented. The third and final chapter shows that the ulvan polysaccharide-rich fraction (UPRF) isolated from *U. rigida* and *U. pseudorotundata* presented similar chemical and structure composition. Similar antioxidant capacity was obtained with increasing potential in response to the increment of polysaccharide concentrations. Both UPRF presented moderate toxicity against HCT-116 cell lines and a selectivity index ≥ 3, suggesting a good potential for use in pharmaceutical products. In general, this thesis contributes to the understanding of nutrients biofiltration present in aquaculture effluents using cultures of two *Ulva* species through the physiological performance of algae and subsequent use of biomass for biotechnological applications.

Keywords: Aquaculture, Biofiltration, Algal biomass, Photosynthesis, Nitrogen, *Ulva* spp., Ulvan.

LISTA DE FIGURAS

Capítulo 2

LISTA DE TABELAS

Capítulo 1

Capítulo 3

LISTA DE ABREVIATURAS E SIGLAS

α_{ETR}: photosynthetic efficiency
A: Absorptance of the algal thallus
ABTS: 2,2'-azino-bis(3-ethylbenzothiazoline-6-sulphonic acid)
ATP: adenosine triphosphate
C:N: carbon and nitrogen ratio
Chl *a*: Clorofila *a*
Chl *b*: Clorofila *b*
CHN: carbon, hydrogen, and nitrogen
DW: dry weight
E_k: saturation irradiance
Eo: incident irradiance of a lamp
E_{PAR}: PAR irradiance (µmol photons m^{-2} s^{-1}) obtained by HOBO
Et: transmitted irradiance
ETR: electron transport rate
ETR_{max}: maximum electron transport rate
ETR_{situ}: Electron Transport Rates *in situ*
F_t: basal fluorescence emitted by an organism pre-acclimated to light conditions
F_0: intrisic fluorescence from the antenna of fully oxidized PSII
FAO: Food and Agriculture Organization of the United Nations
F_{II}: fraction of cellular chlorophyll *a* associated with the light harvesting complex of PSII
F_m: maximum fluorescence of PSII after a saturating light pulse
F_m': maximum fluorescence in light, induced by a saturating pulse
FT-IR: Fourier Transform Infrared Spectroscopy
F_v/F_m: optimal or maximal quantum yield of PSII
F_v: variable fluorescence corresponding to the difference between F_m and F_0
FW: fresh weight
G-361: human malignant melanoma
Gal: galactose
GC-MS: Gas Chromatography–Mass Spectrometry
Glc: glucose
GlcA: glucouronic acid
GOGAT: glutamine:2-oxoglutarate amino-transferase
GR: Growth rates
GS: glutamine synthetase
HACAT: mmortalized human keratinocytes
HCT-116: human colon cancer cell line
IBGE: Instituto Brasileiro de Geografia e Estatística
IC_{50}: half maximal inhibitory concentrations
IMTA: Integrated Multi-Trophic Aquaculture
KH_2PO_4: Potassium phosphate monobasic

KNO_3: Potassium nitrate
MCL: Maximum Composite Likelihood
MTT: 3-(4,5-dimethylthiazol-2-yl)-2,5- diphenyl tetrazolium bromide
N: nitrogen
NH_3: non-ionized ammonia
NH_4^+: ammonium
NH_4Cl: ammonium chloride salt
NO_3^-: nitrate
NPQ: Non-photochemical quenching
NPQ_{max}: maximum non-photochemical quenching
NUE: nutrient uptake efficiency
NUR: nutrient uptake rate
P: phosphorus
PAM: Pulse Amplitude Modulation
PAR: Photosynthetic Active Radiation
PCA: principal component analysis
PCR: polymerase chain reaction
pH: Potencial hidrogeniônico
PO_4^{3-}: phosphate
PSII: photosystem II
Rha: rhamnose
Rib: ribose
RLC: Rapid light curves
RM ANOVA: repeated measures analysis of variance
RuBisCO: Ribulose Bisphosphate Carboxylase-Oxygenase
SI: selectivity index
SNIS: Sistema Nacional de Informações sobre Saneamento
SNK: Student-Newman-Keuls
T: transmittance
TAN: total ammonium nitrogen
U-937: leukemia cell line
UPRF: ulvan polysaccharide-rich fraction
Xyl: xylose
$\Delta F/F_m$': effective quantum yield

SUMÁRIO

INTRODUÇÃO GERAL

A poluição dos recursos hídricos é um problema mundial e crescente, que põe em risco os ecossistemas continentais e costeiros, bem como, a segurança hídrica e alimentar das populações humanas (HÄDER; HELBLING; VILLAFA, 2021). Estima-se que 40% da população mundial vive em uma faixa de até 100 km da costa (FINKL, 2016) e sua sobrevivência dependa da utilização direta ou indireta dos ecossistemas locais. No entanto, a enorme carga de resíduos gerados por essas populações, em grande parte, não recebe tratamento, ou ele é apenas parcial, degradando os ecossistemas e comprometendo seus serviços ambientais e a qualidade da vida humana e marinha (LOTZE et al., 2006; VITOUSEK, 1997). No Brasil, 58% da população total do país vive na zona costeira (IBGE, 2018). De acordo com dados disponibilizados pelo SNIS (SISTEMA NACIONAL DE INFORMAÇÕES SOBRE SANEAMENTO, 2021) menos de 60% da população possui coleta de esgoto, sendo que somente 50,8% do esgoto gerado é tratado. Além da descarga de efluentes domésticos nas zonas costeiras, a indústria, o uso de fertilizantes agrícolas também são atividades em expansão responsáveis pel escoamento de elevada carga de nutrientes e outros contaminantes nos corpos hídricos. Nesse cenário, atividades antropogênicas são causadoras da contínua emissão de nutrientes impactando a qualidade da água e comprometendo as bacias hidrográficas continentais e costeiras (HÄDER; HELBLING; VILLAFA, 2021).

A descarga de efluentes ricos em nutrientes nos ambientes aquáticos impacta a biodiversidade de diversas formas, sendo o fenômeno de eutrofização uma das mais preocupantes (HÄDER; HELBLING; VILLAFA, 2021). Águas costeiras eutrofizadas são cada vez mais reportadas em diversas regiões do mundo (DIAZ; ROSENBERG, 2008), evidenciando certa incapacidade da sociedade moderna em controlar os impactos negativos do desenvolvimento humano. A eutrofização é caracterizada pela entrada excessiva de nutrientes nos corpos d'água, especialmente nas formas de compostos nitrogenados e fosforados. O abundante aporte desses compostos altera a estrutura da biota aquática qualitativa e quantitativamente, e estudos apontam a eutrofização como responsável pelo colapso de ecossistemas (KHAN; MOHAMMAD, 2014; LE MOAL et al., 2019). O desequilíbrio ocorre uma vez que a entrada excessiva de nitrogênio e fósforo nos corpos d'água leva ao crescimento descontrolado de plantas aquáticas e algas oportunistas, causando alterações na comunidade fitoplanctônica, bem como afetando as relações predador-presa, a transferência de nutrientes e o consequente desbalanço nos

diferentes níveis tróficos (HAN; LIU, 2014; JONES; PINN, 2006; VALIELA et al., 1997).

Aquicultura como atividade impactante ao meio ambiente

Geradora de efluentes ricos em compostos nitrogenados e fosforados, a aquicultura é uma atividade que vem crescendo ao longo dos últimos anos. Entre os anos de 1980 a 2014, a produção de peixes para consumo humano advindos de sistemas de aquicultura cresceu de 9 a 48%, o que torna essa prática cada vez mais necessária diante da crescente demanda por pescado (FAO, 2016). No entanto, a descarga de efluentes ricos em matéria orgânica e nutrientes dissolvidos, tanto em cultivos abertos, quanto em cultivos confinados levanta a atenção aos riscos de poluição ambiental gerados por essa atividade (CHOPIN et al., 2001). De acordo com Wu (1995), dependendo de fatores como a espécie cultivada, ciclo de vida dos animais, densidade dos cultivos e tipo de ração, cerca de 52-95% do teor de nitrogênio e 85% de fósforo na ração pode ser desperdiçado no meio ambiente especialmente na forma de compostos nitrogenados (NH_4^+ e NO_3^-) e fosforados (PO_4^{3-}). Tendo em vista que a produção de animais aquáticos como alimento (principalmente como fonte de proteínas e ácidos graxos) tende a aumentar nas próximas décadas (FAO, 2020) faz-se necessária a adoção de estratégias de cultivo que visem a diminuição do lançamento de efluentes ricos em nutrientes a fim de tornar a aquicultura uma prática menos impactante.

No Brasil, a obtenção de licença ambiental para a implementação da prática de aquicultura deve seguir normativas estabelecidas pelo CONAMA (Conselho Nacional do Meio Ambiente), dentre as quais estão as Resoluções 001, 357 e 430. Tais normas dispõem sobre a regularização da prática de aquicultura no que diz respeito aos impactos ambientais que tal atividade pode acarretar, como por exemplo, a geração de efluentes que põe em risco o meio ambiente, o que não só dificultam a liberação de licencimento ambiental, como também agregam custos em termos de recursos e área de produção, e.g. construção de bacias de sedimentação, uso de biofiltros e bombas centrífugas que demandam energia elétrica. Nesse sentido, o desenvolvimento e aplicação de estratégias que visam o polimento de efluentes advindos dos tanques de cultivo são ambientalmente e economicamente importantes para implementação da prática de aquicultura.

Entre tecnologias sustentáveis, o cultivo multitrófico integrado, conhecido internacionalmente como *Integrated Multi-Trophic Aquaculture* (IMTA), é uma medida

promissora e ainda pouco aplicada no Brasil (REIS; BAUER; MARTINS, 2019). Sistemas IMTA minimizam o impacto da descarga excessiva de nutrientes advindos da aquicultura através do cultivo interligado de organismos de diferentes níveis tróficos dentro do mesmo sistema produtivo. A integração dos cultivos de organismos geradores de efluentes ricos em nutrientes (e.g. peixes, crustáceos) conectados ao cultivo de organismos biofiltradores (e.g. moluscos e algas) permite que o efluente rico em nutrientes seja ciclado pelos cultivos subsequentes (NEORI et al., 2004). Dessa forma, os nutrientes em excesso na água que são gerados por uma espécie são aproveitados pelos demais níveis tróficos (GRANADA et al., 2018). O cultivo de macroalgas como parte de sistemas IMTA é atrativo tanto por questões ambientais, por diminuir a emissão de efluentes ricos em nutrientes, quanto por questões econômicas, através da produção de biomassa algal associada a produção da espécie alvo do maricultor. No entanto, a escolha da alga para compor o sistema IMTA deve atender alguns critérios básicos como: elevada capacidade de crescimento e remoção de compostos nitrogenados; facilidade de cultivo e controle do ciclo de vida; resistência a epífitas e organismos causadores de doenças; ajuste entre características fisiológicas da espécie alvo com as condições fornecidas pelos sistemas de cultivo (NEORI et al., 2004). Nesse sentido, é importante o conhecimento das algas ocorrentes e tolerantes à regiões destinadas aos sistemas de aquicultura, bem como, o possível uso da sua biomassa para aplicações biotecnológicas. Dessa forma, a compreensão dos mecanismos fisiológicos associados à biofiltração, e do desempenho fotossintético de cultivos algais para compor sistemas IMTA é crucial para a otimização do crescimento, aumento da capacidade de biofiltração e também para melhorar as práticas de gestão dos sistemas de tratamento de efluentes de aquicultura.

A produção de algas em sistemas IMTA pode ir além do tratamento dos efluentes, permitindo o aproveitamento comercial da biomassa algal com a obtenção de biomoléculas de elevado valor como proteínas, lipídios, carboidratos, pigmentos fotossintetizantes, dentre outros (BARCELÓ-VILLALOBOS et al., 2017; FIGUEROA et al., 2008).

Biomassa algal e interesses comerciais

Macroalgas marinhas são um grupo diversificado composto por mais de 12.000 espécies incluindo algas vermelhas (Rhodophyta), marrons (Phaeophyceae) e verdes (Chlorophyta). A diversidade de compostos encontrados nas algas marinhas está

associada a mecanismos fisiológicos adaptativos, que lhes permitem sobreviver em condições de constante mudança, como flutuações na disponibilidade de nutrientes, variações na intensidade de luz, temperatura, dessecação e na síntese de defesas químicas contra herbívoros (HURD et al., 2014). Nesse sentido, a biomassa algal pode ser fonte de metabólitos primários (e.g. proteínas, peptídeos, carboidratos, lipídios) e secundários (e.g. pigmentos, compostos fenólicos, florotaninos e aminoácidos tipo micosporina) o que permite o uso da biomassa para diversas finalidades, não só na indústria alimentícia mas também na cosmética, farmacêutica, nutracêutica, bem como a aplicação na agricultura como fertilizantes e bioestimulantes (BUSCHMANN et al., 2017a).

Potencial de macroalgas do gênero *Ulva* para biofiltração de nutrientes e fonte de biomassa

Macroalgas do gênero *Ulva* são cosmopolitas apresentando cerca de 131 espécies taxonomicamente aceitas (GUIRY et al., 2014; MANTRI et al., 2020). Essas por sua vez, são caracterizadas por apresentarem crescimento rápido devido às altas taxas fotossintéticas e rápida absorção de nutrientes nitrogenados (BERMEJO et al., 2019; VIAROLI et al., 1996). As florações de *Ulva* são conhecidas como *green tides* e vem sendo relatadas com cada vez mais frequência nos últimos anos principalmente em áreas eutrofizadas onde são observados níveis elevados de nutrientes na água do mar (LIU et al., 2013; SMETACEK; ZINGONE, 2013; YE et al., 2011). O expressivo crescimento de *Ulva* spp. e sua capacidade em suportar amplas condições climáticas e ecológicas (e.g. amplitude de temperatura e salinidade), leva ao interesse no seu cultivo para remoção de nutrientes sendo alvo de diversos trabalhos que visam a biorremediação de efluentes ricos em nutrientes advindos da aquicultura (ASHKENAZI; ISRAEL; ABELSON, 2019; GUTTMAN et al., 2019; NEORI; COHEN; GORDIN, 1991; SHPIGEL et al., 2019). Além de aplicação como biofiltradoras de efluentes, a biomassa de *Ulva* também apresenta potencial valor para aplicação biotecnológica devido ao teor de proteínas, compostos fenólicos e polissacarídeos presentes na parede celular (BENJAMA; MASNIYOM, 2011; MICHALAK; CHOJNACKA; SAEID, 2017; SHPIGEL et al., 2017).

Estudos realizados nos últimos anos têm explorado a extração e aplicação de polissacarídeos sulfatados da parede celular de *Ulva* denominados ulvanos. Os ulvanos podem representar entre 9 a 36% da biomassa seca de *Ulva* e são majoritarimente

formados pelos monossacarídeos ramnose, ácido glucurônico, ácido idurônico, xilose, galactose, glicose e manose. Atividades biológicas de ulvanos vem sendo descritas com potencial anticoagulante, imunomodulador, anticancerígeno, antioxidante, antiviral, anti-hiperlipidêmico, dentre outros (KIDGELL et al., 2019a; QI et al., 2012; TZIVELEKA; IOANNOU; ROUSSIS, 2019a). A bioatividade dos ulvanos está ligada à sua similaridade com moléculas celulares de ocorrência natural em animais, como glicosaminoglicanos e proteoglicanos as quais, por sua vez, estão envolvidas em processos biológicos. No entanto, características estruturais de ulvanos, como peso molecular, grau de sulfatação e constituição dos açúcares, podem interferir na bioatividade desses polissacarídeos (KIDGELL et al., 2019a). Dessa forma, a composição de ulvanos obtidos de diferentes espécies de *Ulva*, bem como o ambiente de cultivo e condições ecofisiológicas prévias das algas, podem influenciar significativamente na sua bioatividade.

Contextualização do trabalho

Tendo em vista que algas do gênero *Ulva* apresentam características vantajosas para cultivo em sistemas IMTA, o presente trabalho foi estruturado abordando os seguintes tópicos: (1) avaliação da biofiltração dos cultivos de *Ulva* spp. para a remoção de nutrientes visando a depuração de efluentes advindos da aquicultura; (2) acompanhamento de aspectos fisiológicos dos cultivos algais; (3) direcionamento da biomassa para aplicações biotecnológicas, com o intuito de valorização da biomassa algal gerada nos sistemas de cultivo. Os capítulos desta tese correspondem aos diferentes experimentos realizados. O primeiro capítulo descreve experimentos utlizando cultivos de algas da espécie *U. pseudorotundata* avaliando a biofiltração e performance fisiológica de cultivos submetidos a duas diferentes fontes de nitrogênio (NH_4^+ e NO_3) simulando a descarga de efluentes advindos de cultivos de peixes. O segundo capítulo apresenta e compara a utilização de cultivos de algas das espécies *U. pseudorotundata* e *U. rigida* para biofiltração de efluentes advindos de tanques de peixes da espécie *Chelon labrosus*. Este capítulo também buscou comparar o crescimento, produção e constituição da biomassa algal gerada ao longo do período experimental. Os experimentos retratados no capítulo 1 e 2 foram realizados em escala semi-piloto de cultivo, sob condições não controladas de temperatura e luz. O uso de técnicas de medidas de fluorescência *in vivo* da clorofila-a através de fluorímetros de amplitude modulada permitiu a obtenção de parâmetros e estimativas de desempenho fotossintéticos das algas. O terceiro e último

capítulo apresenta e discute a potencial utilização de polissacarídeos extraídos da biomassa de *U. pseudorotundata* e *U. rigida* para indústria farmacológica através da caracterização dos polissacarídeos extraídos e de ensaios biológicos de atividade antioxidade e de citotoxicidade em 3 linhagens celulares cancerígenas (câncer de cólon, melanoma e leucemia) e 1 linhagem de células não cancerígenas (queratinócitos). A figura 1 apresenta o resumo gráfico do presente trabalho.

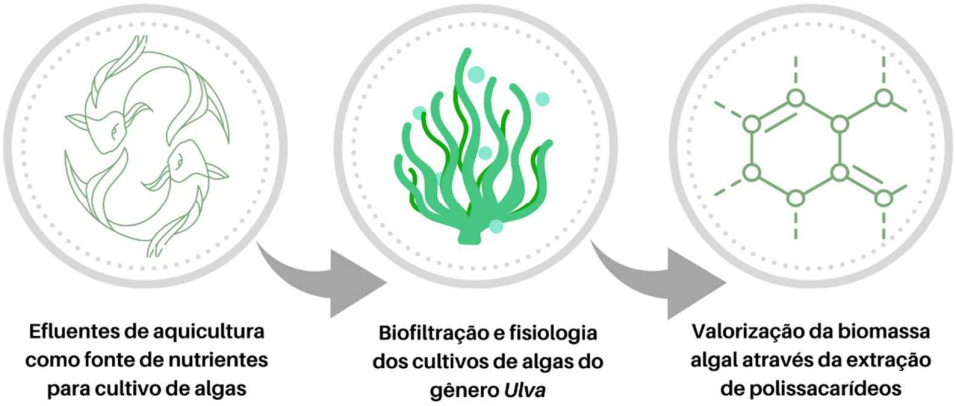

Figure. 1 Resumo gráfico da abordagem desenvolvida na presente tese ilustrando o uso do cultivo de algas do gênero *Ulva* como biofiltro para purificação de efluentes advindos da aquicultura. A biomassa obtida foi direcionada para a obtenção de polissacarídeos para valorização da biomassa.

OBJETIVOS

1. OBJETIVO GERAL

Avaliar aspectos de remoção de compostos inorgânicos nitrogenados através do cultivo de algas do gênero *Ulva* com a perspectiva de biorremediação de efluentes advindos da aquicultura e utilização da biomassa algal para obtenção de polissacarídeos para aplicação biotecnológica na indústria farmacêutica.

2. OBJETIVOS ESPECÍFICOS

Capítulo 1: **Short-term nutrient removal efficiency and photosynthetic performance of *Ulva pseudorotundata* (Chlorophyta): potential use for Integrated Multi-Trophic Aquaculture (IMTA)**

O presente capítulo teve como objetivo principal avaliar a aplicação do cultivo de algas da espécie *Ulva pseudorotundata* para compor sistemas multitróficos integrados.

Buscou-se avaliar o desempenho de biofiltração, performance fotossintética e composição de biomassa dos cultivos. Também foi alvo do estudo comparar a remoção dos nutrientes de duas concentrações iniciais de biomassa algal e a eficiência desses cultivos em remover distintas fontes de concentrações iniciais de nitrogênio inorgânico: NH_4^+ e NO_3^-.

Capítulo 2: **Growth, biofiltration and photosynthetic performance of *Ulva* spp. cultivated in fishpond effluents: An outdoor system study.**

O presente capítulo teve como objetivo comparar o cultivo de *Ulva pseudorotundata* e *Ulva rigida* em efluentes de peixes *Chelon labrosus* para remoção de nutrientes inorgânicos dissolvidos (NH_4^+, NO_3^- e PO_4^{3-}), performance fotossintética, crescimento, produtividade e composição elementar e bioquímica da biomassa.

Capítulo 3: **Characterization, antioxidant and cytotoxicity activity of ulvan polysaccharide-rich fraction obtained from *Ulva pseudorotundata* and *Ulva rigida* and their potential for pharmaceutical application.**

O presente capítulo teve como objetivo realizar a caracterização e identificação dos constituintes elementares e estruturais de polissacarídeos extraídos de *U. pseudorotundata* e *U. rigida*. Neste capítulo também buscou-se avaliar o potencial uso dos polissacarídeos obtidos da biomassa algal para indústria farmacêutica através de obtenção da capacidade antioxidante e citotoxicidade dos polissacarídeos em testes *in vitro*.

CAPÍTULO 1

Manuscrito em revisão pelo periódico *Journal of Applied Phycology*
reproduced with permission from Springe Nature B.V.

Short-term nutrient removal efficiency and photosynthetic performance of *Ulva pseudorotundata* (Chlorophyta): potential use for Integrated Multi-Trophic Aquaculture (IMTA)

Thaís Fávero Massocato[a], Victor Robles-Carnero[c], Julia Vega[c], Eduardo de Oliveira Bastos[b], Antonio Avilés[c], José Bonomi-Barufi[a], Leonardo Rubi Rörig[a], Félix L. Figueroa[c]

[a] Pos-Graduate Program in Biotechnology and Biosciences, Phycology Laboratory, Department of Botany, Biological Sciences Center, Federal University of Santa Catarina, Florianópolis 88040-900, Santa Catarina, Brazil

[b] Phycology Laboratory, Department of Botany, Biological Sciences Center, Federal University of Santa Catarina, Florianópolis 88040-900, Santa Catarina, Brazil

[c] Malaga University. Institute of Blue Biotechnology and Development (IBYDA), Experimental Center Grice Hutchinson, Lomas de San Julián, 2, E-29004 Malaga, Spain

1. ABSTRACT

Short-term $N\text{-}NH_4^+$ and $N\text{-}NO_3^-$ removal by *Ulva pseudorotundata* under different initial nutrient concentrations and biomass stocking densities, monitoring in parallel photosynthetic parameters obtained by Pulse-Amplitude-Modulation (*PAM*) *Fluorometry* of chlorophyll-*a* and evaluating biomass characteristics (CHN, proteins, carbohydrates) was investigated. The results showed that *U. pseudorotundata* cultivated under solar radiation in a land-based out-door pilot scale was efficient in removing $N\text{-}NH_4^+$ and $N\text{-}NO_3^-$ even in concentrations as high as 500 µmol L^{-1} ensuring complete water remediation in a period of 24 h and in all experimental conditions tested, although differences were observed depending on the stocking density and type of N-source. Treatments with $N\text{-}NH_4^+$ showed faster N removal than those with $N\text{-}NO_3^-$, however, treatments with $N\text{-}NO_3^-$ demanded more photosynthetic energy. Part of the ammonium removed in the respective treatments may have been volatilized as a combined effect of the pH increase related to photosynthesis and aeration in the tanks. The results presented here establish the fundamental parameters for the use of *U. pseudorotundata* as a biofiltering organism for effluents with high concentrations of $N\text{-}NH_4^+$ and $N\text{-}NO_3^-$.

Keywords

Algal biomass, aquaculture, biofiltration, chlorophyll-*a* fluorometry, nitrogen, photosynthesis

2. INTRODUCTION

Nutrient discharge plays an important role in natural ecosystems, particularly when considering anthropogenic impacts on water resources (LE MOAL et al., 2019). Considering different nutrient elements, nitrogen and phosphorus are present in high concentrations in aquaculture effluents and the discharge in the natural environment can produce negative impacts (HERATH; SATOH, 2015). In the context of aquaculture, depending on factors such as species type, size of culture organism, stocking density and feeding rate, about 52-95% of N and 85% of P content in the feed can be wasted into the environment (WU, 1995). The disposal of these nutrients not only represents an economic and sanitary problem that raises production costs and requires regular water changes in land-based systems, but also an environmental problem leading to eutrophication of adjacent areas (NAYLOR et al., 2021). As the production of aquatic animals as food (mainly as protein and fatty acid source) tends to increase in the next few decades (FAO, 2020), these problems will be exacerbated unless new strategies are adopted to make animal aquaculture more sustainable. The application of seaweeds as biofilters to remove nutrient loads can become an environmental friendly practice, especially when associated with aquaculture fish production (BUSCHMANN; TROELL; KAUTSKY, 2001; CHOPIN et al., 2001; NEORI et al., 2004; TROELL et al., 2003). Moreover, seaweed biomass is a source of valuable compounds that can be used in a huge range of biotechnology processes and increase the overall profitability of aquaculture activities (Barceló-villalobos et al. 2017; FAO 2018; Vega et al. 2020; Kalasariya et al. 2021). Considering this, the fundamental understanding of the physiological mechanisms behind biofiltration and photosynthetic performance of seaweeds is essential for growth optimization, enhancement of biofiltration capacity and also to improve management practices of aquaculture effluents treatment systems.

Nitrogen in inorganic forms is present in aquaculture effluents especially as ionic forms of ammonium (NH_4^+) and nitrate (NO_3^-), which are taken into the cell and stored by seaweeds through different mechanisms (ROLEDA; HURD, 2019). NO_3^- is described to be taken up by active transport, which occurs against a concentration gradient provided by mechanisms on membrane transport systems, e.g. carrier proteins, and is energy dependent (HARRISON; HURD, 2001). In contrast, NH_4^+ uptake is reported to be through passive transport and demands less energy since it enters cells by passive

diffusion down a concentration gradient (HURD et al., 2014). Assimilation and storage of NO_3^- and NH_4^+ also differ from each other. Studies indicate that once inside the cell, NH_4^+ is not stored in large concentrations and is immediately metabolized to amino acids through glutamine and glutamate synthase in the chloroplasts (TAYLOR; REES, 1999). NO_3^- can be stored in its inorganic form in cellular vacuoles and the cytoplasm, or get converted into NH_4^+ involving activity of two enzymes: nitrate and nitrite reductases (ROLEDA; HURD, 2019). Regulation of this enzymatic pathway is associated with electron transport rates of photosynthesis via the formation of reductant power compounds (NADPH and ferredoxin) (HUPPE; TURPIN, 1994). Consequently, it is suggested that NO_3^- uptake and assimilation is an energy-dependent process which requires energy from the photochemical reactions of photosynthesis (PRITCHARD et al., 2015).

Measurements that assess photosynthetic performance of land-based cultivated seaweeds allow fundamental understanding of their physiological status and capacity to respond to stress events, becoming an essential tool to understand the growth conditions in any production system (FIGUEROA et al., 2006). Photosynthetic activity in aquatic organisms can be estimated by quantifying the accumulation of organic carbon or the production of O_2. Nonetheless, those methods require laborious techniques e.g. specific optodes, clark type electrodes, chemical titration, radiolabeled ^{14}C inorganic carbon, or Membrane Inlet Mass Spectrometry. An alternative and complementary methodology is the estimation of quantum yields from chlorophyll fluorescence using Pulse Amplitude Modulation (PAM) (MAXWELL; JOHNSON, 2000). The PAM, designed to measure the *in vivo* chlorophyll-*a* fluorescence of photosystem II (PSII), has become a widely-used technique to study algal physiology since it is rapid, non-intrusive and easily usable *in situ* (JEREZ et al., 2016; MASOJÍDEK et al., 2011). The PAM *in vivo* chlorophyll-*a* fluorometers enable quantifying the performance of photosystem II (photochemical) and the relative loss of light dissipated energy (non-photochemical processes). Several photosynthetic parameters can be estimated using PAM: effective quantum yield ($\Delta F/F_m$'), as an indicator of the acclimation of PSII, due to the redox state of the reaction centers; the optimal or maximal quantum yield of PSII (F_v/F_m), which indicates the maximal photochemical efficiency of PSII, and also the physiological state of the culture and photoinhibition; electron transport rate (ETR) through PSII, used as an estimator of

photosynthetic capacity and productivity (Maxwell and Johnson 2000). The use of PAM to estimate photosynthetic activity has been described for different microalgae and seaweed culture systems (Gómez-Pinchetti et al. 1998; Celis-Plá et al. 2021; Rearte et al. 2021). Moreover, aspects obtained by fluorescence parameters could infer culture performance associated with bio-optical properties of the organisms. Stress can be detected by the variations of PAM-associated variables as decrease of F_v/F_m and maximal ETR, allowing estimation of photoinhibition (MATA et al., 2006). Moreover, fluorescence parameters are usable to estimate energy loses, such as those linked to non-photochemical mechanisms (Figueroa et al., 2020).

Among the seaweed species used as biofilters *Ulva* genus stands out since, in addition to being highly efficient in removing nutrients from the water (Copertino et al. 2009; Al-Hafedh et al. 2014; Macchiavello and Bulboa 2014), it also has a fast growth rate, wide geographical distribution (MANTRI et al., 2020) and potential for biomass application (BENJAMA; MASNIYOM, 2011; KIDGELL et al., 2019b; SHPIGEL et al., 2017, 2018). Several authors have reported aspects of chlorophyll-*a* measurements in order to elucidate *Ulva* spp. metabolism and nutrient uptake (FAN et al., 2014; GORDILLO; FIGUEROA; NIELL, 2003; SHAHAR et al., 2020). In this connection it is important to verify the possible influence of different N-sources present in fish effluents ($N\text{-}NH_4^+$ produced by animal metabolism and $N\text{-}NO_3^-$ generated after bacterial nitrification) on algal physiology, as determined by different photosynthetic parameters, and on biomass characteristics, obtained by elemental and biochemical analyses. In the present article we evaluated the performance of *U. pseudorotundata* in removing $N\text{-}NH_4^+$ and $N\text{-}NO_3^-$ as its sole nitrogen source in levels above reported from fish tanks in a cycle of 24 hours under outdoor conditions. Simultaneous measurements of nutrient biofiltration capacity and photosynthetic performance were carried out, as well as their effects on biomass composition, in a land based out-door pilot-scale cultivation, considering different initial biomass and nutrient concentrations.

3. MATERIAL AND METHODS

Algal biomass collection and experimental design

Floating specimens of *Ulva pseudorotundata* Cormaci, G.Furnari & Along were collected from the salt marshes in the bay of Cádiz (36°29'-36º30'N, 6º8'-6º10'W)

Andalucía Province, Spain in June and October, 2020. The biomass was transported in thermal boxes, protected from light, to the Grice Hutchinson research center at the Universidad de Málaga where algae cultivation and experiments were conducted. The seaweed was cleaned to remove epiphytes, epibionts and sediments. *Ulva* biomass was then cultivated in 500 L rectangular-shaped tanks containing artificial seawater and supplemented twice a week with NH_4Cl and KNO_3 (300 µmol L^{-1}) and KH_2PO_4 (48 µmol L^{-1}). The salinity and pH of the seawater used for the maintenance were 35 and 8.0 ± 0.2, respectively. Seaweed biomass was grown suspended in the water column by air diffusers situated at the bottom of each tank under ambient conditions of temperature and light. After collection, some small pieces of algal material were separated for species-level identification using molecular methods. Molecular identification was performed by the amplification and sequencing of the partial rbcL gene, using published primer pairs: SHF1 and SHR4 (HEESCH et al., 2009). Species-level identification and phylogenetic analysis are detailed explained by Massocato et al. (2022).

The experiments of biofiltration capacity and photosynthetic performance of *U. pseudorotundata* were conducted in batches of 24 hours. The experimental set-up consisted in verified different nitrogen sources of nutrients, seaweed biomass stocking densities, and nutrient's initial concentrations. Treatments with the same nitrogen source and nutrient concentrations were run simultaneously resulting in six rounds of experiments. All experiments started at 9:00 am (local time) and the tanks were exposed to full sunlight. Temperature and irradiance (Photosynthetic Active Radiation, PAR) in the tanks were recorded every 15 minutes using HOBO Pendant® Temperature/Light Data Logger (UA-002-64). Integrated daily irradiance (kJ m^{-2}) was calculated from PAR data to obtain total light energy received by cultures during experimental time. At the beginning and end of the experiments pH measurements were taken in each tank to estimate the overall variation. The abiotic parameters of pH, salinity (35.8 ± 2.0) and conductivity (54.6 ± 2.8 mS) were measured using a portable device (LAQUAact PH110, LAQUAact-EC120). At the beginning of all experiments, *U. pseudorotundata* biomass, previously submitted to a starvation period of 5 days (without added N and P), was weighed at initial stocking densities of 6.0 and 10.0 g fresh weight (FW) L^{-1} and placed into three replicate tanks (n = 3) with 200 L seawater medium under above mentioned culture conditions. The seaweed stocking densities used in this study were chosen based

on the high uptake efficiency in removing N-NH_4^+, N-NO_3^-, and P-PO_4^{3-} by *Ulva lactuca* in similar stocking densities when cultivated in outdoor conditions and receiving discharge water from an abalone culture center (MACCHIAVELLO; BULBOA, 2014).

To evaluate the effects of different nutrient concentrations on nutrient removal and photosynthetic performance, three concentrations of each N-source (NH_4^+ or NO_3^-) were used separately: 150, 300 and 500 µmol L^{-1}. Those concentrations were chosen based on data reported in fish tanks by Figueroa et al. (2012) and Abreu et al. (2011) with N-NH_4^+ and N-NO_3^-, with maximum values ranged from 200 µmol L^{-1} and 450 µmol L^{-1}. Nutrient's concentrations were obtained by adding NH_4Cl as a source of ammonium and KNO_3 as a source of nitrate. To avoid P shortage of nitrogen uptake in the higher N concentrations (500 µmol L^{-1}) an approximate ratio of 17:1 (PROVASOLI; MCLAUGHLIN; DROOP, 1957) was obtained by adding 29 µmol L^{-1} PO_4^{3-} (KH_2PO_4) in all treatments. To evaluate the removal of N-NH_4^+ and N-NO_3^- over time, a 10 mL water sample was taken from each tank after 60, 180, 300, 420 and 1440 minutes from the beginning of the experiment. Water samples were filtered (GF/F Whatman) and stored at −20 °C in polyethylene flasks for later analysis. In the meantime, algal samples were taken out of the same tanks for chlorophyll-*a* fluorescence measurements in order to determine the photosynthetic performance of algal cultivation.

Nutrient analysis

To determine changes in concentration of N-NH_4^+ and N-NO_3^- , water samples were analyzed colorimetrically using a continuous flow automated analyzer (Technicon AA-2) according to the methods described by Grasshoff et al., (1999). The reduction in nutrient concentration between the time intervals is expressed as a percentage and defined as nutrient uptake efficiency (NUE) and was calculated by equation 1 assessing the changes in N-NH_4^+ and N-NO_3^- concentrations:

$$\text{NUE } (\%) = 100 - \left[\left(\frac{C_{t+1} \times 100}{C_t}\right)\right] \quad (1)$$

where C_t represents the initial concentration of nutrients, C_{t+1} represents the concentration of nutrients after t+1. The amount of nutrients removed per unit of time per volume by seaweed dry weight represent the nutrient uptake rate (NUR) and is determined from changes in N-NH_4^+ and N-NO_3^- according to equation 2:

$$\text{NUR } (\mu\text{mol g}^{-1}\text{ DW h}^{-1}) = \frac{(C_t \times V_t) - (C_{t+1} \times V_{t+1})}{B \times \Delta_t} \quad (2)$$

where C_t represents the initial concentration of nutrients, V_t represents the initial volume of water (in L), C_{t+1} represents the concentration of nutrients after t+1, V_{t+1} represents the volume of water after t+1 (in L); B represents the dry biomass used (in grams), and Δ_t represents the time interval between t and t+1 (in hours).

Photosynthetic performance

To evaluate the photosynthetic performance of *U. pseudorotundata, in vivo* chlorophyll-*a* fluorescence was measured using two different fluorometers, a Pocket-PAM (Gademann Instruments, Würzburg, Germany) and a Junior PAM (Walz GmbH, Effeltrich Germany) connected to a PC running WinControl software.

In-situ estimation of Electron Transport Rate

Electron Transport Rates *in situ* (ETR_{situ}) were measured by Pocket-PAM, at the beginning and end of the experiment, corresponding to the time 15 and 1440 min. Measurements were done using five samples (pseudoreplication) from each tank. Effective quantum yield of Photosystem II (PSII) was calculated using equation 3:

$$\frac{\Delta F}{F_m'} = \frac{(F_m' - F_t)}{F_m'} \quad (3)$$

and was automatically obtained with the Pocket PAM, where F_m' is the maximum fluorescence in light induced by a saturating pulse, and F_t is the basal fluorescence emitted by an organism pre-acclimated to light conditions. Absorptance of the algal thallus was calculated as A = 1 - T, as reported by Figueroa et al. (2009), where T is the transmittance estimated by the equation 4:

$$T = \frac{E_t}{E_o} \quad (4)$$

where E_o is the incident irradiance of a lamp determined by a sensor Li-189 (LI-COR Ltd, Nebraska, USA) connected to a radiometer Li-250 (LI-COR Ltd, Nebraska, USA), and E_t is the transmitted irradiance, measured by placing a small piece of the thallus above the PAR sensor. ETR_{situ} was calculated using equation 5 (GENTY; BRIANTAIS; BAKER, 1989):

$$\mathrm{ETR}_{situ}\ (\mu\mathrm{mol\ electrons\ m^{-2}\ s^{-1}}) = \frac{\Delta F}{F_{\mathrm{m}}'} \times \mathrm{E_{PAR}} \times \mathrm{A} \times \mathrm{F_{II}} \quad (5)$$

where ETR_{situ} is the electron transport rate associated with Photosystem II (µmol electrons m^{-2} s^{-1}); $\Delta F/F_m'$ is the effective quantum yield of Photosystem II; E_{PAR} was the PAR irradiance (µmol photons m^{-2} s^{-1}) obtained by HOBO at the same time of the measurements; A was the Absorptance of the algal thallus; and F_{II} represents the fraction of cellular chlorophyll-*a* associated with the light harvesting complex of PSII being 0.5 the value green algae (GRZYMSKI; JOHNSEN; SAKSHAUG, 1997).

Ex-situ (laboratory) measurements of Rapid light-responses curves

Rapid light curves (RLC) were determined using the Junior-PAM and data were obtained at four moments corresponding to 15, 180, 420 and 1440 minutes of experiment. Samples of *U. pseudorotundata* were transported under dark conditions from the outdoor tanks to the laboratory and kept at least 15 min in darkness. The optimal quantum yield (F_v/F_m), an indicator of maximal quantum efficiency, was obtained from the first saturating pulse after a dark period and determined by the equation 6:

$$\frac{F_{\mathrm{v}}}{F_{\mathrm{m}}} = \frac{(F_{\mathrm{m}} - F_0)}{F_0} \quad (6)$$

where F_0 is the basal fluorescence of fully oxidized reaction centers; F_m is the maximal fluorescence of PSII after a saturating light pulse (0.4 s, approx. 9000 µmol photons m^{-2} s^{-1}), and F_v is the variable fluorescence corresponding to the difference between F_m and F_0.

Next, to estimate the electron transport rate (ETR), the same samples were exposed for 30s to twelve increasing irradiances (25, 45, 66, 90, 125, 190, 285, 420, 625, 845, 1150, and 1500 µmol photons m^{-2} s^{-1}) of actinic light followed by a saturating light pulse. ETR was calculated using equation 7 after the exposure of each light irradiance.

$$\mathrm{ETR\ (II)} = (\mu\mathrm{mol\ electrons\ m^{-2}\ s^{-1}}) = \frac{\Delta F}{F_{\mathrm{m}}'} \times \mathrm{E_{PAR}} \times \mathrm{A} \times \mathrm{F_{II}}\ (7)$$

ETR versus irradiance obtained from light curves were fitted according to Eilers and Peeters (1988) models to estimate the variables of maximum electron transport rates (ETR_{max}) and photosynthetic efficiency (α_{ETR}).

Elemental and biochemical analysis of the biomass

At the beginning and end of each experimental batches, biomass was collected from all treatments, washed with MiliQ-water to remove salt, freeze-dried, and 2 mg were submitted for carbon, hydrogen, and nitrogen content analyses using a LECO CHNS-932 elemental analyser (Michigan, USA) in the Research Support Central Services (SCAI, University of Málaga, Spain). C, H and N values were expressed as percentage of dry mass and the C:N ratio was determined. Protein content was estimated according to Shuuluka et al. (2013) by multiplying the total N by a factor of 5.45. Carbohydrate content was colorimetrically measured according to Dubois et al. (1956).

Data analysis

The data from each treatment were tested for normality (Shapiro–Wilk's test) and homogeneity of variance (Cochran's test). Since assumptions were obtained, data from nutrient analysis (changes in concentrations, NUE and NUR) were analyzed with repeated measures analysis of variance (RM ANOVA). For data obtained from photosynthesis coefficients a factorial ANOVA was performed to evaluate interactions between N-source (two levels: $N\text{-}NH_4^+$ and $N\text{-}NO_3^-$), nutrient concentrations (three levels: 150, 300, and 500 µmol L^{-1}), biomass densities as factors (two levels: 6 and 10 g L^{-1}), and incubation time. Data from elemental and biochemical analyses were submitted to a factorial ANOVA to assess what were the factors influencing data variability of initial and final biomass composition. In both ANOVAs, the factors utilized were N-source, nutrient concentrations, and initial biomass concentration. When significant differences were observed ($p < 0.05$), the Student-Newman-Keuls (SNK) multiple post hoc comparison test was applied. Statistical analyses were performed using STATISTICA 12 software (StatSoft, Inc. 2011).

In an attempt to visualize in a more integrated way the relationships between the multiple variables and parameters determined in each experiment, a principal component analysis (PCA) was performed based on a correlation matrix of the data, using PAST

software, version 3.2 (HAMMER; HARPER; RYAN, 2001). The variables that composed the matrix were: NUR and NUE at 60, 180, 300, 420 and 1440 min of experiment, ETR_{situ} at 15 and 1440 min of experiment, ETR_{max} and F_v/F_m at 15, 180, 420 and 1440 min of experiment, C:N ratio, percentage of carbohydrates and percentage of protein in the initial and final times of the experiment. Some variables were removed from the final analysis because they had low loadings on the first two principal component axes (average daily temperature, average daily pH, integrated daily irradiance) or because they were collinear with other variables (CNH contents). All data were transformed by logarithmization to reduce the amplitude of values of the different variables. Since the PCA analysis does not present significance data (p), a Pearson correlation analysis was also performed among the same data used in the PCA. Correlations were considered significant if $p < 0.05$.

4. RESULTS

Abiotic parameters

The average irradiance value recorded during the day considering all the experiments was 145.52 ± 20.65 µmol photons m^{-2} s^{-1} and the total light energy received by the cultures varied between 938.89 and 1,552.19 kJ m^{-2}. The water temperature in the algae tanks varied between 10.72 °C and 23.85 °C, with a global average value of 16.43 ± 2.92°C. Irradiance and temperature evolution during the experiments can be seen in Supplementary Material (Fig. S1). The final pH was significantly influenced by the interaction of nitrogen source and initial nitrogen concentration (ANOVA: $F(2) = 113.5$, $p < 0.001$, tables S1, S2). The values varied from 8.15 to 8.58 for treatments with $N\text{-}NH_4^+$ and from 8.40 to 9.82 for treatments with $N\text{-}NO_3^-$ (Fig. S2).

Nutrient removal

Considering the total experimental time of 1440 min (24 h), the reduction of nitrogen nutrients was complete for both $N\text{-}NH_4^+$ and $N\text{-}NO_3^-$ treatments (Fig. 1). However, some differences were visible and statistically significant considering nutrient's initial concentration, biomass density, and incubation time of experiment (table S3). The reductions were more abrupt in the treatments with $N\text{-}NH_4^+$ (Fig. 1a, b),

especially in the first 60 min and at the lowest initial concentration (150 µmol L^{-1}). Regarding the biomass density, the reductions were greater in the treatments with 10 g L^{-1} (RM ANOVA, SNK; $p < 0.001$). In treatments with N-NO_3^- (Fig. 1c, d) the smoothest pattern of reduction was similar between treatments with different initial biomass densities, following almost linear trends. These results were influenced by the interaction between the factors initial concentrations, exposure time and biomass densities (RM ANOVA: N-NH_4^+ = $F(10) = 52.9$, $p < 0.001$; N-NO_3^- = $F(10) = 4.3$, $p < 0.001$).

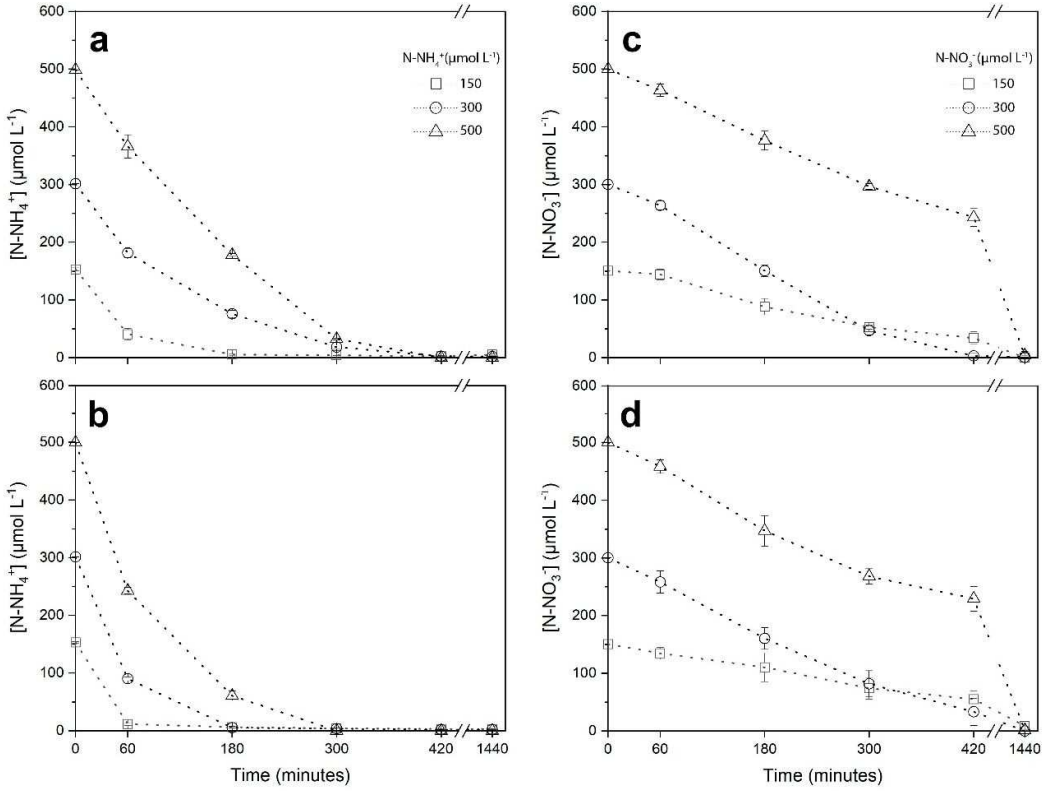

Figure 1. Changes in concentrations of nitrogen nutrients during 1440 minutes of incubation with *U. pseudorotundata* under different nutrient initial concentrations. (a) NH_4^+ with 6 g FW L^{-1}; (b) NH_4^+ with 10 g FW L^{-1}; (c) NO_3^- with 6 g FW L^{-1}; (d) NO_3^- with 10 g FW L^{-1} of stocking biomass. The data represents the means ± SD for n = 3.

By analyzing the nutrient removal efficiency (NUE) data, the nutrient removal patterns become clearer (Fig. 2, table S4). For treatments with 6 g L^{-1} of N-NH_4^+, the removal reaches 90% already at 180 min in the case of the initial concentration of 150 µmol L^{-1}, and at 300 min for concentrations of 300 and 500 µmol L^{-1} (Fig. 2a). In treatments with 10 g L^{-1} of N-NH_4^+ the removal reaches 90% in 180 min for the initial

concentrations of 150 and 300 µmol L^{-1} (RM ANOVA, SNK; $p > 0.100$), taking a little longer (300 min) for the concentration of 500 µmol L^{-1} (Fig. 2b). In contrast, for N-NO_3^- treatments, both biomass presented similar removal efficiencies and no significant difference was observed in 60 min (RM ANOVA, SNK; $p > 0.600$) (Fig. 2c, d). For 6 g L^{-1}, removal efficiencies above 90% were only observed at 1440 min with 150 and 500 µmol L^{-1} and at 420 min with 300 µmol L^{-1} (RM ANOVA, SNK; $p > 0.900$) (Fig. 2c). In a similar manner, when biomass density was 10 g L^{-1} this removal efficiency was only reached after 1440 min (RM ANOVA, SNK; $p > 0.700$) (Fig. 2d).

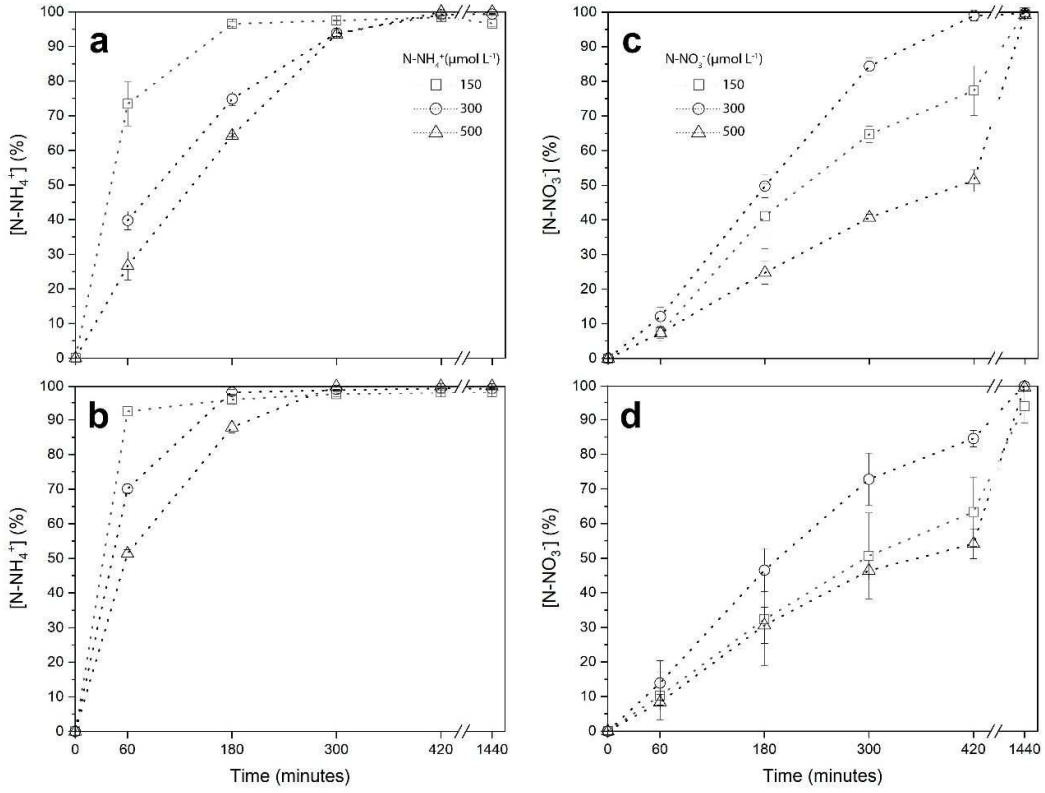

Figure 2. NH_4^+ and NO_3^- removal efficiency – NUE (%) by *U. pseudorotundata* over 1440 min of incubation under different nutrient initial concentrations. (a) NH_4^+ with 6 g FW L^{-1}; (b) NH_4^+ with 10 g FW L^{-1}; (c) NO_3^- with 6 g FW L^{-1}; (d) NO_3^- with 10 g FW L^{-1} of stocking biomass. The data represents the means ± SD for n = 3.

The nutrient uptake rates (NUR) also exhibited different patterns for the different N-sources (Fig. 3, table S5). For N-NH_4^+ values decreased continuously over time for both biomass densities used (Fig. 3a, b). In treatments with 6 g L^{-1} of biomass similar results were showed throughout the experiment for initial concentrations of 150 and 300

µmol L^{-1}, and a decay was observed from a maximum of 149.8 ± 10.0 µmol g^{-1} DW h^{-1} to a minimum of 7.7 ± 0.2 µmol g^{-1} DW h^{-1} between 60 and 1440 min of experiment (Fig. 3a). For initial concentrations of 500 µmol L^{-1} a maximum uptake rate of 180.4 ± 7.3 µmol g^{-1} DW min^{-1} was observed after 60 min and a minimum value of 26.0 ± 0.0 µmol g^{-1} DW h^{-1} was observed at the end of the experiment (Fig. 3a). A similar pattern was observed for treatments with 10 g L^{-1} of biomass (Fig. 3b). The maximum uptake rates occurred after the first 60 min of the experiment for concentrations of 500 µmol L^{-1} (193.0 ± 4.2 µmol g^{-1} DW h^{-1}), followed by concentrations of 300 µmol L^{-1} and 150 µmol L^{-1} (106.4 ± 2.5 µmol g^{-1} DW min^{-1}) (Fig. 3b). At the end of the experiment, the uptake rate decreased to minimum levels of 4.7, 9.4 and 15.6 µmol g^{-1} DW h^{-1}, respectively for the three initial concentrations used.

In contrast, the uptake rate of cultures treated with N-NO_3^- showed a different trend. The values in the initial 60 min were low when compared to the treatments with N-NH_4^+ (14.3 ± 3.7 µmol g^{-1} DW h^{-1} in cultures with 150 µmol L^{-1} and 45.6 ± 0.19 µmol g^{-1} DW h^{-1} in cultures with 300 and 500 µmol L^{-1}), increasing a little between 180 and 300 min, decreasing again thereafter (Fig. 3c, d). The values did not show statistical differences among the factors: nutrient's initial concentrations, biomass densities, and time (RM ANOVA: N-NO_3^- = $F(8) = 1.41$, $p = 0.21$). For cultures with biomass density of 6 g L^{-1}, N-NO_3^- uptake rate rose initially from 60 min to 180 min, with small variation in values up to 300 min, decreasing progressively until the end (1440 min) (Fig. 3c). Maximum value of 63.3 ± 1.8 µmol g^{-1} DW h^{-1} was reached at 180 min by the treatment with 300 µmol L^{-1} (Fig. 3c). For cultures with 10 g L^{-1} of biomass, the N-NO_3^- uptake rate occurred at an almost constant rate (between 12.3 ± 5.1 and 10.3 ± 1.7 µmol g^{-1} DW h^{-1}) in incubations with 150 µmol L^{-1}, decreasing at the end to 4.4 ± 0.2 µmol g^{-1} DW h^{-1} (Fig. 3d). In incubations with 300 and 500 µmol L^{-1} of N-NO_3^- the maximum uptake rates occurred after 180 min reaching values of 35.0 ± 4.8 and 38.4 ± 6.6 µmol g^{-1} DW h^{-1}. At the end of the experiment, the same treatments decreased to 9.4 and 15.6 µmol g^{-1} DW h^{-1}, respectively.

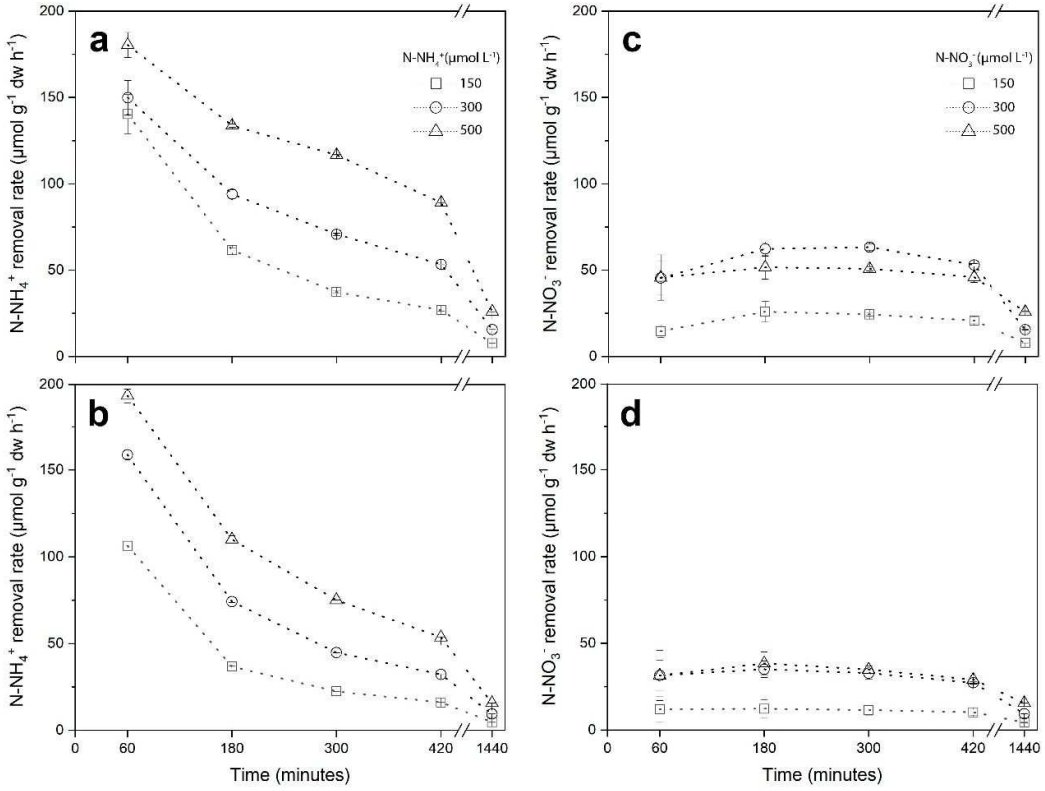

Figure 3. NH_4^+ and NO_3^- uptake rates - NUR (µmol g^{-1} DW h^{-1}) by *U. pseudorotundata* over 1440 min of incubation under different nutrient initial concentrations. (a) NH_4^+ with 6 g FW L^{-1}; (b) NH_4^+ with 10 g FW L^{-1}; (c) NO_3^- with 6 g FW L^{-1}; (d) NO_3^- with 10 g FW L^{-1} of stocking biomass. The data represents the means ± SD for n = 3.

Photosynthetic performance

In-situ estimation of Electron Transport Rate

Photosynthetic Electron Transport Rates (ETR) through PSII measured *in situ* (Fig. 4) were significantly affected by the interaction of N-source, nutrient concentrations, and time (ANOVA: $F(2) = 13.74$, $p < 0.001$). Then, considering this interaction, a significant decay on ETR_{situ} was verified in the concentrations of 150 and 300 µmol L^{-1} from 15 min to 1440 min using N-NH_4^+ as a source of nutrient (ANOVA, SNK; $p < 0.001$). For N-NO_3^-, in the same time interval, a decay on ETR_{situ} was observed for the concentration of 300 µmol L^{-1} (ANOVA, SNK; $p < 0.001$) and no statistical difference was observed for treatments of 150 µmol L^{-1} (ANOVA, SNK; $p = 0.09$) and 500 µmol L^{-1} (ANOVA, SNK; $p = 0.13$).

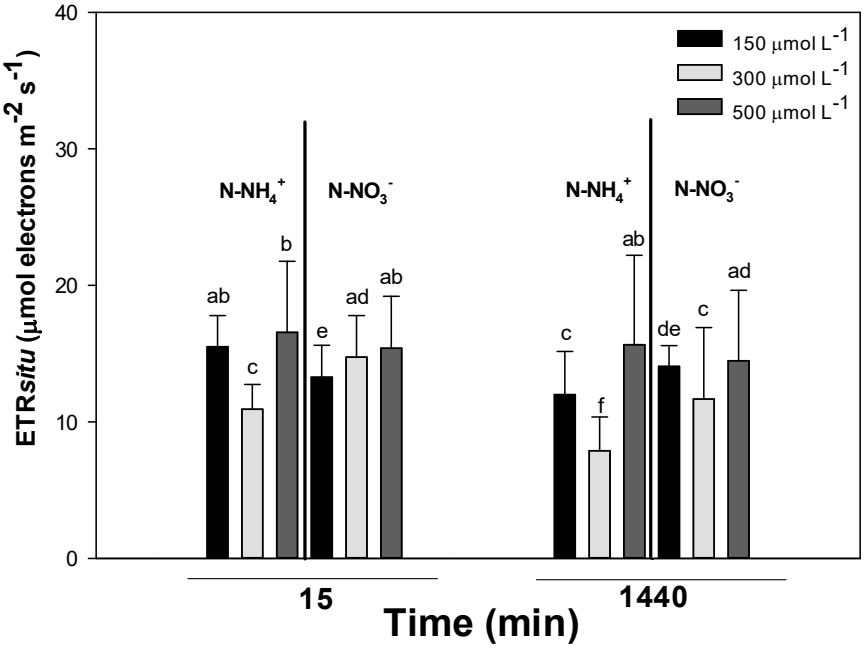

Figure 4. *In situ* electron transport rate (ETR_{situ}) expressed as µmol electrons m^{-2} s^{-1} of *U. pseudorotundata* after 15 and 1440 min cultivated in NH_4^+ and NO_3^- under different concentrations: 150, 300, and 500 µmol L^{-1}. The figure represent only conditions where significant factor effects were detected by multifactorial ANOVA (*biomass density:nutrient source:nutrient's initial concentrations:incubation time*). Bars are means ± SD; different letters indicate statistically significant ($p < 0.05$) of differences for n = 5.

Ex-situ rapid light-responses curves

The maximal quantum yield (F_v/F_m), which is used as a sensitive indicator of seaweed photosynthetic performance, was significantly affected (ANOVA: $F_v/F_m = F(6) = 3.58$, $p < 0.05$) by the interaction among *U. pseudorotundata* biomass density, nutrient concentrations and time, but no significant difference (ANOVA, $F(6) = 0.87$, $p = 0.52$) was found between the different N-source treatments (Fig. 5). The F_v/F_m significantly decreased after 420 min of experiment just for cultures with 6 g L^{-1} of biomass, cultivated on 150 µmol L^{-1} of nutrients. At this point, the minimal value of F_v/F_m observed was 0.35 ± 0.11.

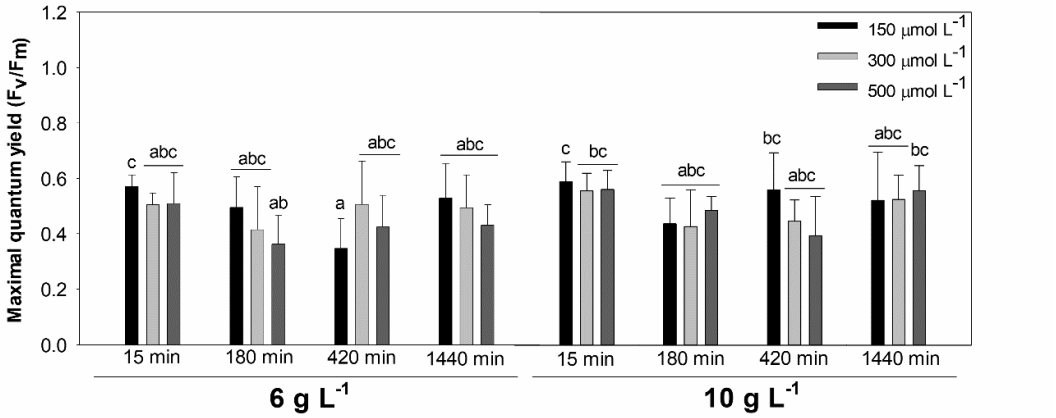

Figure 5. Diurnal changes of maximum quantum yield (F_v/F_m) of *U. pseudorotundata* during 1440 minutes cultivated on two densities of biomass (6 g L^{-1} and 10 g L^{-1}) under different initial concentrations of NH_4^- and NO_3^-: 150, 300, and 500 µmol L^{-1}. The figure represents only conditions where significant factor effects were detected by multifactorial ANOVA (*biomass density:nutrient source*:*nutrient's initial concentrations:incubation time*). Bars are means ± SD; different letters indicate statistically significant ($p < 0.05$) of differences for n = 3.

Maximal electron transport rate (ETR_{max}), described as an indicator of photosynthetic capacity, was influenced by a significant interaction (ANOVA: $F(6) = 6.46$, $p < 0.05$) among N-source, nutrient concentrations and time, but not by biomass density (ANOVA: $F(6) = 0.65$, $p = 0.69$; Fig. 6). In an overview, the ETR_{max} showed the lowest values in the N-NH_4^+ treatments at 15 min of the experiment, although some data at later times, especially among N-NH_4^+ treatments, did not show significant differences.

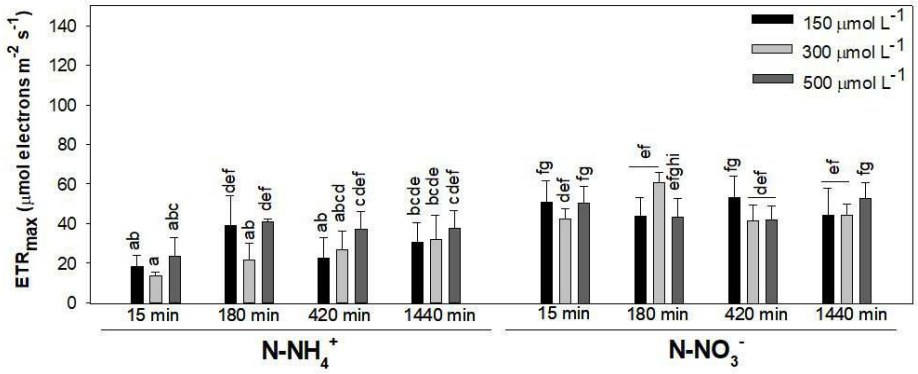

Figure 6. Diurnal changes of maximum electron transport rate (ETR_{max}) measured *ex situ* of *Ulva pseudorotundata* during 1440 minutes in NH_4^+ and NO_3^- on two densities of biomass 6 g L^{-1} and 10 g L^{-1} under different initial concentrations: 150, 300, and 500 µmol L^{-1}. The figure represent only conditions where significant factor effects were detected by multifactorial ANOVA (*biomass density:nutrient source*:*nutrient's initial concentrations:incubation time*). Bars are means ± SD; different letters indicate statistically significant ($p < 0.05$) of differences for n = 3.

The α_{ETR}, considered as a descriptor of photosynthetic efficiency, was significantly affected by the interaction among biomass density, nutrient concentration and time (ANOVA: $\alpha_{ETR} = F(6) = 3.60$, $p < 0.05$) (Fig. 7), but no significantly difference (ANOVA, $p = 0.59$) was found between the different N-source treatments. Data obtained from α_{ETR} showed a slight decrease at evening (420 min) for the treatment 150 µmol L^{-1} and 6 g L^{-1} of biomass.

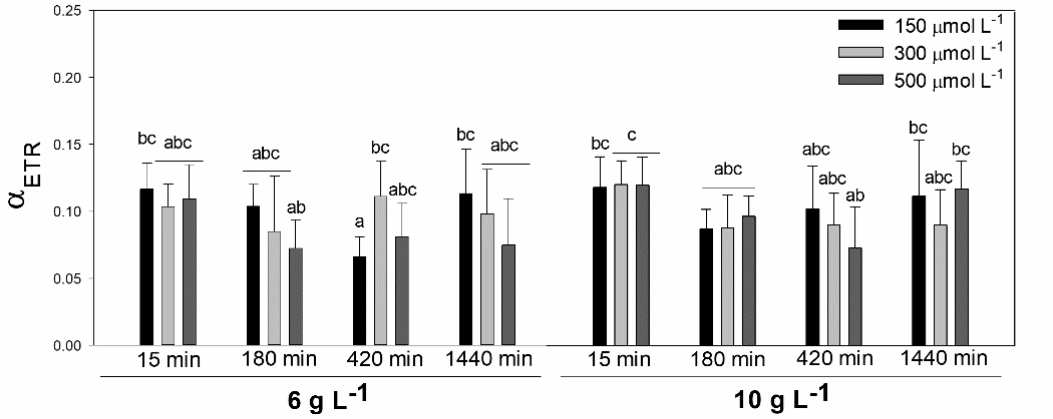

Figure 7. Diurnal changes of photosynthetic efficiency (α_{ETR}) of *Ulva pseudorotundata* during 1440 minutes in NH_4^+ and NO_3^- on two densities of biomass 6 g $L^{-1}$and 10 g L^{-1} under different initial concentrations: 150, 300, and 500 µmol L^{-1}. The figure represent only conditions where significant factor effects were detected by multifactorial ANOVA (*biomass density:nutrient source*:*nutrient's initial concentrations:incubation time*). Bars are means ± SD; different letters indicate statistically significant ($p < 0.05$) of differences for n = 3.

Elemental and biochemical composition

The elemental composition of *U. pseudorotundata* biomass at the initial time of the experiments presented significant variability related to the combined conditions used (significant interaction among the factors nitrogen source, initial nutrient concentration and initial algae biomass) (Table S6, Fig. 8a). Regarding the initial carbon content, the values ranged from 30.7 to 36.5% under N-NH_4^+ and from 32.1 to 35.5% under N-NO_3^-, presenting differences among treatments (ANOVA: $F(2) = 7.0$, $p < 0.05$). However, there was no significant difference in the final carbon values between the treatments, which presented a general average value of 32.3 ± 2.7% (ANOVA: $F(2) = 0.07$, $p = 0.94$, Fig. 8b). Initial nitrogen content also showed differences among treatments (ANOVA: $F(2) = 3.92$, $p < 0.05$, Fig. 8b), but final values showed significant differences only for nitrogen source (ANOVA: $F(1) = 37.02$, $p < 0.05$, Fig. 8b). The initial values ranged from 2.5 to 3.8% in the experiments treated with N-NH_4^+, and from 3.8 to 4.6% in the experiments treated with N-NO_3^-, and the final values were lower in treatments with N-NH_4^+ (3.1% ± 0.5 SD) than for those with N-NO_3^- (4.0% ± 0.4 SD). The initial hydrogen content, in turn, varied significantly between 4.4 and 5.4% for treatments with N-NH_4^+ and between 5.7 and 6.3% for treatments with N-NO_3^- (ANOVA: $F(2) = 10.47$, $p < 0.05$, Fig. 8b). The final values were influenced only by the nitrogen source (ANOVA: $F(1) = 6.62$, $p < 0.05$, Fig. 8b), with lower values for N-NH_4^+ treatments (5.23% ± 0.2 SD) when compared to N-NO_3^- treatments (5.43% ± 0.2 SD). Finally, the C:N ratio also showed significantly different initial values ranging from 9.5 to 14.5 in the treatments with N-NH_4^+ and from 7.8 to 9.2 in the treatments with N-NO_3^- (ANOVA: $F(2) = 7.83$, $p < 0.05$, Fig. 8b). Final values were also influenced by nitrogen source with higher values for N-NH_4^+ treatments (10.9 ± 1.4 SD) when compared to N-NO_3^- treatments (7.9 ± 0.6 SD) (ANOVA: $F(1) = 80.92$, $p < 0.05$, Fig. 8b). Regarding the biochemical composition (Fig. 9, tables S7-S9), the protein content followed the same pattern described above for nitrogen content, since the protein value derives from this variable, with initial values ranging from 13.7 to 20.9% for the treatments with N-NH_4^+ and 20.5 to 25.1% for treatments with N-NO_3^- (ANOVA: $F(2) = 3.92$, $p < 0.05$, Fig. 9a). Final values, were lower for N-NH_4^+ treatments (16.8% ± 2.5 SD) than for N-NO_3^- treatments (22.0% ± 2.2 SD) (ANOVA: $F(1) = 37.02$, $p < 0.05$,, Fig. 9b). The initial carbohydrate concentration was not influenced by the interaction

between nitrogen source, initial nutrient concentration and initial algae biomass, with average values of 36.9 (± 4.4 SD) for treatments with N-NH_4^+ and 31.8 (± 6.0 SD) for treatments with N-NO_3^- (ANOVA: $F(2) = 0.14$, $p = 0.87$, Fig. 9a). At the end, the values were influenced by the interaction between nitrogen source and algal biomass density (ANOVA: $F(1) = 4.94$, $p < 0.05$,), being higher in treatments with N-NH_4^+ (36.83% ± 6.14 SD) than in those treated with N-NO_3^- (29.53% ± 5.34 SD), especially for initial algal biomass of 6 g L^{-1} which reached 38.9% (Fig. 9b).

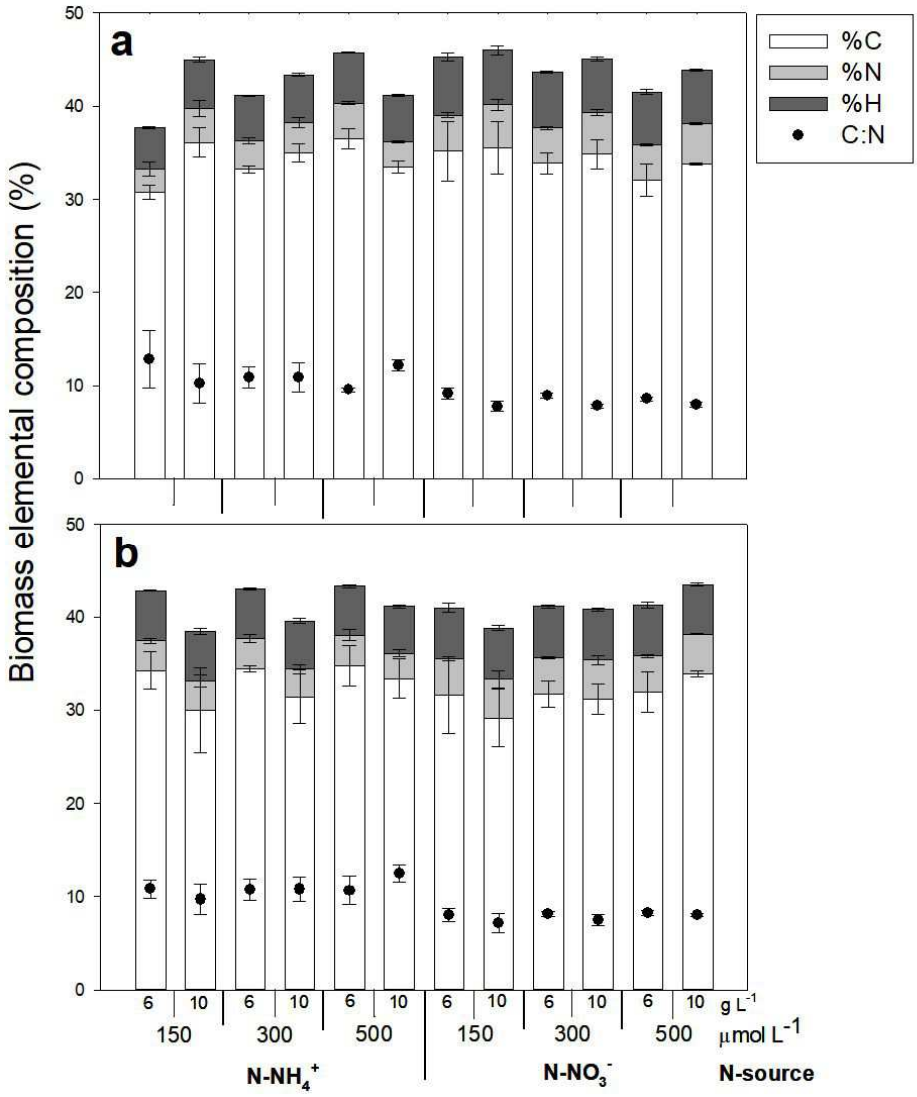

Figure 8. Elemental composition of the dry biomass of *Ulva pseudorotundata* cultivated in different nitrogen sources (NH_4^+ and NO_3^-), nutrient initial concentrations (150, 300 and 500 µmol L^{-1}) and biomass

densities (FW 6 and 10 g L^{-1}). Data are presented as percentage of carbon, nitrogen and hydrogen (CHN) and C:N ratio obtained at initial (a) and final (b) time of the experiments. Values are mean ± SD (n = 3).

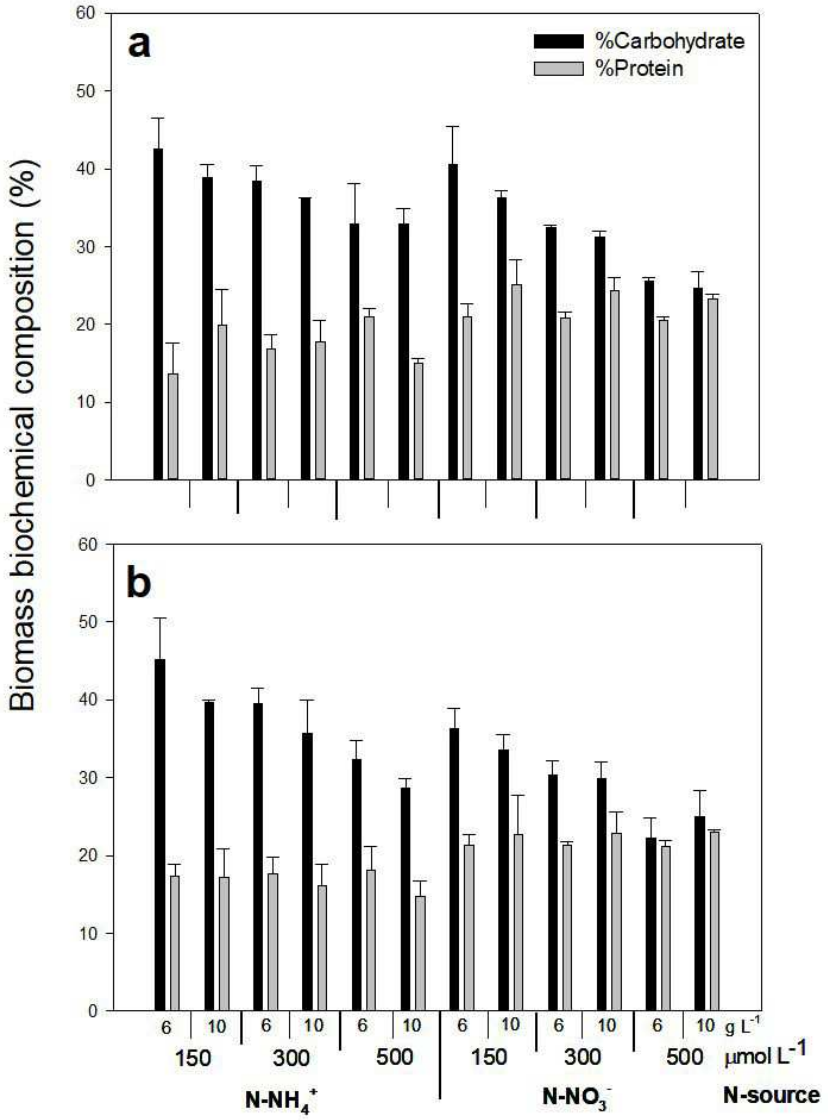

Figure 9. Biochemical composition of the dry biomass of *Ulva pseudorotundata* cultivated in different nitrogen sources (N-NH_4^+ and N-NO_3^-), nutrient initial concentrations (150, 300 and 500 µmol L^{-1}) and biomass densities (FW 6 and 10 g L^{-1}). Data are presented as percentage of carbohydrate and protein obtained at initial (a) and final (b) time of the experiments. Values are mean ± SD (n = 3).

Principal Component Analysis

The PCA showed in an integrated way the main relationships among the variables determined in the experimental tanks. In the presented analysis (Fig. 10) the first principal component explained 58.5% of the variance and the second component 23.3% of the variance. The first component axis clearly showed differences between the treatments with $N\text{-}NH_4^+$ and $N\text{-}NO_3^-$, where the NUR at 60 min and NUE at 180 and at 300 min were the variables with greater load in the treatments with $N\text{-}NH_4^+$ (positive side of component 1). The initial and final C:N ratios also showed greater loads in the first component than in the second, although with low values. In opposition, photosynthetic parameters like ETR_{situ} at 15 and 1440 min, ETR_{max} at 15 min and also initial and final protein contents were higher for $N\text{-}NO_3^-$, treatments (negative side of component 1). In the second principal component, NUR at 144, 180, 300 and 420 min showed high loadings in the positive side of the axis, in opposition with F_v/F_m data and initial and final carbohydrate contents in the negative side of the axis.

Observing Pearson's correlation matrix among these variables (Table S10) it is possible to verify that most of the relationships described above based on PCA, whether positive or negative, are statistically validated ($p < 0.05$), evidencing that the main trends shown in the PCA can be confirmed.

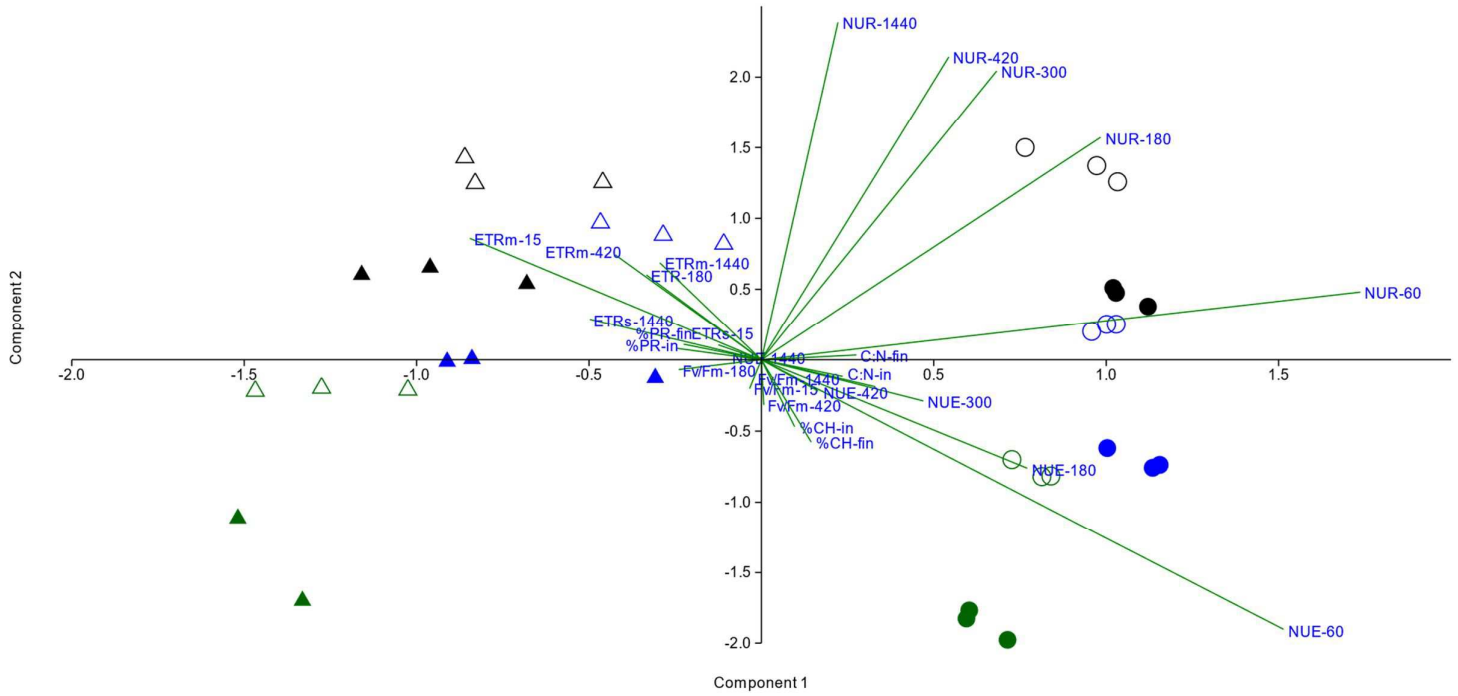

Figure 10. Principal Component Analysis performed with data from nutrient removal experiments by *Ulva pseudorotundata* subjected to two types of nitrogen source (NH_4^+ and NO_3^-). Circles represent NH_4^+ treatments and triangles represent NO_3^- treatments. Empty and filled symbols indicate treatments with 6 g L^{-1} and 10 g L^{-1} of initial biomass, respectively. Symbols in green, blue and black indicate 150, 300 and 500 µmol L^{-1} of nitrogen nutrient, respectively. NUR is nutrient uptake rate, NUE is nutrient uptake efficiency, ETR_s is electron transport rate in situ, ETR_{max} is the maximal electron transport rate, F_v/F_m is the maximal photochemical efficiency of PSII. The numbers associated with these abbreviations are the measurement times in min. C:N is the carbon to nitrogen ratio, %CH is the percentage of carbohydrates and %PR is the percentage of protein, *ini* and *fin* representing initial and final time of the experiment, respectively.

Table 1 Maximal removal efficiency of nutrients by seaweed selected to play a role as biofilter in different types of cultivation.

Species	Type of cultivation	Incubation time	Nutrient source	Nutrient concentrations ($\mu mol.L^{-1}$)	Nutrient uptake efficiency (%)	Reference
Ulva pseudorotundata	outdoor conditions - closed system	5 hours (300 min)	NH_4Cl	500 µmol L^{-1}	> 90% ammonium	Present work
		24 hours (1440 min)	KNO_3	500 µmol L^{-1}	100% nitrate	
Ulva clathrata	outdoor conditions - flow-through system	15 hours	Integrated with shrimp effluent (*Litopenaeus vannamei*)	51 to 60 µmol L^{-1}	82-85%TAN (total ammonia-N)	Copertino et al. (2009)
				< 2.0 µmol L^{-1}	50% phosphate	
Ulva lactuca	outdoor conditions - flow-through system	-	Integrated with fish effluent (*Oreochromis spilurus*)	4.44 µmol L^{-1}	97.54% TAN (total ammonia-N)	Al-Hafedhet al. (2014)
				12 µmol L^{-1}	16.4-24.03% phosphate	
Ulva lactuca	outdoor conditions - flow-through system	-	Integrated with fish effluent (*Haliotis rufescens*)	0.889 ± 0.112 µmol L^{-1}	86-100% ammonium	Macchiavello & Bulboa (2014)
				7.21 ± 0.47 µmol L^{-1}	65-83% nitrate	
				0.97 ± 0.26 µmol L^{-1}	13-65% phosphate	
Ulva ohnoi	laboratory conditions - Algal Turf Scrubber (ATS) system	24 hours (1440 min)	NH_4Cl	182.94 µmol L^{-1}	99.3% ammonium	Salvi et al. (2021)
			$Na_2HPO_4 \cdot 7H_2O$	92.3 µmol L^{-1}	100% phosphate	
Ulva prolifera	laboratory conditions - closed system	48 hours	KNO_3	194.8 ± 9.8 µmol L^{-1}	99.24% nitrate	Fan et al. (2014)
			KH_2PO_4	25.8 ± 0.6 µmol L^{-1}	91.30% phosphate	
Codium fragile	laboratory conditions - closed system	6 hours	NH_4Cl	150 µmol L^{-1}	99.5% ammonium	Kang et al. (2007)
Gracilaria cervicornis	laboratory conditions - closed system	5 hours	NH_4Cl	5 µmol L^{-1}	85.3% ammonium	Carneiro et al. (2011)
			KNO_3	5 µmol L^{-1}	97.5% nitrate	
			KH_2PO_4	5 µmol L^{-1}	81.6% phosphate	
Gracilaria vermiculophylla	laboratory conditions - closed system	4 hours	NH_4Cl	150 µmol L^{-1}	63% ammonium	Abreu et al. (2011a)
			$NaNO_3$	450 µmol L^{-1}	33% nitrate	
Hydropuntia cornea	outdoor conditions - flow-through system	-	Integrated with fish effluent (*Sparus aurata*)	10 to 200 µmol L^{-1}	99.55% TAN (total ammonia-N)	Figueroa et al. (2012)
	indoor conditions - flow-through system			10 to 200µmol L^{-1}	96.23% TAN (total ammonia-N)	
Kappaphycus alvarezii	indoor tanks - flow-through system	-	Integrated with fish effluent (*Trachinotus carolinus*)	4.4±0.8 µmol L^{-1}	70.54% ammonium	Hayashi et al. (2008)
				190.6±23.7 µmol L^{-1}	18.2% nitrate	
				12.6±2.7 µmol L^{-1}	50.84% nitrite	
				15.2±1.7 µmol L^{-1}	26.76% phosphate	

5. DISCUSSION

In the present study we investigated the short-term removal of N-NH_4^+ and N-NO_3^- by *U. pseudorotundata* under different initial nutrient concentrations and biomass densities, monitoring nutrient removal efficiencies, photosynthetic parameters and evaluating biomass characteristics. The results showed that *U. pseudorotundata* cultivated under solar radiation in a land-based pilot scale was efficient in removing N-NH_4^+ and N-NO_3^- even in concentrations as high as 500 μmol L^{-1} ensuring complete water remediation in all experimental conditions tested, although differences were observed depending on the stocking density and type of N-source. Despite the fact that both nutrient sources were extinguished after 1440 min of incubation, N-NH_4^+ was removed more efficiently by *U. pseudorotundata* cultivation. On the other hand, N-NO_3^- was more slowly removed, being completely eliminated only after 1440 min of incubation. This difference in uptake rate was reflected in photosynthesis, where a tendency towards an increase in photosynthetic parameters, especially for maximum electron transport rates (ETR_{max}), was observed when *U. pseudorotundata* was incubated with N-NO_3^-. The biomass characteristics, despite showing some heterogeneity at the beginning of the experiments, were at the end similar between treatments with different nitrogen sources.

Regarding abiotic parameters monitored during the experiments, temperature and irradiance conditions reflected the characteristics of the time of year in which they were carried out (late autumn and beginning of winter in Southern Spain), with some differences between experiments related to meteorological events. As the experiments lasted 24 h (1440 min), there were no large fluctuations in these variables during each experiment. On the other hand, the pH increased throughout the experiments as a result of photosynthetic activity and showed differences related to the nitrogen nutrient source and its initial concentration, with significantly higher values for the treatments with N-NO_3^-. The lower pH values for the ammonium treatments are partially related to the acidic character of the ammonium chloride salt (NH_4Cl), which was used as a source of N-NH_4^+ (BARROSO; PEREIRA; NAHAS, 2006). Potassium nitrate (KNO_3), which was used as source of N-NO_3^- does not have this acidic character resulting in greater increases in the pH of its treatments. In addition, the growth of algae in N-NH_4^+ generates a decrease in pH due to the release of H^+ ions to the medium. In contrast, growth in N-NO_3^- causes an

increase in pH as a function of the release of OH^- ions (COLLOS; HARRISON, 2014; RAVEN; SMITH, 1976).

The two parameters used to evaluate nutrient removal evidenced the efficiency of *U. pseudorotundata* for biofiltration processes. While the NUE considers the relative removal of nutrient by time in a specific experimental unit, the NUR represents the removal by time and by volume of water, normalized by the dry mass of algae. NUE values showed that $N\text{-}NH_4^+$ removal reached about 97% after 300 min (5 h) of experiment, which is within the range of values reported in the literature for other marine algae species (ABREU et al., 2011b; CARNEIRO; FREIRE; MARINHO-SORIANO, 2011; KANG et al., 2008a). Furthermore, these results corroborate those reported for other *Ulva* species grown under lower initial concentrations of $N\text{-}NH_4^+$ (Copertino et al. 2009; Al-Hafedh et al. 2014; Salvi et al. 2021) (Table 1). Regarding $N\text{-}NO_3^-$, *U. pseudorotundata* showed more than 60% of removal efficiency after 420 min when cultivated at initial concentrations of 150 and 300 μmol L^{-1}. An equivalent efficiency in the removal of $N\text{-}NO_3^-$ as the only source of N was observed by (ABREU et al., 2011b) when cultivating *Gracilaria vermiculophylla* with 50 μmol L^{-1} of initial concentration. At the end of the experiment (24h) the removal of $N\text{-}NO_3^-$ reached up to 90% in the three initial concentrations tested. Contrasting results were described by Fan et al. (2014) in experiments with *U. prolifera* cultured with 503 μmol L^{-1} of initial concentration $N\text{-}NO_3^-$ showing a maximum of 36.24% removal at the end of the experiment (48h).

Biomass stock density is a critical factor for biofiltration systems as it has a direct influence on nutrient uptake efficiency (AL-HAFEDH; ALAM; BUSCHMANN, 2014; COHEN; NEORI, 1991; MAO et al., 2009). For $N\text{-}NH_4^+$, the removal rate by *U. pseudorotundata* was influenced by stocking densities, that is, the reduction in $N\text{-}NH_4^+$ concentrations occurred faster when the biomass density was higher. This trend is in agreement with studies carried out with other species, but which used similar biomass stocks, as is the case of *U. lactuca* (COHEN; NEORI, 1991), *G. vermiculophylla* (ABREU et al., 2011a), *G. chilensis* and *U. lactuca* (MACCHIAVELLO; BULBOA, 2014). However, Abreu et al. (2011b) and Macchiavello and Bulboa (2014) observed values of nutrient uptake inversely proportional to stocking densities, while Cohen and Neori (1991) did not observe significant differences. Of course, other factors can also explain these differences, such as crop irradiance, temperature, aeration, genotypic and

phenotypic aspects and physiological status of the species and even the shape of the culture tank.

The fast removal efficiency (NUE) of $N\text{-}NH_4^+$ by *U. pseudorotundata* is reflected in the observed values of the $N\text{-}NH_4^+$ uptake rates (NUR). The NUR obtained for $N\text{-}NH_4^+$ was nonlinear in time and exhibited three distinct phases. First, a strong removal was observed during the first 180 min of experiment on both biomass densities and could be explained by the term "surge uptake" (ROLEDA; HURD, 2019) as a mechanism of fast uptake of a nutrient over a short period of time. Second, a relatively constant phase was observed between 180 and 420 min, followed by a decrease as a third phase. The similar surge uptake of $N\text{-}NH_4^+$ was also reported by Salvi et al. (2021) for *U. ohnoi* in the first 15 min of incubation time. In laboratory experiments with *U. lactuca*, Pedersen (1994) previously described the three uptake rate phases as observed in the present study, and the period of surge uptake of $N\text{-}NH_4^+$ was observed between 10-60 min. In contrast, different patterns were observed in treatments with $N\text{-}NO_3^-$. We verified an increasing uptake rate until 300 min of experiment, followed by a decreasing trend. Similar results were noticed for *U. prolifera* which showed a saturated uptake rate for $N\text{-}NO_3^-$ with a maximum of 28.4 ± 1.7 μmol g^{-1} DW h^{-1} in an initial concentration of 195 μmol L^{-1} (FAN et al., 2014). In this case, the authors considered that external $N\text{-}NO_3^-$ concentrations were high enough to fill the intracellular N pools. Although in our work *U. pseudorotundata* demonstrated a decay on uptake rate under higher concentrations, a complete removal of $N\text{-}NO_3^-$ was observed in 1440 min of experiment, even during dark periods (between 420 and 1440 min) signalizing non-saturated internal N pools with $N\text{-}NO_3^-$ as N source even with 500 μmol L^{-1} as initial concentrations.

The results discussed above indicate that the concentrations of nitrogenous nutrients and the initial algal biomass used in our experiments were not sufficient to saturate or cause negative effects on the physiology of *U. pseudorotundata,* and that the systems can operate with higher algal biomass and nutrient concentrations than those tested, as long as there is no interference to the irradiance distribution. Considering this, it is possible that an improvement in the nutrient removal process can be obtained by manipulating the effluent flow between different algae cultures, alternating periods of starvation with periods of high concentrations.

Ale et al. (2011) described that the uptake of $N\text{-}NH_4^+$ by *U. lactuca* was higher even when $N\text{-}NO_3^-$ and $N\text{-}NH_4^+$ were supplied together, indicating that the nature of

nitrogen uptake by the species was selective. Experiments with organic (urea and glycine) and inorganic (N-NH_4^+ and N-NO_3^-) nitrogenous nutrients showed that *U. prolifera* assimilated N-NH_4^+ faster than N-NO_3^-, and also suggested a more efficient absorption of inorganic nutrients than organic ones. The faster N-NH_4^+ removal compared to N-NO_3^- by *U. pseudorotundata* evidenced in our study can be attributed to the different mechanisms of absorption, assimilation and incorporation of these nutrients in the cell, since NO_3^- has a higher energy requirement for its absorption and assimilation compared to NH_4^+ (PRITCHARD et al., 2015). Our results showed a trend towards higher ETR_{max} values in treatments with N-NO_3^-, which indicates a greater flow of electrons from photosynthesis necessary for the process of reducing NO_3^- to NH_4^+, and then to amino acids and proteins.

Photosynthetic parameters can be used to evaluate the physiological status of seaweed cultivation related to multiple factors of system conditions e.g. temperature, aeration, light irradiance and nutrient supply (Figueroa et al. 2006, Figueroa et al. 2009, Shahar et al. 2020). In respect to maximal quantum yield of PSII (F_v/F_m), our results showed that this parameter, which indicates the maximal algal photosynthetic efficiency, was not influenced by nitrogen source. However, nutrient concentrations, biomass densities and the period of the day contributed to statistical differences. Distinct results were obtained with *U. fasciata* cultivated with N-NO_3^- and total ammonium nitrogen (TAN) in which F_v/F_m was affected by the nitrogen source (SHAHAR et al., 2020). In that study, *U. fasciata* was described to present higher F_v/F_m when cultivated with N-NO_3^-, and the authors justify the lower photosynthetic activity in cultures supplied with TAN than N-NO_3^- due to a possible toxicity of the free NH_3^+. In our case no difference in F_v/F_m was observed between treatments with the two different types of N-source, suggesting no toxicity response at the tested conditions.

When cultivated in IMTA systems algae are subjected to considerable variations in the luminous environment which can lead to photoinhibition and photochemical damage. Photoinhibition mechanisms, recognized as a reversible interruption of the photosynthetic electron transport chain to protect seaweed against overexposure to solar radiation (MAXWELL; JOHNSON, 2000), are usually observed in photosynthetic studies, when F_v/F_m is monitored along the day (FIGUEROA et al., 2020). F_v/F_m usually decreases in periods of higher photosynthetically active radiation (PAR), signalizing photoinhibition and increased energy dissipation (FIGUEROA et al., 2020). In this

study, however, this variation did not exhibit a marked depression during the afternoon (between 180 and 420 min of experiment) suggesting that the maximum quantum yield, also considered a stress indicator, was not influenced by the different nitrogen sources. Although our cultures were not exposed to high ambient irradiance since it was winter time with cloudy days, the minimal values of F_v/F_m were observed in cultures with 150 µmol L^{-1} and 6 g L^{-1} of biomass indicating that low algal biomass densities and nitrogen concentrations caused photoinhibition on *U. pseudorotundata*. This corroborates the results obtained by Huovinen et al. (2006) who observed that in treatments with N-NH_4^+, the recovery responses of *Grateloupia lanceola* were modified as a function of the nutrient concentration. Moreover, under higher ammonium concentrations (300 µmol L^{-1}) the cultures improved the mechanisms of recovery against high irradiance. In this way Korbee et al. (2005) pointed out that under N-limited conditions, seaweed physiological mechanisms, such as photosynthetic capacity and photoprotection, could be affected. Also, Henley et al. (1991) described that under N-NO_3^- supply *U. rotundata* reduced photoinhibition at noon during daily cycles suggesting that greater nitrogen availability make the algae more resilient to these negative effects. In this sense, the monitoring of F_v/F_m could be an applicable information to avoid photochemical damage when, for example, seaweed is cultivated in conditions under low fluxes of nutrients or starvation conditions in order to improve the efficiency of nutrients removal from mariculture farm effluents.

The elemental and biochemical composition of the biomass was determined to verify if the treatments, even in short-time (24h), would induce detectable changes, either among different treatments or between the initial and final times. The protein content values obtained for *U. pseudorotundata* (general average = 19.7%) were similar to those reported in the literature for other species (BIKKER et al., 2016; CASTRO-GONZÁLEZ et al., 1996; LAKSHMI et al., 2020), and the carbohydrate content (general average = 33.8%) was slightly higher than those mentioned by other authors. Also, the biomass presented greater heterogeneity in the elemental and biochemical composition in the initial experimental times, presenting itself with more homogeneous characteristics at the end of the experiments. The initial heterogeneity is probably associated with small differences in the biomass characteristics of the algae used as inoculum, since they may have come from different culture ponds. This result may be indicating that the algae physiology progresses towards a homogenization of the composition, even with varying

conditions. However, this hypothesis must be evaluated with reservations, since the experimental time of only 24 h may not have been enough to consolidate responses of the varied conditions on the algae composition.

An important point to be considered is that part of the $N\text{-}NH_4^+$ removed from the respective treatments may have been eliminated from the liquid medium by volatilization and not necessarily incorporated into the biomass. This situation is possible due to the increase in pH related to photosynthesis, associated with the aeration of the tanks. Ammonium (NH_4^+) can be converted to non-ionized ammonia (NH_3), which is volatile and even toxic to fish and other organisms. The relative concentration of each form is strongly dependent on pH and, to a lesser extent, on temperature and salinity. Under typical seawater conditions (pH 8.0 and 20°C) there is only about 10% ammonia. As the pH increases, the ammonia concentration increases dramatically. The proportion of unionized ammonia increases 10-fold for each unit increase in pH and 2-fold for each 10°C increase in temperature in the 0-30°C range (Erickson, 1985). Thus, considering the volatility of ammonia, there can be significant losses in tanks where algal photosynthesis promotes increases in pH, especially if there is aeration (Collos and Harrison, 2014). The pH of the tanks, although not continuously monitored, showed a considerable increase at the end of the experiments. As there was intense aeration, the probability of NH_3 losses, reflecting a reduction of dissolved NH_4^+ is very high. In a context of bioremediation, however, the effect of algal photosynthesis would be, in any case, contributing to the reduction of dissolved nitrogen, which would be partially assimilated by the biomass and partially volatilized. The lost of ammonium due to variation of seawater pH and temperature was reported in the green microalga *Chlorella fusca* grown in freshwater enriched by centrate (PERALTA; JEREZ; FIGUEROA, 2019).

Although not all results regarding photosynthetic parameters have showed significant differences between treatments with $N\text{-}NH_4^+$ and $N\text{-}NO_3^-$, the principal component analysis showed in an integrated way the important trends mentioned above, facilitating the understanding of the relationships among data. The $N\text{-}NH_4^+$ and $N\text{-}NO_3^-$ treatments were distributed on opposite sides of the principal components plane, especially on the first axis. $N\text{-}NO_3^-$ treatments were generally positively associated with ETR_{max} values, but also with protein content and some other photosynthetic parameters, while $N\text{-}NH_4^+$ treatments were positively associated with NUE values. Such results show

that the monitoring of photosynthetic parameters in algae based nutrient removal systems produces a good, fast and practical physiological diagnosis of the algae, allowing, eventually, to verify if the algae are using NH_4^+ or other forms of nitrogen that demand more energy to absorption and assimilation. This can help, for example, in the management of systems with regard to greater exposure of the cultivation tanks to light, or the harvesting of surplus biomass to reduce self-shading.

Concluding remarks

Our pilot scale experiments demonstrated that *U. pseudorotundata* rapidly removed more than 98% of $N\text{-}NH_4^+$ in different initial concentrations and biomass densities suggesting a certain versatility of this alga with regard to possible variations in these parameters – typical situations found in effluent remediation systems. In respect to $N\text{-}NH_4^+$, the best performance was obtained with initial biomass of 10 g L^{-1} and initial concentrations up to 300 µmol L^{-1}. Using $N\text{-}NO_3^-$ as N-source, a removal efficiency above 93% required 24 h. In the reality of effluents from marine fish farming, for example, both nitrogen sources, in addition to others, will be present, with $N\text{-}NH_4^+$ being absorbed (and also volatilized) more quickly, and $N\text{-}NO_3^-$ more slowly, acting as a nutrient for long-term maintenance of algae (PRITCHARD et al., 2015). If, on the one hand, algal photosynthesis raises the pH and makes more ammoniacal nitrogen available in the form of non-ionized ammonia, on the other hand, the absorption capacity of algae and the volatilization forced by aeration can compensate for this increase, reducing the risk of ammonia toxicity for fish. As for other *Ulva* species, the biomass produced has a number of uses, including feed for the fish themselves in a circular system (BIKKER et al., 2016).

The monitoring of photosynthetic parameters by PAM fluorescence in parallel with the determination of nutrient removal parameters allowed to verify, in a practical and sensitive way, that the uptake and assimilation of $N\text{-}NO_3^-$ demands more energy than in the case of $N\text{-}NH_4^+$. Since the PAM fluorescence data allow us to estimate the energy transfer efficiency of the PSII, the results obtained in this study also contributes to elucidate seaweed photosynthesis performance by *in situ* and *ex situ* measurements from a cultivation under environmental growing conditions. This greater demand for light energy for uptake and assimilation of $N\text{-}NO_3^-$ in relation to $N\text{-}NH_4^+$ suggests different managements in culture and/or remediation systems with regard to biomass density to be

used, timing of harvesting of the grown biomass and other aspects that influence the luminous environment of cultivation or remediation systems.

When practiced inland, IMTA systems could vary in terms of systems design and scale. The results obtained in the present study could be applied for systems in which the effluent flows between different algae cultures, alternating periods of starvation with periods of high concentrations. In this scenario, while a tank will receive effluent, the other one can be maintained under starvation conditions in order to increase the efficiency of nutrient removal from fish farm effluents. Moreover, we concluded that *U. pseudorotundata* can be cultivated in effluents coming directly from fish tanks (rich in $N\text{-}NH_4^+$) or receiving effluents from bacterial biofilters, in which $N\text{-}NO_3^-$ may predominate, being possible, if some care and management are considered, the almost total removal of nitrogen nutrients in a period of 24 h.

Finally, our data qualify *U. pseudorotundata*, a species native to the Spanish Mediterranean coast, as another candidate *Ulva* species for managed use in bofiltration of aquaculture effluents, either in land based or in integrated multitrophic aquaculture systems.

6. ACKNOWLEDGMENTS

We sincerely thank the Federal University of Santa Catarina (UFSC) and University of Malaga (UMA), especially the faculty members and technical staff of the Laboratory of Phycology (LAFIC - UFSC), Laboratory of Fotobiología y Biotecnología de Organismos acuáticos (FYBOA - UMA), research center Grice Hutchinson (UMA), and Servicios Centrales de Apoyo a la Investigación (SCAI - UMA) for providing space and resources for this work. We also thank Marta G. Sanchez, Fabian Lopez, David Paniagua, Roberto Abdala, Nathalie K. Peinado, and Ellie Bergstrom for their support and assistance in carrying out experiments, data collection and manuscript revision. Financial resources and scholarships were provided by: Andalusia Government (Spain) in the frame of the Projects (1) FACCO- UMA18-FEDER JA-162 and NAZCA-PY20-00458, Santa Catarina State Foundation for Research and Innovation Support (FAPESC process no 03/2017, Brazil), and Coordination for the Improvement of Higher Education Personnel (CAPES/PRINT process nos. 88887.470102/2019-00, Brazil). We also thanks the Conselho Nacional de Desenvolvimento Científico e Tecnológico (CNPq) for providing Post-Doctoral scholarship to E. O. Bastos (process no. 151637 / 2020-2) and financial support through research grants. This study is part of the Doctoral thesis of the first author to the UFSC Graduate Program in Biotechnology and Bioscience, Santa Catarina, Brazil.

Data availability statement

The datasets generated during and/or analysed during the current study are available from the corresponding author on reasonable request.

Competing Interests

The authors declare have no competing interests as defined by Springer, or other interests that might be perceived to influence the results and/or discussion reported in this paper.

Authors Contribution Statement

Massocato, T., Vega, J., Robles-Carnero, V., Avilés, A., Bonomi-Barufi, J., Rörig, L., and Figueroa, F. participated in the experimental design.
Massocato, T., Vega, J., and Robles-Carnero, V. participated in the experimental execution.
Massocato, T., Vega, J., Robles-Carnero, V., and Avilés, A. dedicated for the chemical analysis.
Massocato, T., Robles-Carnero, V., Bastos, E., Bonomi-Barufi, J., Rörig, L., and Figueroa, F. participated in the execution of statistical analysis and data interpretation.
Massocato, T., Bastos, E., Bonomi-Barufi, J., Rörig, L., and Figueroa, F. wrote, review and editing the manuscript text.
Bonomi-Barufi, J., Rörig, L., and Figueroa, F. supervised and provided funding acquisition.

7. SUPPLEMENTARY MATERIAL

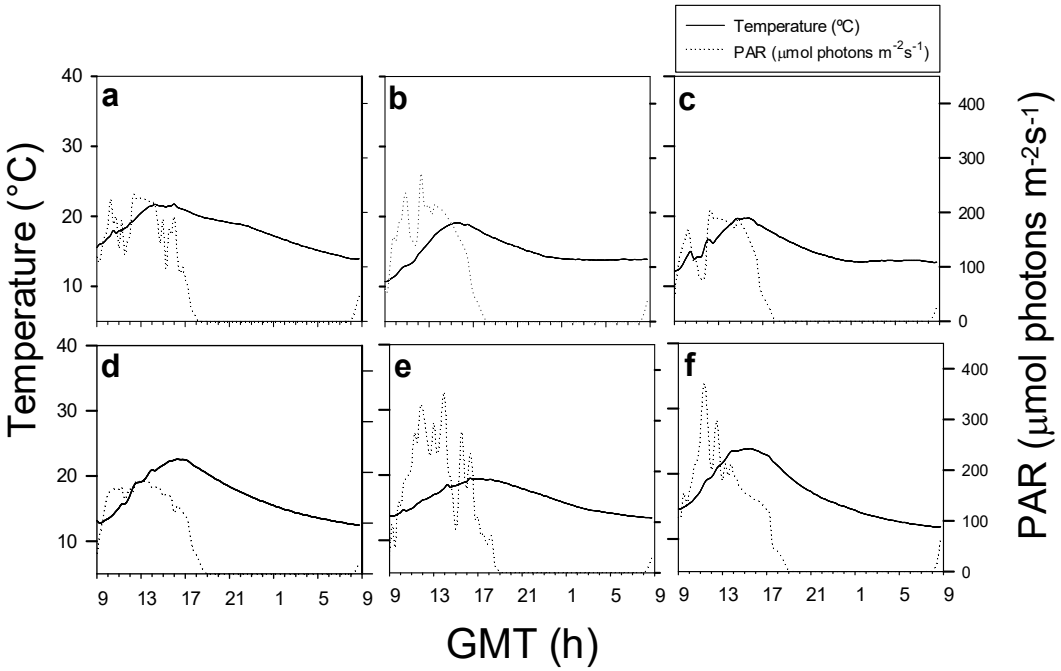

Figure supplementary 1. Temperature (ºC) and PAR: photosynthetically active radiation (µmol photons $m^{-2}s^{-1}$) against experimental period in GMT (h) of *U. pseudorotundata* cultivation in different combinations of nitrogen sources ($N\text{-}NH_4^+$ and $N\text{-}NO_3^-$), biomass densities (6 g L^{-1} and 10 g L^{-1}), and nutrient initial concentrations: 150, 300, and 500 µmol L^{-1}. (a): $N\text{-}NH_4^+$/6 g L^{-1} and 10 g L^{-1}/150 µmol L^{-1}; (b): $N\text{-}NH_4^+$/6 g L^{-1} and 10 g L^{-1}/300 µmol L^{-1}; (c): $N\text{-}NH_4^+$/6 g L^{-1} and 10 g L^{-1}/500 µmol L^{-1}; (d): $N\text{-}NO_3$/6 g L^{-1} and 10 g L^{-1}/150 µmol L^{-1}; (e): $N\text{-}NO_3$/6 g L^{-1} and 10 g L^{-1}/300 µmol L^{-1}; (f): $N\text{-}NO_3$/6 g L^{-1} and 10 g L^{-1}/500 µmol L^{-1}.

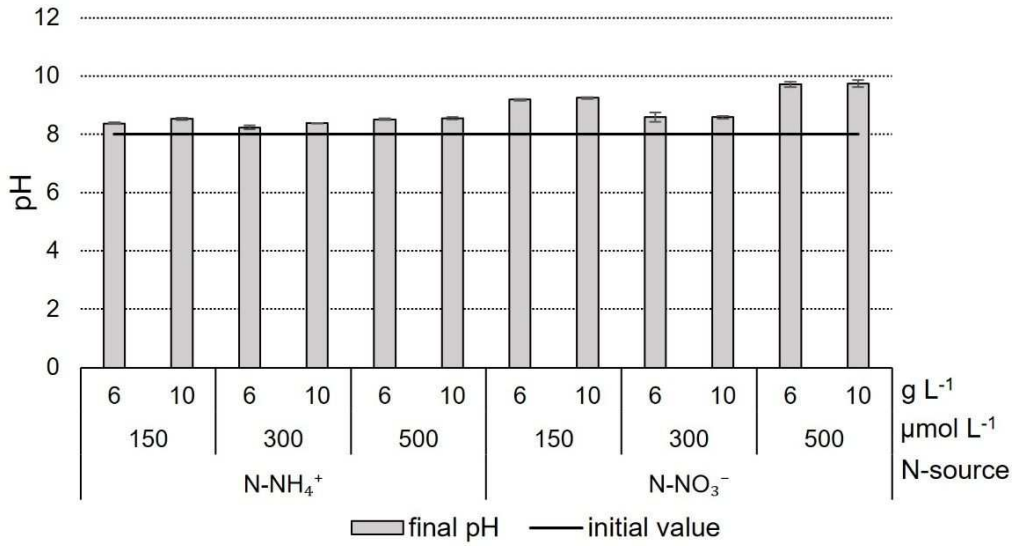

Figure supplementary 2. pH measurements in the end of experiment of *U. pseudorotundata* under different combinations of nitrogen sources (N-NH_4^+ and N-NO_3^-), biomass densities (6 g L^{-1} and 10 g L^{-1}), and nutrient initial concentrations: 150, 300, and 500 µmol L^{-1}. Values are mean ± SD (n = 3).

Table supplementary 1. Multifactorial ANOVA effects for pH measurements in the end of experiment of *U. pseudorotundata* under different combinations of nitrogen sources (N-NH_4^+ and N-NO_3^-), biomass densities (6 g L^{-1} and 10 g L^{-1}), and nutrient initial concentrations: 150, 300, and 500 µmol L^{-1}. *df:* degree of freedom; *F*: F-statistic. The significance differences ($p < 0.05$) are shown in bold.

Source	***df***	***F***	***p***
Nutrient source (1)	1	904.70	0.00
Nutrient's initial concentration (2)	2	254.70	0.00
Biomass density (3)	1	8.00	0.01
(1) x (2)	2	**113.50**	**0.00**
(1) x (3)	1	3.50	0.07
(2) x (3)	2	1.00	0.40
(1) x (2) x (3)	2	0.80	0.46

Table supplementary 2. Results of the post hoc SNK test concerning changes pH measurements in the end of experiment of *U. pseudorotundata* under different combinations of nitrogen sources ($N\text{-}NH_4^+$ and $N\text{-}NO_3^-$) and nutrient initial concentrations: 150, 300, and 500 µmol L^{-1}. Different letters indicate significant differences ($p < 0.05$).

N-source	Nutrient's initial concentration (µmol L^{-1})		
$N\text{-}NH_4^+$	150	8.45 ± 0.01	a
	300	8.31 ± 0.04	c
	500	8.53 ± 0.01	ab
$N\text{-}NO_3^-$	150	9.21 ± 0.01	d
	300	8.59 ± 0.08	b
	500	9.72 ± 0.02	e

Table supplementary 3. Results of the post hoc SNK test concerning changes in concentrations of N-$NH4^+$ and N-NO_3^- at 0, 60, 180, 420, and 1440 minutes considering nutrient's initial concentrations (150, 300, and 500 µmol L^{-1}) and biomass densities (FW 6 g L^{-1} and FW 10 g L^{-1}) *of U. pseudorotundata*. Different letters indicate significant differences ($p < 0.05$).

Nutrient's initial concentration (µmol L^{-1})	Biomass density (FW g L^{-1})	Time (min.)	Nutrient's concentrations							
			$N\text{-}NH_4^+$				$N\text{-}NO_3^-$			
150	6	0	153.02	±	2.64	h	150.57	±	0.60	f
		60	40.74	±	10.14	d	138.85	±	9.32	f
		180	5.28	±	1.05	a	88.32	±	14.13	de
		300	3.85	±	0.49	a	52.95	±	3.61	bc
		420	2.34	±	0.46	a	33.99	±	10.79	b
		1440	5.10	±	1.23	a	0.00	±	0.00	a
	10	0	153.11	±	1.38	h	150.60	±	0.60	f
		60	11.55	±	2.26	ab	134.65	±	10.41	f
		180	6.27	±	1.57	a	101.51	±	25.26	e
		300	3.92	±	1.24	a	74.01	±	18.64	cd
		420	3.12	±	0.37	a	54.95	±	14.91	b
		1440	2.90	±	0.61	a	9.07	±	7.33	a
300	6	0	301.40	±	0.18	k	300.13	±	0.13	i
		60	181.52	±	7.92	i	263.76	±	8.01	h
		180	75.84	±	5.99	f	150.64	±	10.15	f
		300	18.41	±	2.96	b	46.83	±	7.45	b
		420	2.51	±	1.45	a	3.11	±	4.56	a
		1440	1.85	±	0.32	a	1.10	±	1.90	a
	10	0	301.42	±	0.03	k	300.13	±	0.23	i
		60	90.18	±	3.39	g	258.25	±	19.16	h
		180	5.28	±	2.70	a	160.44	±	18.76	f
		300	3.40	±	0.64	a	81.70	±	22.68	de
		420	1.87	±	0.41	a	46.38	±	23.77	bc
		1440	2.05	±	0.70	a	0.00	±	0.00	a
500	6	0	498.88	±	0.12	m	500.05	±	0.09	m
		60	365.84	±	20.39	l	463.47	±	10.61	l
		180	178.13	±	2.29	i	376.22	±	16.28	k
		300	32.40	±	1.36	c	296.72	±	4.99	i
		420	0.00	±	0.00	a	243.05	±	15.96	gh
		1440	0.00	±	0.00	a	4.03	±	6.98	a
	10	0	499.52	±	0.12	m	500.21	±	0.25	m
		60	242.83	±	5.57	j	458.39	±	11.75	l
		180	60.60	±	8.12	e	346.98	±	26.26	j
		300	0.00	±	0.00	a	268.01	±	13.14	h
		420	0.00	±	0.00	a	229.29	±	21.49	g
		1440	0.00	±	0.00	a	1.65	±	1.65	a

Table supplementary 4. Results of the post hoc SNK test concerning nutrient's uptake efficiency (%) of *U. pseudorotundata.* after 60, 180, 420, and 1440 minutes under diferent N-source ($N\text{-}NH_4^+$ and $N\text{-}NO_3^-$) and nutrient's initial concentrations (150, 300, and 500 μmol L^{-1}). Different letters indicate significant differences ($p < 0.05$).

			Nutrient's uptake efficiency							
Nutrient's initial concentration (μmol L^{-1})	Biomass density (FW g L^{-1})	Time (min.)	$N\text{-}NH_4^+$				$N\text{-}NO_3^-$			
150	6	0-60	73.41	±	6.36	f	7.78	±	1.92	a
		0-180	96.55	±	0.71	ijk	41.33	±	9.49	cd
		0-300	97.48	±	0.10	ijk	64.83	±	2.53	ef
		0-420	98.47	±	0.33	k	77.43	±	7.18	gh
		0-1440	96.66	±	0.85	ijk	100.00	±	0.00	j
	10	0-60	92.45	±	1.52	h	10.60	±	6.66	a
		0-180	95.91	±	1.01	hijk	32.57	±	13.40	bc
		0-300	97.44	±	0.79	ijk	50.82	±	12.57	d
		0-420	97.96	±	0.24	jk	63.49	±	10.05	e
		0-1440	98.11	±	0.38	k	93.96	±	4.88	ij
300	6	0-60	39.77	±	2.64	b	12.12	±	2.65	a
		0-180	74.84	±	1.98	f	49.81	±	3.36	d
		0-300	93.89	±	0.98	hij	84.40	±	2.48	hi
		0-420	99.17	±	0.48	k	98.96	±	1.52	j
		0-1440	99.39	±	0.11	k	99.63	±	0.63	j
	10	0-60	70.08	±	1.12	e	13.95	±	6.45	a
		0-180	98.25	±	0.89	k	46.54	±	6.29	d
		0-300	98.87	±	0.20	k	72.77	±	7.57	eg
		0-420	99.38	±	0.14	k	84.55	±	2.35	h
		0-1440	99.32	±	0.23	k	100.00	±	0.00	j
500	6	0-60	26.67	±	4.08	a	7.32	±	2.11	a
		0-180	64.29	±	0.47	d	24.76	±	3.26	b
		0-300	93.50	±	0.27	hi	40.66	±	0.99	cd
		0-420	100.00	±	0.00	k	51.40	±	3.20	d
		0-1440	100.00	±	0.00	k	99.19	±	1.40	j
	10	0-60	51.39	±	1.11	c	8.36	±	2.39	a
		0-180	87.87	±	1.62	g	30.63	±	5.27	bc
		0-300	100.00	±	0.00	k	46.42	±	2.64	d
		0-420	100.00	±	0.00	k	54.16	±	4.30	df
		0-1440	100.00	±	0.00	k	99.67	±	0.33	j

Table supplementary 5. Results of the post hoc SNK test concerning nutrient's uptake rate (g^{-1} DW h^{-1}) of *U. pseudorotundata.* after 60, 180, 420, and 1440 minutes under diferent N-source ($N\text{-}NH_4^+$ and $N\text{-}NO_3^-$) and nutrient's initial concentrations (150, 300, and 500 µmol L^{-1}). Different letters indicate significant differences ($p < 0.05$).

Nutrient's initial concentration (µmol L^{-1})	Biomass density (FW g L^{-1})	Time (min.)	Nutrient's uptake rate $N\text{-}NH_4^+$				$N\text{-}NO_3^-$			
150	6	0-60	140.35	±	11.42	p	14.65	±	3.67	ac
		0-180	61.56	±	1.35	j	25.94	±	6.01	c
		0-300	37.29	±	0.68	g	24.41	±	1.05	c
		0-420	26.91	±	0.55	ef	20.82	±	1.94	ac
		0-1440	7.70	±	0.18	a	7.84	±	0.03	bd
	10	0-60	106.44	±	2.52	m	11.99	±	7.49	ab
		0-180	36.80	±	0.39	g	12.30	±	5.09	abc
		0-300	22.43	±	0.03	de	11.52	±	2.89	ab
		0-420	16.11	±	0.14	bc	10.27	±	1.67	ab
		0-1440	4.71	±	0.02	a	4.43	±	0.25	d
300	6	0-60	149.85	±	10.02	q	45.46	±	9.93	ac
		0-180	93.98	±	2.47	l	62.29	±	4.17	c
		0-300	70.75	±	0.69	k	63.33	±	1.83	c
		0-420	53.37	±	0.23	i	53.04	±	0.82	ac
		0-1440	15.60	±	0.01	bd	15.57	±	0.10	bd
	10	0-60	158.83	±	2.52	r	31.49	±	14.58	ab
		0-180	74.22	±	0.67	k	35.01	±	4.76	abc
		0-300	44.81	±	0.09	h	32.85	±	3.44	ab
		0-420	32.18	±	0.05	fg	27.26	±	0.76	ab
		0-1440	9.38	±	0.02	ac	9.40	±	0.01	d
500	6	0-60	180.37	±	7.31	s	45.74	±	13.18	ac
		0-180	133.65	±	1.01	o	51.60	±	6.80	c
		0-300	116.62	±	0.33	n	50.83	±	1.24	c
		0-420	89.09	±	0.02	l	45.89	±	2.86	ac
		0-1440	25.98	±	0.01	ef	25.83	±	0.37	bd
	10	0-60	193.00	±	4.15	t	31.44	±	8.99	ab
		0-180	110.00	±	2.03	m	38.40	±	6.62	abc
		0-300	75.12	±	0.02	k	34.92	±	1.99	ab
		0-420	53.65	±	0.01	i	29.10	±	2.31	ab
		0-1440	15.65	±	0.00	bc	15.62	±	0.05	d

Table supplementary 6. Results of the post hoc SNK test concerning elemental composition of dried *U. pseudorotundata* biomass before cultivation in different combinations of nitrogen sources ($N\text{-}NH_4^+$ and $N\text{-}NO_3^-$), biomass densities (6 g L^{-1} and 10 g L^{-1}), and nutrient initial concentrations: 150, 300, and 500 µmol L^{-1}. Content of the parameters: carbon (C), nitrogen (N), and hydrogen (H) are presented as their percentage of alga biomass. C:N ratio was obtained from the measurements of %C and %N. Values are mean (± SD), n = 3. Letters represent statistical differences ($p < 0.05$, SNK).

Nutrient source	Nutrient's initial concentration (µmol L^{-1})	Biomass density (g L^{-1})	%C	%N	%H	C:N
$N\text{-}NH_4^+$	150	6	30.75 ± 0.76 b	2.51 ± 0.72 d	4.42 ± 0.08 e	14.47 ± 1.09 d
		10	36.09 ± 1.59 a	3.65 ± 0.85 abc	5.26 ± 0.28 ad	10.20 ± 2.13 abc
	300	6	33.21 ± 0.38 ab	3.08 ± 0.35 ad	4.84 ± 0.07 d	10.88 ± 1.19 bc
		10	34.96 ± 0.98 ab	3.27 ± 0.50 acd	5.13 ± 0.18 d	10.85 ± 1.61 bc
	500	6	36.50 ± 1.06 a	3.83 ± 0.20 abc	5.41 ± 0.09 abd	9.53 ± 0.23 ab
		10	33.45 ± 0.63 ab	2.76 ± 0.09 ad	4.95 ± 0.07 d	12.15 ± 0.59 c
$N\text{-}NO_3^-$	150	6	35.20 ± 3.20 a	3.85 ± 0.31 abc	6.26 ± 0.40 c	9.16 ± 0.61 ab
		10	35.57 ± 2.80 a	4.61 ± 0.59 b	5.84 ± 0.50 abc	7.76 ± 0.53 a
	300	6	33.87 ± 1.14 ab	3.81 ± 0.16 abc	6.01 ± 0.13 bc	8.90 ± 0.28 ab
		10	34.82 ± 1.62 ab	4.47 ± 0.32 b	5.80 ± 0.24 abc	7.81 ± 0.25 a
	500	6	32.10 ± 1.73 ab	3.76 ± 0.09 abc	5.67 ± 0.26 abc	8.54 ± 0.25 ab
		10	33.82 ± 0.11 ab	4.27 ± 0.12 bc	5.75 ± 0.11 abc	7.92 ± 0.24 a

Table supplementary 7. Results of the post hoc SNK test concerning carbohydate composition of dried *U. pseudorotundata* biomass before cultivation in different combinations of nitrogen sources (N-NH_4^+ and N-NO_3^-), biomass densities (6 g L^{-1} and 10 g L^{-1}), and nutrient initial concentrations: 150, 300, and 500 µmol L^{-1}. Since ANOVA results did not indicated significant interaction between factors we represented the results for each factor: nitrogen sources, biomass densities, and nutrient initial concentrations. Values are mean (± SD), n = 3. Letters represent statistical differences ($p < 0.05$, SNK).

%Carb.				
N-source				
	NO_3^-	31.77	± 4.35	a
	NH_4^+	36.95	± 6.03	b
Nutrient's initial concentration (µmol L^{-1})				
	500	29.01	± 8.64	a
	300	34.53	± 7.98	b
	150	39.54	± 6.94	c
Biomass density (g L^{-1})				
	10	33.32	± 4.86	a
	6	35.40	± 6.60	b

Table supplementary 8. Results of the post hoc SNK test concerning carbohydate composition of dried *U. pseudorotundata* biomass at the end of experiment cultivated in different combinations of nitrogen sources (N-NH_4^+ and N-NO_3^-), biomass densities (6 g L^{-1} and 10 g L^{-1}), and nutrient initial concentrations: 150, 300, and 500 µmol L^{-1}. Values are mean (± SD), n = 3. Letters represent statistical differences ($p < 0.05$, SNK).

Nutrient source	Biomass density (g L^{-1})	%Carb.			
N-NO_3^-	10	29.47	±	4.35	a
	6	29.59	±	6.45	a
N-NH_4^+	10	34.69	±	5.34	b
	6	38.97	±	6.42	c

Table supplementary 9. Results of the post hoc SNK test concerning protein composition of dried *U. pseudorotundata* biomass before cultivation in different combinations of nitrogen sources ($N\text{-}NH_4^+$ and $N\text{-}NO_3^-$), biomass densities (6 g L^{-1} and 10 g L^{-1}), and nutrient initial concentrations: 150, 300, and 500 µmol L^{-1}. Values are mean (± SD), n = 3. Letters represent statistical differences ($p < 0.05$, SNK).

Nutrient source	Nutrient's initial concentration (µmol L^{-1})	Biomass density (g L^{-1})	%Prot.			
$N\text{-}NH_4^+$	150	6	13.70	±	3.92	d
		10	19.92	±	4.62	abc
	300	6	16.78	±	1.92	ad
		10	17.82	±	2.72	acd
	500	6	20.89	±	1.09	abc
		10	15.03	±	0.51	ad
$N\text{-}NO_3^-$	150	6	20.97	±	1.71	abc
		10	25.12	±	3.24	b
	300	6	20.75	±	0.89	abc
		10	24.34	±	1.73	b
	500	6	20.46	±	0.51	abc
		10	23.29	±	0.63	bc

Table supplementary 10. Values of Pearson correlations among the following parameters: NUR and NUE (60, 180, 300, 420 and 1440 min of experiment), ETR_{situ} (15 and 1440 min of experiment), ETR_{max} and F_v/F_m (15, 180, 420 and 1440 min of experiment), C:N ratio, percentage of carbohydrates and percentage of protein (initial and final times of the experiment).

	NUR 180min	NUR 300min	NUR 420min	NUR 1440min	NUE 60min	NUE 180min	NUE 300min	NUE 420min	NUE 1440min	ETR_{situ} 15min	ETR_{situ} 1440min	ETR_{max} 15min	ETR_{max} 180min	ETR_{max} 420min	ETR_{max} 1440	F_v/F_m 15min	F_v/F_m 180min	F_v/F_m 420min	F_v/F_m 1440min	C:N Initial	C:N Final	%Carb. Initial	%Carb. Final	%Prot. Initial	%Prot. Final
NUR 60min	**0.86**	**0.66**	**0.56**	0.25	**0.68**	**0.80**	**0.81**	**0.71**	0.17	-0.29	**-0.79**	**-0.80**	**-0.46**	**-0.53**	**-0.46**	0.16	**-0.51**	0.05	**0.33**	**0.68**	**0.86**	0.26	**0.33**	**-0.66**	**-0.73**
	p=0.000	**p=0.000**	**p=0.000**	p=0.145	**p=0.000**	**p=0.000**	**p=0.000**	**p=0.000**	p=0.312	p=0.085	**p=0.000**	**p=0.000**	**p=0.005**	**p=0.001**	**p=0.005**	p=0.366	**p=0.001**	p=0.768	**p=0.050**	**p=0.000**	**p=0.000**	p=0.126	**p=0.047**	**p=0.000**	**p=0.000**
NUR 180min		**0.94**	**0.89**	**0.63**	0.25	**0.47**	**0.62**	**0.59**	**0.39**	-0.30	**-0.60**	**-0.53**	-0.23	-0.27	-0.22	-0.32	**-0.47**	-0.13	0.07	**0.46**	**0.71**	-0.02	0.01	**-0.48**	**-0.53**
		p=0.000	**p=0.000**	**p=0.000**	p=0.146	**p=0.004**	**p=0.000**	**p=0.000**	**p=0.018**	p=0.079	**p=0.000**	**p=0.001**	p=0.179	p=0.117	p=0.203	p=0.058	**p=0.004**	p=0.434	p=0.668	**p=0.005**	**p=0.000**	p=0.912	p=0.938	**p=0.003**	**p=0.001**
NUR 300min			**0.99**	**0.79**	-0.02	0.19	**0.42**	**0.45**	**0.43**	-0.26	**0.39**	0.29	0.05	0.14	0.04	**0.39**	**0.42**	0.15	0.10	0.24	**0.51**	-0.18	0.16	0.28	**0.35**
			p=0.000	**p=0.000**	p=0.895	p=0.256	**p=0.010**	**p=0.007**	**p=0.008**	p=0.132	**p=0.020**	p=0.087	p=0.755	p=0.404	p=0.797	**p=0.020**	**p=0.011**	p=0.397	p=0.569	p=0.166	**p=0.002**	p=0.287	p=0.352	p=0.096	**p=0.039**
NUR 420min				**0.85**	-0.13	0.08	0.32	**0.36**	**0.45**	-0.20	-0.28	-0.18	0.00	-0.08	0.02	**-0.39**	**-0.38**	-0.15	-0.15	0.15	**0.41**	-0.25	-0.23	0.22	0.26
				p=0.000	p=0.459	p=0.637	p=0.057	**p=0.030**	**p=0.006**	p=0.241	p=0.095	p=0.289	p=0.995	p=0.630	p=0.896	**p=0.018**	**p=0.023**	p=0.391	p=0.379	p=0.370	**p=0.012**	p=0.137	p=0.168	p=0.208	p=0.124
NUR 1440min					**-0.38**	-0.28	-0.14	-0.13	**0.43**	0.24	0.10	0.15	0.06	0.05	0.26	**-0.35**	-0.25	-0.12	-0.25	-0.08	0.16	**-0.58**	**-0.56**	0.05	0.02
					p=0.024	p=0.096	p=0.400	p=0.434	**p=0.009**	p=0.159	p=0.576	p=0.377	p=0.734	p=0.767	p=0.122	**p=0.035**	p=0.150	p=0.475	p=0.141	p=0.653	p=0.357	**p=0.000**	**p=0.000**	p=0.780	p=0.886
NUE 60min						**0.93**	**0.75**	**0.63**	-0.12	-0.12	**0.60**	**0.80**	**0.48**	**0.72**	**0.62**	0.21	-0.24	0.20	**0.61**	**0.64**	**0.61**	**0.52**	**0.63**	**-0.57**	**0.64**
						p=0.000	**p=0.000**	**p=0.000**	p=0.487	p=0.482	**p=0.000**	**p=0.000**	**p=0.003**	**p=0.000**	**p=0.000**	p=0.229	p=0.161	p=0.253	**p=0.000**	**p=0.000**	**p=0.000**	**p=0.001**	**p=0.000**	**p=0.000**	**p=0.000**

NUE 180min	**0.91**	**0.83**	0.07	**-0.34**	**-0.74**	**-0.86**	**-0.43**	**-0.61**	**-0.61**	0.12	-0.24	0.10	**0.57**	**0.72**	**0.71**	**0.56**	**0.63**	**-0.64**	**-0.68**
	p=0.000	**p=0.000**	p=0.675	**p=0.041**	**p=0.000**	**p=0.000**	**p=0.009**	**p=0.000**	**p=0.000**	p=0.494	p=0.164	p=0.564	**p=0.000**	**p=0.000**	**p=0.000**	**p=0.000**	**p=0.000**	**p=0.000**	**p=0.000**
NUE 300min		**0.97**	0.22	**-0.57**	**-0.75**	**-0.81**	-0.26	**-0.55**	**-0.51**	0.03	-0.28	0.03	**0.46**	**0.64**	**0.70**	**0.53**	**0.58**	**-0.56**	**-0.67**
		p=0.00	p=0.203	**p=0.000**	**p=0.000**	**p=0.000**	p=0.120	**p=0.001**	**p=0.001**	p=0.846	p=0.102	p=0.851	**p=0.004**	**p=0.000**	**p=0.000**	**p=0.001**	**p=0.000**	**p=0.000**	**p=0.000**
NUE 420min			0.24	**-0.66**	**-0.70**	**-0.72**	-0.17	**-0.44**	**-0.49**	0.01	-0.22	0.01	**0.39**	**0.57**	**0.60**	**0.55**	**0.57**	**-0.48**	**-0.58**
			p=0.159	**p=0.000**	**p=0.000**	**p=0.000**	p=0.309	**p=0.007**	**p=0.003**	p=0.953	p=0.202	p=0.945	**p=0.018**	**p=0.000**	**p=0.000**	**p=0.000**	**p=0.000**	**p=0.003**	**p=0.000**
NUE 1440min				-0.01	-0.02	-0.02	0.10	0.10	0.15	0.06	0.10	-0.04	0.04	0.00	0.12	-0.24	-0.30	0.00	-0.04
				p=0.964	p=0.891	p=0.895	p=0.549	p=0.580	p=0.369	p=0.747	p=0.577	p=0.809	p=0.823	p=0.991	p=0.479	p=0.162	p=0.077	p=0.998	p=0.796
ETR_{situ} 15min					**0.48**	**0.34**	-0.02	0.05	0.30	0.09	0.21	0.05	0.04	-0.19	-0.19	**-0.39**	**-0.33**	0.09	0.16
					p=0.003	**p=0.044**	p=0.896	p=0.754	p=0.073	p=0.612	p=0.214	p=0.789	p=0.807	p=0.273	p=0.270	**p=0.020**	**p=0.049**	p=0.618	p=0.348
ETR_{situ} 1440min						**0.76**	**0.55**	**0.37**	**0.57**	0.19	**0.53**	0.07	-0.14	**-0.56**	**-0.67**	**-0.57**	**-0.55**	**0.50**	**0.62**
						p=0.000	**p=0.000**	**p=0.027**	**p=0.000**	p=0.276	**p=0.001**	p=0.670	p=0.432	**p=0.000**	**p=0.000**	**p=0.000**	**p=0.000**	**p=0.002**	**p=0.000**
ETR_{max} 15min							**0.54**	**0.66**	**0.49**	0.03	**0.40**	-0.16	**-0.45**	**-0.65**	**-0.73**	**-0.43**	**-0.51**	**0.54**	**0.68**
							p=0.001	**p=0.000**	**p=0.002**	p=0.848	**p=0.015**	p=0.337	**p=0.006**	**p=0.000**	**p=0.000**	**p=0.010**	**p=0.002**	**p=0.001**	**p=0.000**
ETR_{max} 180min								**0.47**	0.24	0.01	**0.34**	-0.25	-0.11	**-0.37**	**-0.35**	-0.23	-0.29	0.32	**0.35**
								p=0.004	p=0.154	p=0.934	**p=0.040**	p=0.143	p=0.514	**p=0.028**	**p=0.035**	p=0.174	p=0.083	p=0.056	**p=0.034**
ETR_{max} 420min									0.27	0.06	**0.38**	**-0.36**	**-0.35**	**-0.36**	**-0.43**	-0.13	**-0.35**	**0.34**	**0.46**

ETR_{max} 1440min	p=0.116	p=0.707	**p=0.021**	**p=0.033**	**p=0.039**	**p=0.031**	**p=0.009**	p=0.434	**p=0.034**	**p=0.041**	**p=0.004**
		-0.10	0.26	-0.15	-0.22	**-0.35**	**-0.34**	**-0.45**	**-0.48**	**0.34**	0.30
		p=0.548	p=0.122	p=0.385	p=0.192	**p=0.034**	**p=0.041**	**p=0.006**	**p=0.003**	**p=0.046**	p=0.077
F_v/F_m 15min			**0.47**	0.09	0.27	0.00	-0.18	0.12	0.06	0.10	0.04
			p=0.004	p=0.612	p=0.105	p=0.994	p=0.291	p=0.487	p=0.707	p=0.560	p=0.798
F_v/F_m 180min				-0.01	0.07	-0.09	**-0.39**	-0.10	-0.27	0.15	**0.35**
				p=0.957	p=0.692	p=0.601	**p=0.018**	p=0.558	p=0.112	p=0.391	**p=0.034**
F_v/F_m 420min					0.11	0.00	-0.14	0.03	0.05	0.02	0.17
					p=0.520	p=0.988	p=0.412	p=0.875	p=0.759	p=0.893	p=0.315
F_v/F_m 1440min						**0.47**	**0.38**	0.17	0.22	**-0.41**	**-0.40**
						p=0.004	**p=0.022**	p=0.329	p=0.189	**p=0.012**	**p=0.016**
C:N Initial							**0.75**	**0.47**	**0.48**	**-0.94**	**-0.59**
							p=0.000	**p=0.004**	**p=0.003**	**p=0.000**	**p=0.000**
C:N Final								0.26	0.29	**-0.76**	**-0.89**
								p=0.132	p=0.090	**p=0.000**	**p=0.000**
%Carb. Initial									**0.87**	**-0.39**	**-0.33**
									p=0.000	**p=0.018**	**p=0.048**

%Carb. Final	**-0.41 p=0.014**	**-0.34 p=0.042**
%Prot. Initial		**0.57 p=0.000**

CAPÍTULO 2

Artigo disponível no periódico *Frontiers in Marine Science* - edição: Boosting the Potential of Algae for Biomass Production, Valorisation, and Bioremediation
DOI: 10.3389/fmars.2022.981468
Front. Mar. Sci as the original publisher of that content

Growth, biofiltration and photosynthetic performance of *Ulva* spp. cultivated in fishpond effluents: an outdoor study

Massocato, T. [1*], Robles, V.[2], Moreira, B.[1], Castro-Varela, P.[2], Pinheiro-Silva, L.[3], Oliveira, W.[4], Veja, J.[2], Avilés, A.[2], Bonomi-Barufi, J.[1], Rörig, L.[1†], Figueroa, F.L.[2†]

[1]Phycology Laboratory, Department of Botany, Federal University of Santa Catarina, Florianópolis, Brazil

[2]Andalusian Institute of Blue Biotechnology and Development (IBYDA), Experimental Centre Grice Hutchinson, Department of Ecology, Malaga University, Malaga, Spain

[3]Laboratory of Freshwater Ecology, Department of Ecology and Zoology, Federal University of Santa Catarina, Florianópolis, Brazil

[4]Multiuser Laboratory of Biology Studies (LAMEB), Department of Botany, Federal University of Santa Catarina, Florianópolis 88040-900, Santa Catarina, Brazil

[†]These authors have contributed equally to this work and share last authorship

1. ABSTRACT

Anthropogenic impacts on water resources, especially by nutrient discharge, is a worldwide problem in marine coastal areas. In this context, seaweed cultivation in aquaculture wastewater can be considered as an alternative for effluent mitigation, where the biomass becomes a source of valuable compounds. The current study examined the potential use of the seaweeds *Ulva pseudorotundata* and *Ulva rigida* to remove nutrients to treat effluents from the culture of *Chelon labrosus*. Two experiments were conducted under pilot-scale conditions to evaluate the nutrient uptake, photosynthetic activity, and biomass production of the seaweed species cultivated under 50 and 100% effluent concentrations. Photosynthetic parameters were determined by *in vivo* chlorophyll *a* fluorescence associated to photosystem II 3 times a day to estimate photosynthetic performance and seaweed physiology throughout the experiment: optimal quantum yield (F_v/F_m), *in situ* and *ex situ* electron transport rate (ETR), photosynthetic efficiency (α_{ETR}), saturation irradiance (E_k), and the maximum non-photochemical quenching (NPQ_{max}). To evaluate seaweed metabolism and biomass compounds, elemental and biochemical composition were analyzed in the beginning and end of each experiment. Results regarding the nutrient source showed that both species removed more than 65% of ammonium after 3 hours of experimentation. At the end of the experiments, up to 94.8% of the initial ammonium was sequestered from the effluent. Additionally, after 5 days of cultivation under 50% fish effluent both *Ulva* species were able to remove more than 85% of the nitrate. Although a decrease in uptake efficiency was observed in cultures with 100% fish effluent, at the end of the experiment more than 440 μmol L^{-1} of nitrate was removed, considering all treatment conditions. The biomass values showed that growth rates of seaweed cultivated in 100% effluent were higher than those obtained in 50% effluent. Moreover, when cultivated in the 100% effluent concentration, a significant increment in protein content was detected in both *Ulva* species. Our results contribute to the understanding of biofiltration and photosynthetic performance of two different *Ulva* species in order to improve growth optimization, enhancement of biofiltration capacity and also to boost management practices of seaweed cultivation in aquaculture effluent treatment systems.

Keywords

Aquaculture, biofiltration, *in vivo* chlorophyll-*a* fluorescence, nitrogen, photosynthesis, *Ulva pseudorotundata*, *Ulva rigida*.

2. INTRODUCTION

Eutrophication and the exploitation of natural resources resulting from anthropogenic activity have drastically modified marine coastal areas in the past few decades (LOTZE et al., 2006; SMITH; TILMAN; NEKOLA, 1999). Furthermore, climate change is a threat to marine ecosystems, which is an emerging concern for coastal and ocean resilience. According to the United Nations Decade of Ocean Science for Sustainable Development (2021-2030) (UNESCO, 2018), political strategy and scientific knowledge will be required in the coming years in order to mitigate risk and develop sustainable practices. Hence, the search for innovative technologies that promote structural transformation and sustainable solutions is imperative, aiming to reduce the impact of economic activities on natural resources. The algal industry is an emerging sector that can be exploited in terms of blue bioeconomy, since it holds a very high potential from an economic, social and environmental perspective (ARAÚJO et al., 2021). Algae production also plays an important role in ecosystem services and has the potential to mitigate climate change by reducing carbon emissions (FROEHLICH et al., 2019). The diversity of micro- and macroalgae (or seaweed) represents a source of a vast number of valuable compounds, which can be applied to biotechnological approaches in the cosmeceutical, pharmaceutical, agricultural and food industries (BUSCHMANN et al., 2017a; JUSADI et al., 2021; VEGA et al., 2021)

According to the Food and Agriculture Organization of the United Nations (FAO, 2020), world algae aquaculture production has increased over the years, reaching 32.4 million tons of biomass in 2018, which is dominated by seaweeds. Much of the productivity is still limited to countries in Eastern and Southeastern Asia, however, as bioeconomic development grows worldwide, seaweed farming is gaining attention, especially in European countries. Many different technologies have been developed to produce seaweed, and their incorporation in fish, crustacean, and mollusc farms is growing as well. Integrating Multi-Trophic Aquaculture (IMTA) systems consists of the coupling of seaweed production with mariculture waste waters, which decreases the amount of inorganic nutrients in the discharge effluent. IMTA systems are considered an eco-friendly practice since they reduce the impact of the aquaculture industry and increase the overall profitability of fish production through the cultivation of algal biomass which can be applied in different economic sectors (CHOPIN et al., 2001; NEORI et al., 2004; SHPIGEL et al., 1993). When practiced inland, IMTA systems require a deep understanding of broad concepts such as: systems design and scale, seaweed

biomass quality and value, and how to improve the efficiency of algae species to absorb and remove nutrients from mariculture waste. Seaweed culture conditions (e.g. depth, light, stocking density, water turnover rates) and specific properties of the seaweed species (e.g. biology and physiology) are the main factors contributing to the nutrient reduction efficiency and uptake rate. Moreover, understanding 1) how seaweed biofiltering performance changes over diurnal and seasonal cycles, 2) which local seaweed strains/species can perform better in biofiltering effluents, and 3) what factors, other than light and nutrients, may narrow seaweed production, is also important for the successful implementation of integrated aquaculture systems (TROELL et al., 2003). Thus, great efforts are made to understand algal physiology in order to improve growth optimization, upscaling of production volumes, enhancement of biofiltration capacity, and management practices of seaweed cultivation in aquaculture effluent treatment systems.

The green macroalgae genus *Ulva* is one of the most studied seaweeds for its use as a biofilter of dissolved nutrients from mariculture effluents. *Ulva* has a worldwide distribution, with 131 taxonomically recognized species (GUIRY et al., 2014), playing an important ecological role in marine nutrient cycling and provisioning a source of food and habitat for a diversity of species. *Ulva* spp. are frequently associated with the formation of massive algal aggregations denominated “green tides", commonly in eutrophicated areas where elevated nutrient levels in seawater are observed (LIU et al., 2013; SMETACEK; ZINGONE, 2013; YE et al., 2011). Fast growth rates, phenotypic plasticity, the ability to rapidly remove nutrients, and the potential for various biomass applications make these robust seaweeds stand out for cultivation in onshore and offshore systems (GUTTMAN et al., 2018; NEORI et al., 2003; STEINHAGEN et al., 2022). Many studies demonstrate the efficiency of using *Ulva* spp. as a biofilter of fish effluents since it rapidly absorbs organic and inorganic nutrients, especially ammonium (BEN-ARI et al., 2014; COHEN; NEORI, 1991; DEL RÍO; RAMAZANOV; GARCÍA-REINA, 1996; NARDELLI et al., 2019). Under outdoor conditions, the efficiency of ammonia removal by *Ulva* in IMTA systems may reach more than 80%, which greatly improves the quality of mariculture effluents (AL-HAFEDH; ALAM; BUSCHMANN, 2014; COPERTINO; TORMENA; SEELIGER, 2009; MACCHIAVELLO; BULBOA, 2014). Moreover, dried *Ulva* spp. biomass can contain up to 40% protein (SHAHAR et al., 2020; SHPIGEL et al., 2019), and is a source of cell wall polysaccharides that are sought after for biotechnology applications (KIDGELL et al., 2019a). In this context, *Ulva* spp. can act as bioremediators by extracting

waste nutrients from mariculture effluents and converting them into biomass that may be beneficial as a source of raw material. Nonetheless, nutrient uptake performance and growth rate can vary among species, depending on local environmental conditions (photoperiod and temperature) and the characteristics of the cropping system (nutrient loads, salinity, turbidity) which can affect the biofiltration performance and the cultivation biochemical composition.

Ulva species have also been used as a model organism in ecophysiology studies where relationships between photosynthesis and chlorophyll-*a* fluorescence have been explored (CRUCES et al., 2019; OSMOND et al., 1993). Photosynthesis assessments of *Ulva* spp. using Pulse Amplitude Modulation (PAM) of chlorophyll-*a* fluorescence has allowed inferences about the process of photoinhibition and the triggering of photoinhibitory damage and photoprotection mechanisms. Cruces et al. (2019) evaluated the photosynthetic performance of *U. rigida* using PAM and were able to quantify electron transport rates and aspects of photoinhibition in response to diurnal changes in solar radiation. Electron transport rates measured by PAM can also vary with nitrate concentration. Cabello-Pasini and Figueroa (2005) demonstrated that the maximum rate of electron transport (ETRmax) of *U. rigida* increased with the increase of nitrate in the medium. Figueroa et al. (2020) conducted experiments with *U. rigida* cultivated under predicted values of pCO_2, nutrient enrichment and temperature that showed multiple aspects of photosynthetic parameters obtained by PAM measurements and provided information about the physiological impacts of future global changes.

Researches with other seaweed species showed that PAM was a useful tool to evaluate photosynthetic responses of seaweed cultured under multiple factors such as irradiance (FIGUEROA et al., 2006; KANG et al., 2008b; MATA et al., 2006), temperature (FIGUEROA et al., 2009b), system aeration (FIGUEROA et al., 2006), and different nitrogen sources (SHAHAR et al., 2020). Understanding photosynthesis and the biofiltration process can help to improve aspects of IMTA cropping systems. In the present study, two seaweed species naturally occurring in the Mediterranean and with potential for use in biofiltration (*U. pseudorotundata* and *U. rigida*) were evaluated for their (1) ability to remove dissolved inorganic nutrients (NH_4^+, NO_3^- and PO_4^{3-}), (2) photosynthetic performance, (3) biomass productivity, and (4) biomass elemental and biochemical composition. The experiments were carried out on a land-based pilot scale using fishpond effluents at two different concentrations. The main objective was to compare and parameterize the two species for use in biofiltration processes associated with IMTA systems.

3. MATERIAL AND METHODS

Algal material collection and culture conditions

The *Ulva* species used in this study were collected in two different places: in the bay of Cádiz (36º30'N, 6º10'W), where specimens were collected from salt marsh areas, and in the bay of Málaga (36°42'N, 4°19'W), where *Ulva* sp. specimens were collected fixed to rocky intertidal shores, both situated in Andalusia, Spain (**Figure 1**). The algae were transported to the Grice Hutchinson Research Center at Malaga University where the experiments were conducted. After collection, small pieces of algal material were separated for species-level identification using molecular methods. Clean and healthy fronds of *Ulva* were maintained in rectangular tanks (200 L; 1 m^2 surface area and 50 cm depth) and exposed to full solar radiation in which air diffusers situated at the bottom of each tank kept the algae unattached and suspended. Prior to the experiments, seaweed biomass was grown in artificial seawater and supplemented twice a week with NH_4Cl (300 µmol L^{-1}), KNO_3 (300 µmol L^{-1}) and KH_2PO_4 (48 µmol L^{-1}). The salinity and pH of the seawater were 35 and 8.0, respectively.

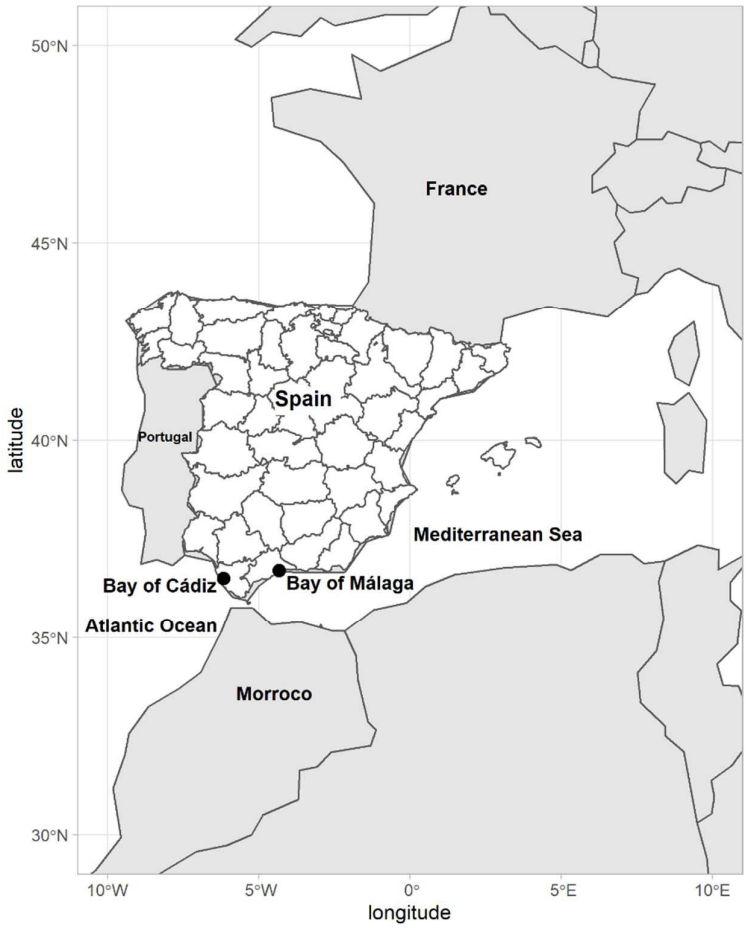

Figure 1. Map of Spain indicating the sites sampled in the present study.

Species-level identification and phylogenetic analysis

Algal samples were dried in silica-gel and submitted to DNA extraction, amplification, sequencing, and identification. The large subunit of the plastid-encoded Ribulose Bisphosphate Carboxylase-Oxygenase (RuBisCO) gene region (rbcL) was amplified in a polymerase chain reaction (PCR) using published primer pairs SHF1 (CCGTTTAACTTATTACACGCC) and SHR4 (TTACATCACCACCTTCAGATGC) (HEESCH et al., 2009). The following were added to each sample: 0.25µl of Taq DNA polymerase (5u/µl) (Qiagen), 2.5µl of CoralLoad PCR Buffer, 2.5µl of dNTPS (2mM), 5µl of Q-solution, 3.5µl MgCl (2µl for H3) (25mM), 1µl of each primer (10µM), 2 µl of total DNA, and 7.25u of MiliQ water, leading to a final volume of 25 µl. PCR proceeded as follows: denaturation at 94°C for 3 minutes, followed by 40 cycles of 94°C for 1 minute and 30 seconds of denaturation, 37°C for 2 minutes for annealing step,

and then 72°C for 3 minutes for final extension. The strings were aligned and edited in Geneious 10.0.9. The species identification was carried out through BLASTn and compared in the GenBank database.

The evolutionary history was inferred by using the Maximum Likelihood method and Kimura 2-parameter model (KIMURA, 1980). The bootstrap consensus tree inferred from 1000 replicates (FELSENSTEIN, 1985) was taken to represent the evolutionary history of the taxa analyzed. Branches corresponding to partitions reproduced in less than 50% bootstrap replicates were collapsed. Initial tree(s) for the heuristic search were obtained by applying the Neighbor-Joining method to a matrix of pairwise distances estimated using the Maximum Composite Likelihood (MCL) approach. A discrete Gamma distribution was used to model evolutionary rate differences among sites (5 categories (+G, parameter = 0.1073)). The rate variation model allowed for some sites to be evolutionarily invariable ([+I], 45.04% sites). This analysis involved 19 nucleotide sequences. There were a total of 675 positions in the final dataset. Evolutionary analyses were conducted in MEGA11 (TAMURA; STECHER; KUMAR, 2021).

Experimental design

To assess the biofiltration capacity of the seaweed, two consecutive experiments were conducted using effluents from the cultivation of *Chelon labrosus* (Osteichthyes, Mugilidae). The fish effluent was obtained from a closed recirculating water system connected to a filter with chemoautotrophic nitrifying bacteria. Chemical composition of the effluents was characterized prior to experiments by ion chromatography (METROHM 863 Compact IC Autosampler). The first experiment was performed during 5 days using an effluent diluted to 50% with tap water. For the second one, we used pure effluent and it lasted 4 days. At the beginning of each experiment, *U. pseudorotundata* and *U. rigida* biomass was weighed at initial stocking densities of 6.0 g FW L^{-1} (n = 3). These seaweed stocking densities were established based on previous studies of *U. lactuca* cultivated in abalone culture effluent which demonstrated high uptake efficiency in removing NH_4^+, NO_3^-, and PO_4^{3-} (MACCHIAVELLO; BULBOA, 2014). Both experiments started at 1:00 pm (local time) and the algae were kept without nutrients before the beginning of the experiments to provide starvation conditions. During experiments, pH, dissolved oxygen, and salinity were measured daily using portable devices (LAQUAact PH110, HANNA Instruments) (Table S1). Temperature and Photosynthetically Active Radiation (PAR, λ = 400-700 nm) were recorded every 15 minutes

from HOBO data loggers (Zippo-HOBO U12, SQ-212 PAR) installed in one of the tanks. Integrated daily irradiance (kJ m^{-2}) was calculated from PAR data to obtain total light energy received by cultures during the experiment.

Biofiltration capacity

To evaluate the nutrient removal performance of the algae, water samples were obtained from each tank three times a day for N-NO_3^- analysis (morning 8:00 - 9:00, noon 12:00 - 13:00 and evening 16:00 - 17:00); and once a day for NH_4^+ and PO_4^{3-} analysis (evening 16:00 - 17:00), except the first day, when samples were taken at 13:00 and 16:00. Aliquots of 10 mL were filtered (GF/F Whatman) and stored at −20°C in polyethylene flasks for further analysis using a segmented flow analyzer (SFA; Seal Analytical autoanalyzer QuAAtro) according to the methods described by (GRASSHOFF; KREMLING; EHRHARDT, 1999).
Nutrient uptake efficiency (NUE) was calculated as:

$$\mathbf{NUE}\ (\%) = \mathbf{100} - \left[\left(\frac{\boldsymbol{C_{t+1}} \times \mathbf{100}}{\boldsymbol{C_t}}\right)\right]$$

where C_t represents the initial concentration of nutrients, C_{t+1} represents the concentration of nutrients after t+1. The nutrient uptake rate (NUR), which represents the amount of nutrients removed per unit of time, per volume, per unit of seaweed dry weight, was determined from changes in nutrient concentrations according to the following equation:

$$\mathbf{NUR}\ (\boldsymbol{\mu mol\ g^{-1}\ DW\ h^{-1}}) = \frac{(\mathbf{C_t} \times \mathbf{V_t}) - (\mathbf{C_{t+1}} \times \mathbf{V_{t+1}})}{\mathbf{B} \times \boldsymbol{\Delta_t}}$$

where C_t represents the initial concentration of nutrients, V_t represents the initial volume of water (in L), C_{t+1} represents the concentration of nutrients after t+1, V_{t+1} represents the volume of water after t+1 (in L), B represents the dry biomass used (in grams), and Δ_t represents the time interval between t and t+1 (in hours).

Photosynthetic performance

Photosynthetic performance was assessed at the same time points as nitrate sampling described above by *in vivo* chlorophyll-a fluorescence of Photosystem II (PSII) measured *in situ* and *ex situ*. Measurements *in situ* were conducted using a Pocket-PAM (Gademann

Instruments, Würzburg, Germany) on five algal samples from each tank to obtain the effective quantum yield of PSII ($\Delta F/F_m'$) using the equation:

$$\frac{\Delta F}{F_m'} = \frac{(F_m' - F_t)}{F_m'}$$

where F_m' is the maximum fluorescence in light, induced by a saturating pulse, and F_t, the basal fluorescence emitted by an organism pre-acclimated to light conditions. The data of $\Delta F/F_m'$ obtained was used to calculated the Electron Transport Rate (ETR_{situ}) associated with PSII according to Genty et al. (1989):

$$\mathbf{ETR_{situ}}\ (\mu\mathbf{mol\ electrons\ m^{-2}\ s^{-1}}) = \frac{\Delta F}{F_m'} \times E_{PAR} \times A \times F_{II}$$

where $\Delta F/F_m'$ is the effective quantum yield of PSII, E_{PAR} is the PAR (µmol photons m^{-2} s^{-1}) obtained by HOBO at the same time of the measurements, A was the absorptance of the algal thallus, and F_{II} was a constant that represents the fraction of cellular chlorophyll *a* associated with the light harvesting complex of PSII being 0.5 the value for green algae (FIGUEROA; CONDE-ALVAREZ; GOMEZ, 2003). Absorptance of the algal thallus was calculated according to (FIGUEROA et al., 2009b) as follows:

$$A = 1 - \frac{E_t}{E_0}$$

where E_o is the incident irradiance of a lamp determined by a sensor Li-189 (LI-COR Ltd, Nebraska, USAd) connected to a radiometer Li-250 (LI-COR Ltd, Nebraska, USA), and E_t is the transmitted irradiance, measured by placing a small piece of the thallus above the PAR sensor.

Ex situ measurements consisted of rapid light-response curves (RLC), which were obtained using a Junior PAM (Walz GmbH, Effeltrich Germany) connected to a PC running WinControl software. Algal samples were transported under dark conditions from the outdoor tanks to the laboratory. After dark-adapted for at least 15 min, the maximum quantum yield of PSII F_v/F_m was obtained from the first saturating pulse and determined by the equation:

$$\frac{F_v}{F_m} = \frac{(F_m - F_0)}{F_0}$$

where F_0 is the initial fluorescence of PSII (intrinsic fluorescence from the antenna of fully oxidized PSII); F_m is the maximum fluorescence of PSII after a saturating light pulse (0.4 s, approx. 9000 µmol photons m^{-2} s^{-1}), and F_v is the variable fluorescence corresponding to the difference between F_m and F_0. Afterwards, to estimate the electron transport rate (ETR), the same samples were exposed for 30s to twelve increasing irradiances (25, 45, 66, 90, 125, 190, 285, 420, 625, 845, 1150, and 1500 µmol photons m^{-2} . s^{-1}) of actinic blue light, each one followed by a saturating blue light pulse. ETRs were calculated as previously described and plotted against the actinic light intensities generating light curves that were fitted according to the Eilers and Peeters (1988) model to obtain photosynthetic parameters (ETR_{max}, α_{ETR}, and E_k) in which ETR_{max} represents the maximum electron transport rates, α_{ETR} is the algal photosynthetic efficiency and E_k saturation irradiance for the photosynthetic electron transport. Non-photochemical quenching (NPQ), which corresponds to the total energy dissipation, was calculated after each saturating pulse during the RLCs, and NPQ *versus* irradiance relationships were determined. Curves were then fitted using Eilers and Peeters (1988) models, allowing the calculation of maximum NPQ values (NPQ_{max}). All rapid light curves were fitted using the statistical environment R, version 4.2 (The R Development Core Team, 2022).

Biomass growth and composition

Growth rate, biomass productivity (also known as biomass yield), and biochemical composition were measured from the biomass obtained at the beginning and at the end of the experiments. Growth rates (GR) were calculated according to Lignell and Pedersén (1989):

$$\mathbf{GR}\ (\%\ \mathbf{day^{-1}}) = \left[\left(\frac{W_t}{W_i}\right)^{\frac{1}{t}} - 1\right] \times 100$$

where Wi = initial wet weight, Wt = wet weight after t days and t = days of cultivation. The productivity of the tanks was calculated according to (MATA et al., 2003):

$$\mathbf{Productivity}\ (\mathbf{g\ DW\ m^{-2}\ day^{-1}}) = \frac{\left[\frac{(W_t - W_i)}{t\left(\frac{F_w}{D_w}\right)}\right]}{A}$$

where, W_t = wet weight after t days, W_i = initial wet weight, t = the number of days, (FW/DW) is the fresh weight/dry weight ratio, and A is the area covered by the tank in m^2. To obtain the fresh weight/dry weight ratio, ten samples of ~3 g were dried to constant weight at 60 °C (48–72 h). Triplicate seaweed samples of each tank (~5 g FW) were taken at the beginning and end of the experiments, washed with MiliQ-water to remove salt and freeze-dried for 48h (Telstar Lyoquest-55) for tissue biochemical analysis. 2 mg of dried biomass were submitted for carbon, hydrogen, and nitrogen content analyses using a LECO CHNS-932 elemental analyser (Michigan, USA). C, H and N values were expressed as percentage of dry weight and the C:N ratio was determined.

The daily N content of the produced biomass was also used as an estimate of the biofiltration capacity, being calculated by multiplying the biomass yield by the N content of the seaweeds (MATA; SCHUENHOFF; SANTOS, 2010). Total protein content was estimated according to Shuuluka et al., (2013) by multiplying the total N by a factor of 5.45. Chlorophyll *a* (Chl *a*), chlorophyll *b* (Chl *b*) and total carotenoids (Car) were extracted from samples of the *Ulva* spp. thalli (10-15 mg DW) by incubating them in 5-10 mL of acetone 90% + $C_4Mg_4O_{12}$ for 12 h in the dark at 4°C and then centrifuging for 15 min at 4ºC and 5000 rpm. Subsequently, the absorbances were measured photometrically at 480, 647, 664, and 750 nm (UV-2600 Shimadzu). The contents of Chl *a*, Chl *b*, and Car (mg g^{-1} DW) were calculated according to Ritchie (2006) and Parsons and Strickland (1963), respectively.

Statistical analyses

The averages of integrated daily irradiance and temperature were analyzed to compare experiment 1 and 2 by a test of independent samples (*t*-student) using the STATISTICA 12 software (StatSoft, Inc. 2011). We tested the effect of effluent (two levels), species identity (two levels), hour (five levels), day (five levels) and their interaction on nutrient concentrations (NO_3^-, NH_4^+ and PO_4^{3-}), algal biofiltration capacity (NUE and NUR), photosynthetic performance (F_v/F_m, ETR_{situ}, ETR_{max}), biomass growth (growth rate, productivity, N uptake) and composition (hydrogen, nitrogen, carbon, C:N ratio, protein, Chl *a*, Chl *b*, carotenoids) using analyses of variance (ANOVA) with permutation tests, as implemented in the 'lmPerm' package in R (Wheeler, 2016). We chose permutational methods since they are suitable when sample sizes are small and do not make assumptions about normal distribution. Permutation analysis randomizes the data set while retaining the data structure to generate all possible

permutations of the values obtained in the experiment. Then, the *p*-value is obtained comparing each permuted data set to the raw data set to assess whether the treatment effects are the same or greater. When the null hypothesis was rejected after ANOVA, we followed with Tukey's HSD post-hoc tests for multiple pairwise comparisons.

First, to test for changes in nutrient concentration during the experiment, days (between-group), hours (within-group), species identity (within-group) and their interaction were used as independent variables in a three-way ANOVA, where NO_3^-, NH_4^+ and PO_4^{3-} were used as response variables in each model. Second, to test for differences in the performance of nutrient removal between algal species during the experiment, days (between-group), species identity (within-group), and their interaction were used as predictors in a two-way ANOVA, whereas NUE and NUR were used as response variables in each model. Then, to test for differences in the photosynthetic performance between algal species during the experiment, days (between-group), hours (within-group), species identity (within-group) and their interaction were used as independent variables in a three-way ANOVA, where F_v/F_m, ETR_{situ}, ETR_{max} were used as response variables in each model. Finally, to test for differences in the biomass growth and composition between algal species and effluent concentration, effluent (between-group), species identity (within-group) and their interaction were used as independent variables in a two-way ANOVA, where growth rate, productivity, N uptake, hydrogen, nitrogen, carbon, C:N ratio, protein, Chl *a*, Chl *b* and carotenoids were used as response variables in each model.

Spearman's correlation analyses were performed to measure the strength and direction of associations among chlorophyll-*a* fluorescence parameters (ETR_{situ}, F_v/F_m, ETR_{max}, α_{ETR}, Ek, and NPQ_{max}), and algal nitrate biofiltration capacity (NUE and NUR) using the function *ggpairs* from the 'GGally' package (Schloerke et al., 2021). We used non-parametric statistics since no normal distribution was found (p-value > 0.05; Shapiro test).

Multiple linear models with permutation tests were performed using the 'lmPerm' package in R (Wheeler, 2016) to assess the relationship between nutrient uptake efficiency (NUE) and photosynthetic performance. The variables used as predictors in the models were F_v/F_m, α_{ETR}, E_k, ETR_{max}, NPQ_{max}, and ETR_{situ}. Only significant (p-value < 0.05) predictors were retained in the model (α_{ETR}, NPQ_{max}, and ETR_{situ}). Then, we used simple linear models to assess the relationship between each predictor and NUE. The adjusted coefficient of determination (adjusted-R^2) was used to examine the fraction of the explained variance by the model.

Statistical analyses described above were performed in the R statistical software version 4.2.0 (R Core Team 2022).

4. RESULTS

Molecular identification

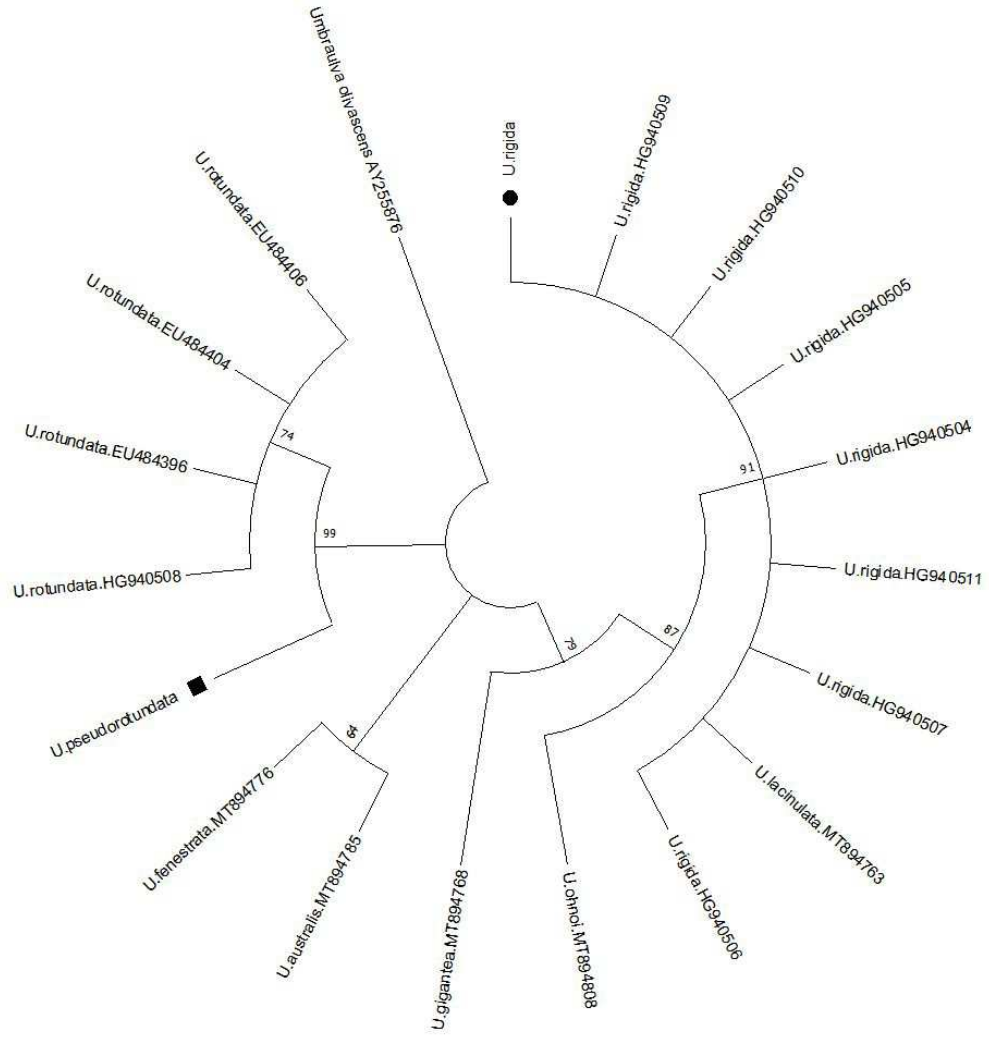

Figure 2. *Ulva* species identification utilized in this study. Molecular identification of algal material, considering a phylogenetic tree obtained by RbcL sequences (SHF1 and SHR4 markers). ■*U. pseudorotundata*; ●*U. rigida*.

Ulva specimens collected from the Spanish Mediterranean coast were identified as *Ulva pseudorotundata*, from the bay of Cádiz, and *Ulva rigida*, from the bay of Málaga (**Figure 2**). Alignment of rbcL DNA sequences obtained from algal samples showed a monophyletic

clade for each species in a phylogenetic tree with the sequences found in GenBank for *U. rigida* and *U. pseudorotundata*. Sequences obtained from *U. pseudorotundata* were grouped in the same clade as *U. rotundata* collected from Ireland (LOUGHNANE et al., 2008; WAN et al., 2017) and, according to Guiry et al., (2014), could be considered as the same species since the specific epithet *rotundata* it's not usual anymore.

Cultivation conditions

The concentration of the main ions presented in *Chelon labrosus* effluents used as culture media for the algae are presented in **Table 1**. Clearly the dominant nitrogen form in the effluents was NO_3^-. Low values of NH_4^+ were detected since the subsequent oxidation of this nutrient was carried out by chemoautotrophic nitrifying bacteria in the fishing system cultivation. The N:P molar ratios were approximately 12 for both effluents, which is about half the typical value for the main algal culture media used (e.g. F/2 and von Stosch; Andersen, 2005).

Table 1. Chemical composition of *Chelons labrosus* effluent used in experiment 1 (50% fish effluent) and experiment 2 (100% fish effluent) for *U. pseudorotundata* and *U. rigida* cultivation. Concentration (µmol L^{-1}) values are mean ± SD, n = 2.

Inorganic nutrients	**$[Cl^-]$**	**$[NO_3^-]$**	**$[PO_4^{3-}]$**	**$[SO_4^{2-}]$**	**$[Na^+]$**	**$[NH_4^+]$**	**$[K^+]$**	**$[Ca^{2+}]$**
Exp. 1	15138.85 ± 2240.62	1671.7 ± 25.59	153.58 ± 7.70	699.02 ± 40.93	14099.50 ± 2181.60	157.4 ± 8.04	342 ± 38.07	496.4 ± 136.61
Exp. 2	15760 ± 192.92	1578.73 ± 15.39	148.1 ± 0.85	764.3 ± 21.29	14937.67 ± 303.28	237.58 ± 0.10	377.24 ± 2.88	831.43 ± 111.13

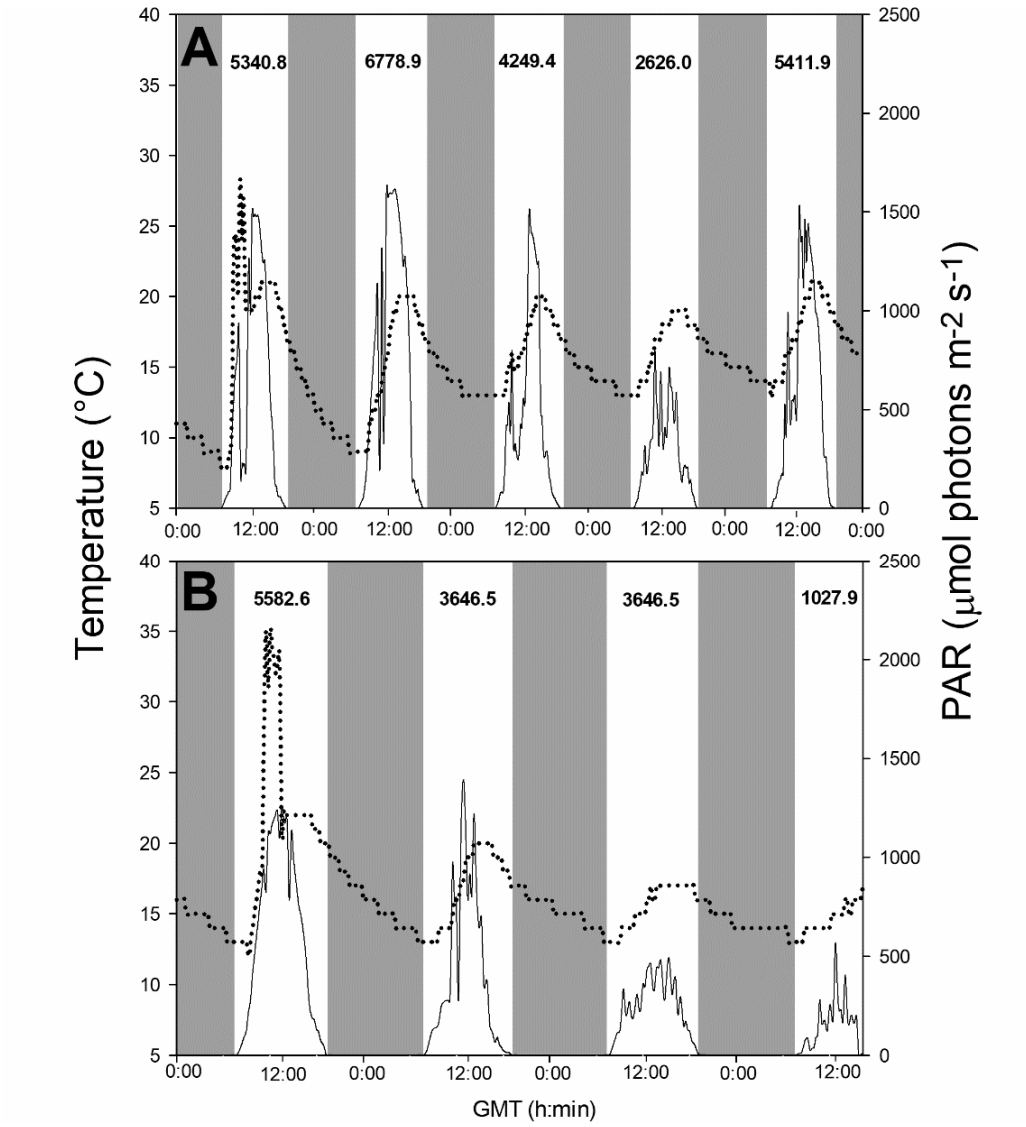

Figure 3. Variation in temperature (°C, dotted line) and photosynthetically active radiation (PAR, µmol photons m^{-2} s^{-1}, solid line) data during the experimental cultivation period of *U. pseudorotundata* and *U. rigida* in fish effluents. (A) daily temperature and daily solar irradiance for experiment 1 (50% fish effluent) and (B) daily temperature and daily solar irradiance for experiment 2 (100% fish effluent). PAR: λ = 400-700 nm. Gray areas correspond to dark periods. The integrated daily irradiance values (kJ m^{-2}) are displayed at the top of the graphs.

Temperature, PAR and daily integrated irradiance obtained from algal tanks during experiments 1 and 2 are presented in **Figure 3**. Temperature and PAR clearly presented daily patterns of low values in the mornings and evenings and higher values at noon. For experiment 1, daily mean values of irradiance varied from 289.88 to 748.29 µmol photons m^{-2} s^{-1} during the experimental period and temperature ranged

from 8.0 to 28.0 °C (**Figure 3A**). For experiment 2, the irradiance oscillated from 149.15 to 603.13 μmol photons m^{-2} s^{-1} and temperature from 12.0 to 35.0 °C (**Figure 3B**). No significant differences were observed between the two experiments when comparing the average values of integrated daily irradiance (*t*-student, $t(7) = 1.526$, $p = 0.17$). The same was observed when comparing the averages of daily temperatures (*t*-student, $t(7) = -0.745$, $p = 0.48$).

Biofiltration performance

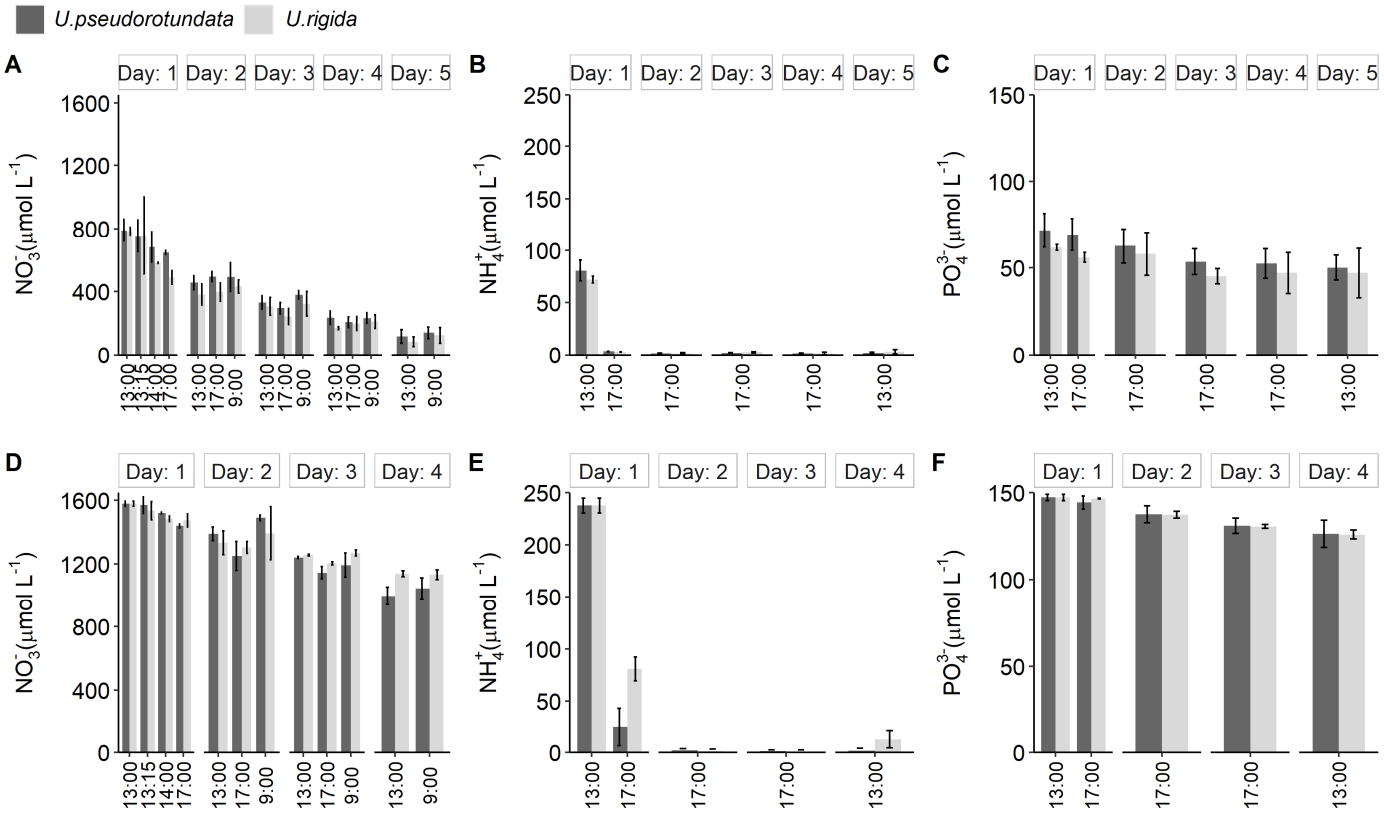

Figure 4. Changes in concentrations of NO_3^-, NH_4^+, and PO_4^{3-} (µmol L^{-1}) during the experimental cultivation of *U. pseudorotundata* and *U. rigida.* A, B and C refer to experiment 1, conducted during 5 days with 50% fish effluent. D, E and F refer to experiment 2, conducted during 4 days with 100% fish effluent. Values are mean ± SD, n = 3.

Both *Ulva* species showed similar capacity for the removal of NO_3^-, NH_4^+, and PO_4^{3-} when cultivated in *C. labrosus* fishpond effluents (**Figure 4**) and significantly reduced concentrations of these nutrients over time in the two experimental conditions (Table S2). Considering NO_3^-, at the end of experiment 1 *U. pseudorotundata* reached a removal of 672.0 ± 86.2 µmol L^{-1} while *U. rigida* removed 700.6 ± 28.0 µmol L^{-1}, but there was no statistical difference between the performances of the two species throughout the experiment (**Figure 4A**, ANOVA: $F(1) = 6073.0$, $p = 0.134$, Table S2). In experiment 2, cultivated with 100% effluent, *U. pseudorotundata* removed about 582.8 ± 41.8 µmol L^{-1} while *U. rigida* was responsible for the reduction of 441.3 ± 26.5 µmol L^{-1} from water, with no significant differences between the two species on the last day (**Figure 4D**, Tukey post hoc test, $p = 1.0$).

NH_4^+ removal was fast and efficient for the two species in both experiments. In experiment 1 both species removed more than 95% of NH_4^+ in just 3 hours, reaching 78.7 ± 9.7 µmol L^{-1} for *U. pseudorotundata* and 69.0 ± 4.9 µmol L^{-1} for *U. rigida* (Figure 4B). A sharp decline was also observed in experiment 2 (**Figure 4E**), leading to a final removal of 225.1 ± 5.6 µmol L^{-1} for *U. rigida* and 236.0 ± 8.6 SD µmol L^{-1} for *U. pseudorotundata*. The removal of PO_4^{3-} was less pronounced than the nitrogen sources, both species being equally efficient at removing about 20 ± 3.3 µmol L^{-1} in both experiments (**Figures 4C,F**).

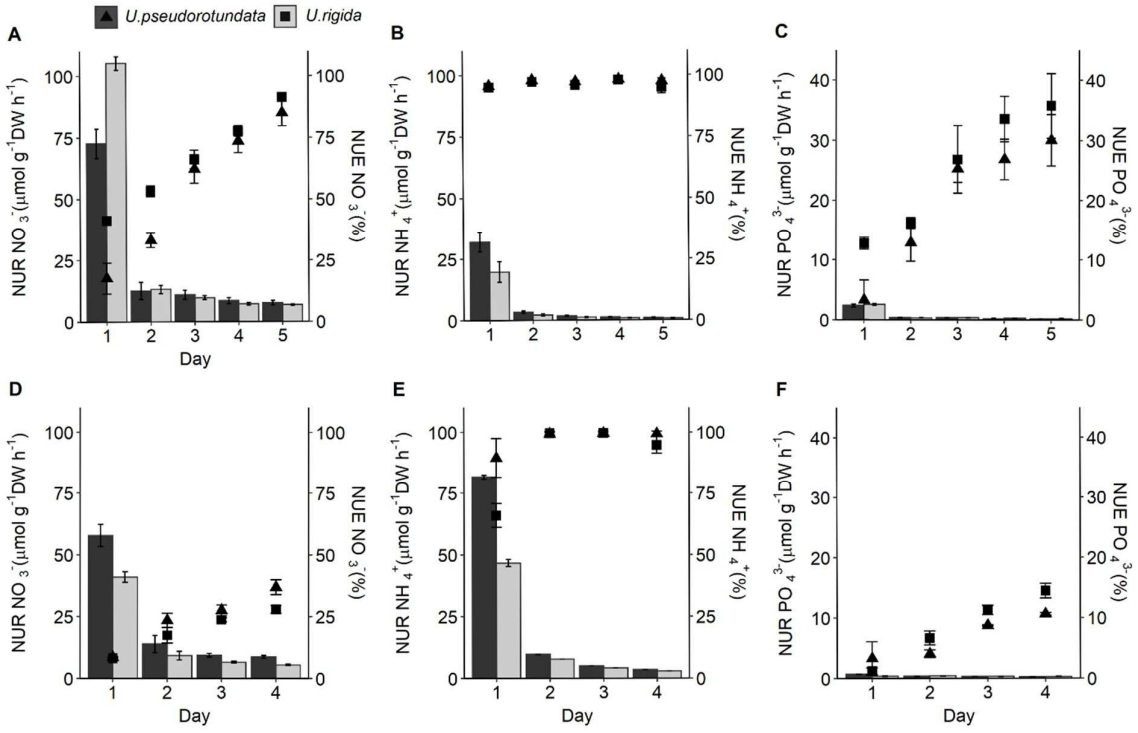

Figure 5. NO_3^-, NH_4^+, and PO_4^{3-} removal rate - NUR (bars) and uptake efficiency - NUE (symbols) by *U. pseudorotundata* and *U. rigida* in fish effluents. A, B and C refer to experiment 1, conducted during 5 days with 50% fish effluent. D, E and F refer to experiment 2, conducted during 4 days with 100% fish effluent. Values are mean ± SD, n = 3.

The two species evaluated showed similar patterns for both biofiltration parameters (NUR and NUE) in the two conditions tested (50% and 100% fish effluent) (**Figure 5**). For nitrogenous nutrients, the uptake rates reached a maximum on the 1st day then decreased over time. In experiment 1, uptake rates for NO_3^- and NH_4^+ differed significantly (ANOVA: NO_3^- = $F(1) = 264.7$, $p < 0.001$; NH_4^+ = $F(1) = 65.1$, $p < 0.001$, Table S3) between the two species **(Figures 5A,B)**. On the 1st day, *U. rigida* exhibited the highest NO_3^- uptake rate (Tukey post hoc test, $p < 0.001$) reaching values of 105 ± 2.7 µmol NO_3^- g^{-1} DW h^{-1} (**Figure 5A**). However, the NH_4^+ uptake rate was higher (Tukey post hoc test, $p < 0.001$) in *U. pseudorotundata* (31.9 ± 4.0 µmol g^{-1} DW h^{-1}) than in *U. rigida* (19.7 ± 4.2 µmol g^{-1} DW h^{-1}) when compared at the same moment (**Figure 5B**). After the initial drop, the uptake rates for NO_3^- and NH_4^+ showed similar patterns until the end of the experiment. In experiment 2, NUR values on the 1st day were different between the two species for both nitrogenous nutrients (Tukey post hoc test, $p <$ 0.001), and *U. pseudorotundata* showed better performance, reaching 57.8 ± 4.5 µmol g^{-1} DW h^{-1} of NO_3^- and 81.8 ± 0.9 µmol g^{-1} DW h^{-1} of NH_4^+ (**Figures 5D,E**).

Maximum uptake efficiency for NO_3^- (NUE) was reached at the end of each experiment and values ranged between 85.1% and 91.3% in experiment 1 and from 29.9% to 36.9% in experiment 2, considering both species (**Figures 5A,D**). NH_4^+ was biofiltered at a high percentage in all cultures just after 3 hours of seaweed treatment in both experiments. On the first day NUE reached at least 95% in experiment 1, while in experiment 2 the values ranged between 65.9-89.5%. At the end of both experiments, the two species removed up to 94.8% of NH_4^+ (**Figures 5B,D**). Regarding PO_4^{3-}, in experiment 1 both species showed equivalent removal rates (ANOVA: $F(1) = 0.019$, $p = 0.155$, Table S3), ranging from 2.4 to 0.2 μmol g^{-1} DW h^{-1} for *U. pseudorotundata* and 2.6 to 0.2 μmol g^{-1} DW h^{-1} for *U. rigida* (**Figure 5C**). However, in experiment 2 there was a significant difference associated with the interaction between *species* and *time* (ANOVA: $F(3) = 0.139$, $p < 0.001$, Table S3), with the NUR for PO_4^{3-} being higher in *U. pseudorotundata* (0.42 ± 0.18 μmol g^{-1} DW h^{-1}) than in *U. rigida* (0.34 ± 0.06 μmol g^{-1} DW h^{-1} (**Figure 5F**).

Photosynthetic performance

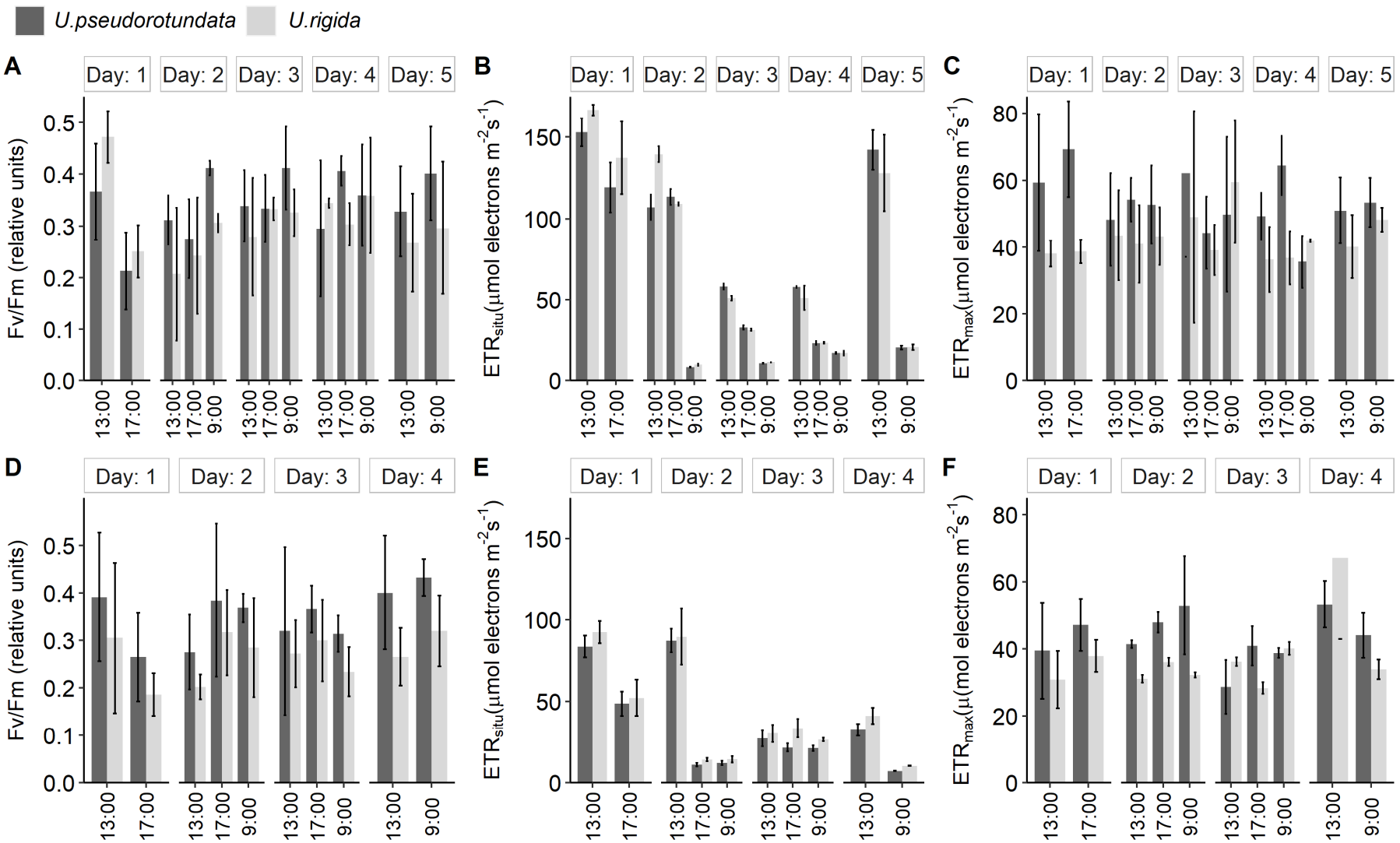

Figure 6. Diurnal changes of photosynthetic parameters: maximum quantum yield (F_v/F_m), *in situ* electron transport rate (ETR_{situ}), and maximum electron transport rate (ETR_{max}) of *U. pseudorotundata* and *U. rigida* in two conditions: 50% fish effluent (5 days): A, B, and C; 100% fish effluent (4 days): D, E, and F. Values are mean ± SD, n = 3.

Photosynthetic parameters measured during the experimental period by PAM-fluorometers are presented in **Figure 6**. In general, both *Ulva* species exhibited similar photosynthetic performance throughout the two experiments, except for electron transport rate measured directly under algal cultivation conditions (ETR_{situ}). Regarding the maximum values of potential quantum yield (F_v/F_m), although the ANOVA analysis showed a significant interaction between *time* and *day* (ANOVA: 50% = $F(6) = 0.112$, $p = 0.014$; 100% = $F(4) = 0.101$, $p = 0.029$, Table S4) such differences were not detected by the Tukey post hoc test ($p > 0.05$), which indicate that there was absence of photoinhibition even when irradiance was highest (**Figures 6A,D**). ETR_{situ} was significantly affected (ANOVA: $F(6) = 1400.8$, $p = 0.008$, Table S4) by the interaction of *species*, *hour*, and *day* just experiment 1 (50% effluent) (**Figures 6B,E**). Maximum electron transport rate (ETR_{max}) was influenced by a significant interaction (ANOVA: $F(4) = 1733.7$, $p < 0.001$, Table S4) between *hour* and *day* only in experiment 2, and no significant difference has been detected between variables in experiment 1 (**Figures 6C,F**).

Photosynthesis-nitrate removal relationship

Table 2. Spearman correlation values between nitrate biofiltration parameters and photosynthetic parameters obtained from *U. pseudorotundata* and *U. rigida* cultivation under two experimental conditions: (1) 50% fish effluent and (2) 100% fish effluent. Symbols indicate significance level: *$p < 0.05$, **$p < 0.01$, ***$p < 0.001$. Values marked with bold indicate statistically significant *p*-values.

	NUR	F_v/F_m	α_{ETR}	E_k	ETR_{max}	NPQ_{max}	ETR_{situ}	Species
NUE	**-0.367***	0.190	**0.312***	-0.123	0.138	0.024	0.052	*U. pseudorotundata*
	-0.110	0.248	**0.506*****	-0.162	0.213	0.010	0.151	*U. rigida*
NUR		**-0.374****	**-0.451*****	**0.393****	**0.261***	0.076	**0.346****	*U. pseudorotundata*
		-0.173	-0.086	0.085	-0.042	**0.510*****	**0.481*****	*U. rigida*
F_v/F_m			**0.781*****	**-0.541*****	-0.164	0.056	**-0.433*****	*U. pseudorotundata*
			0.667***	**-0.588*****	-0.172	0.029	**-0.353****	*U. rigida*
α_{ETR}				**-0.639*****	-0.015	**0.289***	**-0.301***	*U. pseudorotundata*
				-0.482***	0.066	0.145	-0.203	*U. rigida*
E_k					**0.553*****	-0.020	**0.345****	*U. pseudorotundata*
					0.425***	-0.153	0.131	*U. rigida*
ETR_{max}						**0.314***	0.203	*U. pseudorotundata*
						-0.193	-0.034	*U. rigida*
NPQ_{max}							**0.289***	*U. pseudorotundata*
							0.268*	*U. rigida*

Spearman's correlation analysis between the different fluorescence parameters and nitrate biofiltration measurements (NUR and NUE) obtained from *U. pseudorotundata* and *U. rigida* are shown in **Table 2**. The correlations obtained considering the data from experiments 1 and 2 showed that F_v/F_m, as an indicator of photoinhibition, was negatively correlated with ETR_{situ} and saturation irradiance (E_k), but positively correlated with photosynthetic capacity ($\alpha_{ETR.}$). α_{ETR} was positively correlated with NUE, and NPQ_{max} was positively correlated with ETR_{situ}.

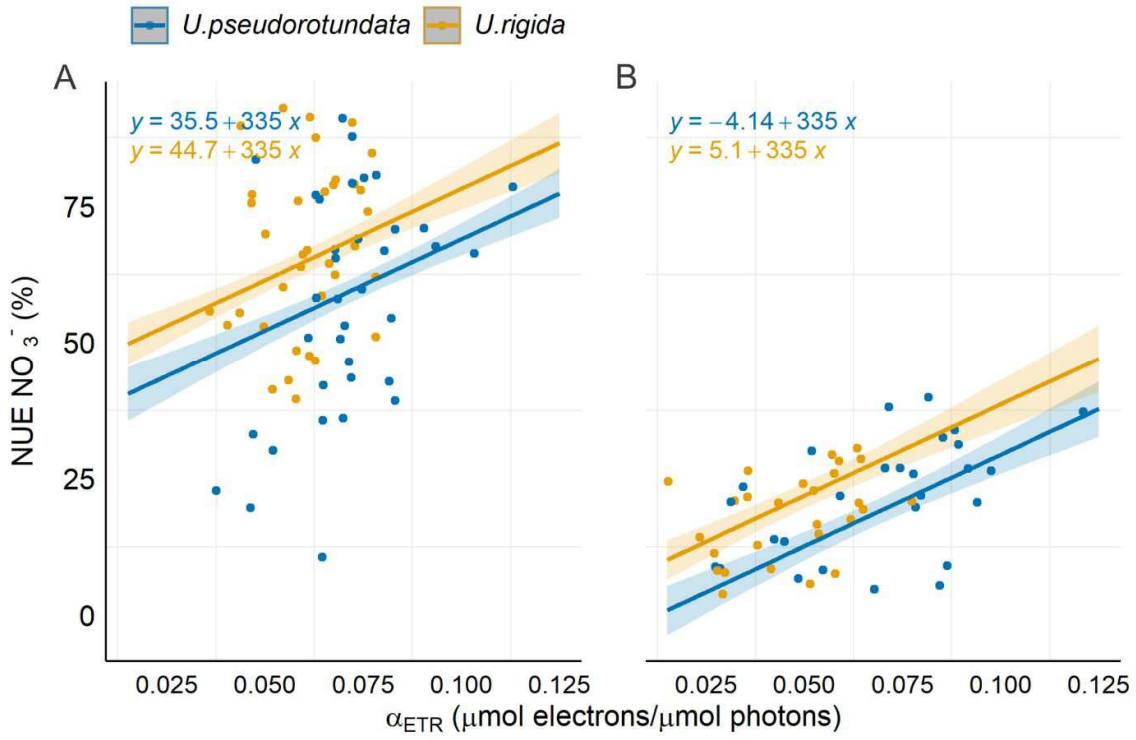

Figure 7. Linear regression model between NO_3^- uptake efficiency (NUE) and photosynthetic efficiency (α_{ETR}) for the species *U. pseudorotundata* and *U. rigida* grown in (A) 50% fish farm effluent and (B) 100% fish farm effluent. The solid line represents the fitted values of the overall model.

The linear regression model revealed that NO_3^- uptake efficiency (NUE) has a positive relationship with photosynthetic efficiency (α_{ETR}) in both *Ulva* species (**Figure 7**). In both experiments, the NO_3^- uptake efficiency significantly increased with increasing α_{ETR} (R^2 = 69.77%, F-statistic = 97.14, p <0.001).

Biomass growth rate, productivity and N content

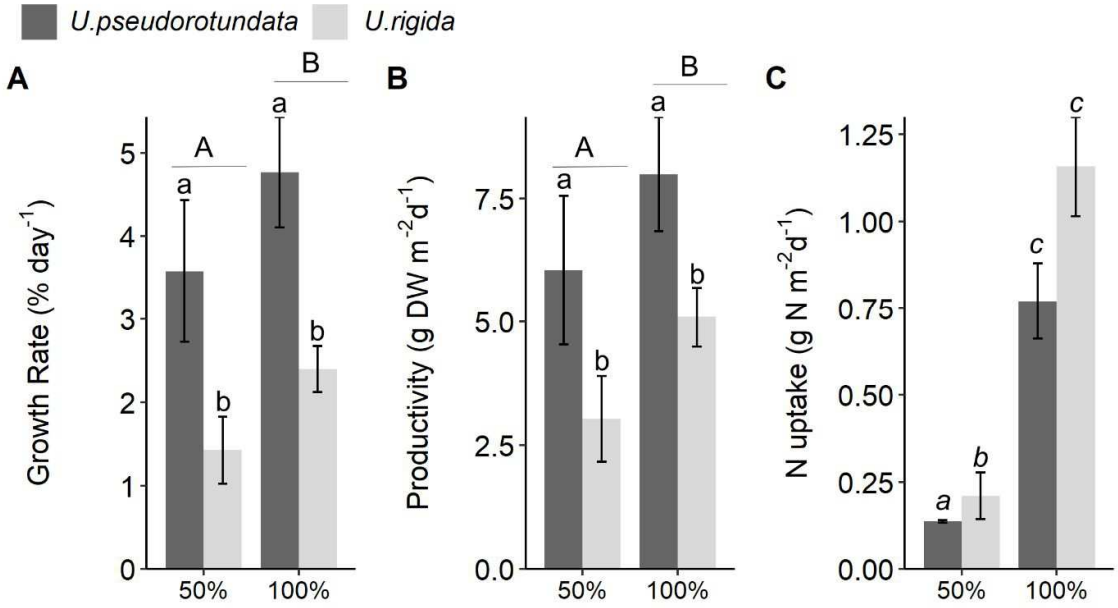

Figure 8. (A) Growth rate (% day^{-1}), (B) productivity (g DW m^{-2} d^{-1}), and (C) nitrogen uptake (g N m^{-2} day^{-1}) of *U. pseudorotundata* and *U. rigida* grown in 50% and 100% fish farm effluents. Values are mean ± SD, n = 3. Different small letters represent differences related to the factor "*species*". Different capital letters represent differences caused by the factor "*effluent concentration*". Different italic letters represent the differences caused by the interaction between the two factors.

The growth rates of both species were higher when cultivated in 100% fish farm effluent (ANOVA: $F(1) = 3.49$, $p = 0.015$, **Figure 8A**, Table S5), with *U. pseudorotundata* showing higher values than *U. rigida* (Tukey post hoc test, $p < 0.001$). Productivity data were significantly influenced by effluent concentration (ANOVA: $F(1) = 12.04$, $p = 0.009$, **Figure 8B**, Table S5), and the highest values were also associated with *U. pseudorotundata* (Tukey post hoc test, $p = 0.002$). Total nitrogen assimilation per tank was higher in *U. rigida* than in *U. pseudorotundata* in the 50% effluent experiment (Tukey post hoc test, $p = 0.005$), but there was no difference between the two species in the 100% effluent experiment (Tukey post hoc test, $p = 0.783$, **Figure 8C**).

Biochemical composition

Table 3. Elemental and biochemical composition of the dry biomass of *U. pseudorotundata* and *U. rigida* grown in different concentrations of fish pond effluent (experiment 1: 50% and experiment 2: 100%). Values of carbon (C), nitrogen (N), hydrogen (H) and protein are presented as a percentage, while the C:N ratio was calculated from the level of C and N in the dry biomass. Pigments: chlorophyll *a*, chlorophyll *b* and carotenoids are presented as concentrations in the biomass (mg g^{-1} DW). Values are mean ± SD (n = 3).

		Time	C	H	N	C:N	Protein	Chl *a*	Chl *b*	Carotenoids
Experiment 1										
50% effluent	*U. pseudorotundata*	Initial	33.13 ± 4.53	5.38 ± 0.91	3.74 ± 0.55	8.86 ± 0.54	20.41 ± 2.98	1.41 ± 0.06	0.50 ± 0.02	0.24 ± 0.01
		Final	32.41 ± 1.83	5.57 ± 0.32	3.87 ± 0.29	8.38 ± 0.18	21.10 ± 1.59	1.49 ± 0.04	0.59 ± 0.02	0.28 ± 0.01
	U. rigida	Initial	37.19 ± 1.61	6.04 ± 0.21	3.85 ± 0.23	9.70 ± 0.97	20.97 ± 1.24	0.79 ± 0.03	0.45 ± 0.02	0.26 ± 0.01
		Final	34.55 ± 1.37	5.70 ± 0.27	3.86 ± 0.25	8.97 ± 0.29	21.03 ± 1.34	1.50 ± 0.07	0.55 ± 0.03	0.26 ± 0.01
Experiment 2										
100% effluent	*U. pseudorotundata*	Initial	32.24 ± 1.94	5.67 ± 0.22	3.47 ± 0.38	9.34 ± 0.58	18.90 ± 2.08	1.20 ± 0.02	0.53 ± 0.02	0.29 ± 0.01
		Final	32.83 ± 0.08	5.70 ± 0.05	4.00 ± 0.20	8.22 ± 0.41	21.81 ± 1.08	1.00 ± 0.02	0.45 ± 0.04	0.24 ± 0.03
	U. rigida	Initial	33.28 ± 1.91	5.52 ± 0.13	3.14 ± 0.01	10.61 ± 0.61	17.10 ± 0.04	0.70 ± 0.18	0.29 ± 0.08	0.15 ± 0.05
		Final	36.84 ± 1.15	5.82 ± 0.11	4.48 ± 0.21	8.23 ± 0.36	24.41 ± 1.15	0.77 ± 0.07	0.25 ± 0.09	0.12 ± 0.04

Biomass elemental and biochemical composition of the two *Ulva* species are presented in Table 3. The contents of carbon, nitrogen and proteins, as well as the C:N ratio, showed significant differences related to the interaction between the factors *effluent concentration* and *time* (ANOVA: C% = $F(1) = 21.135$; N% = $F(1) = 1.131$; Protein% = $F(1) = 33.609$; C:N = $F(1) = 1.933$, $p < 0.05$, Table S6) and an absence of significant differences between species. Both species showed a significant increase in nitrogen and protein content when cultivated in 100% effluent (Tukey post hoc test, $p < 0.001$) while a significant reduction was observed in the C:N ratio between the beginning and end of the experiment (Tukey post hoc test, $p < 0.001$). The hydrogen content were not affected by the effluent concentration (ANOVA, $F(1) = 1.641$, $p = 0.615$, Table S6), but differences were observed between the species (ANOVA, $F(1) = 47.455$, $p = 0.004$, Table S6), with higher values for *U. rigida* (Tukey post hoc test, $p = 0.006$). The chlorophyll-*a* content was influenced by the interaction of the factors *concentration*, *species* and *time* (ANOVA, $F(1) = 0.049$, $p = 0.018$, Table S6) and the highest values were obtained at the end of experiment 1 for both species (Tukey post hoc test, *U. pseudorotundata*: $p < 0.001$; *U. rigida*: $p < 0.001$). Considering both *Ulva* species, there was an increment in Chl *b* when cultivated in 50% effluent (Tukey post hoc test, $p < 0.001$). For carotenoids, considering both *Ulva* species, the higher values were obtained when *Ulva* were cultivated in 50% fish effluent (Tukey post hoc test, $p < 0.001$).

5. DISCUSSION

To develop an efficient integrated system of fish and marine algae biomass production, a deep understanding of the physiology of species used in the system is essential. Cultivation of *Ulva* spp. using fish farming effluents as a culture medium is a promising process, as these algae have a high capacity to remove nutrients. They act as a biofilter and generate biomass with several biomolecules of high economic value such as cell wall polysaccharides (ulvans) and pigments. The improvement of marine algae cultivation systems, as well as their use in bioremediation, implies the selection of native species that are adapted to local conditions, thus avoiding the introduction of exotic species. In the current study, we compared biofiltration capacity, photosynthetic performance, productivity and biomass characteristics of *U. pseudorotundata* and *U. rigida* cultivated in effluents of *Chelon labrosus* ponds. Comparisons

were performed at two effluent concentrations under environmental conditions of light and temperature, simulating commercial production conditions. The results indicated that both *Ulva* species presented similar biofiltration performance to remove dissolved inorganic nutrients (NO_3^-, NH_4^+ and PO_4^{3-}) from fish farm effluents, enabling them as good candidates for use in integrated aquaculture systems.

Biofiltration performance

The investigation of the ability of different seaweed species to biofiltrate nutrients is fundamental for the use of these organisms as nutrient scrubbers of waste waters from mariculture activities. According to Gevaert et al. (2007), *Ulva* species can differ in their ability to uptake and assimilate nutrients due to their adaptation to stressful conditions, such as fluctuations of inorganic nitrogen concentrations. Based on this, we hypothesized that the species used in the present study could have different behaviors since they were collected from different environments. *U. rigida* was collected directly from intertidal rock pools and bare rocks, while *U. pseudorotundata* was obtained from salt marshes where they were floating suspended in the water column. Intertidal algae like *U. rigida* are exposed to a broad range of conditions such as variation in nutrients, oxygen and inorganic carbon concentrations, apart from changes in temperature, desiccation, and pH fluctuations. On the other hand, species like *U. pseudorotundata,* deal with constantly high temperatures, extreme salinities, and intense solar radiation. Despite these different stressful conditions, both species exhibited similar biofiltration performance, removing considerable amounts of nitrate (NO_3^-), ammonium (NH_4^+), and phosphate (PO_4^{3-}) from the experimental tanks. These similar responses suggest high phenotypic plasticity of both species, an important finding for use in bioremediation.

In our experiments both species showed higher uptake efficiency (NUE) for NH_4^+ when compared to NO_3^-, quickly reducing NH_4^+ concentrations at the beginning of the experiment. Our findings of this faster NH_4^+ uptake efficiency is in agreement with previous studies on *Ulva* spp. (SHAHAR et al., 2020; SHPIGEL et al., 2019) and must be related to the mechanisms of uptake and assimilation of different nitrogen forms (ROLEDA; HURD, 2019). Since less energy is required for NH_4^+ assimilation and metabolization into amino acids, *Ulva* spp. tend to remove this nutrient more efficiently than NO_3^-. On the other hand NO_3^- metabolism is described as an energy-dependent mechanism that requires active transport to cross cell walls, followed by storage in intracellular pools such as nitrate and/or metabolization into ammonia

through two-step sequential enzymes (nitrate and nitrite reductase) (HURD et al., 2014). As observed by Shpigel et al. (2019), nitrate uptake by *U. lactuca* initiated only 24 hours after total ammonia depletion, which was suggested by the authors as the time required for nitrate reductase synthesis. A study performed with *U. fasciata* revealed nitrate reductase activity after 28 hours of transfering the algae from a medium with total ammonia nitrogen as the only nitrogenous nutrient to NO_3^- enriched seawater (SHAHAR et al., 2020). Considering the high concentrations of NH_4^+ and NO_3^- available in the effluents used, the remaining stock of NO_3^- measured at the end of the second experiment may be related to a saturation of nitrogen required by algae metabolism. Similar results were described by Fan et al. (2014), which observed that increasing NO_3^- levels, over a concentration of 503 µmol L^{-1}, lead to a decay in NO_3^- uptake rate by *U. prolifera*.

PO_4^{3-} concentrations in the fish farm effluents used in our study were enough to avoid phosphorus limitation for seaweed growth during experimental time. The lower values of PO_4^{3-} removal, when compared to the removal of nitrogenous nutrients, are probably related to the differentiated assimilation rates of these nutrients (Redfield ratio), which is typical of photosynthetic organisms. If, on the one hand, this result suggests that fish farming effluents are not ideally balanced for algal growth, on the other hand, it indicates that this excess of P is not harmful to their growth, since the productivity values were similar in both effluent concentrations.

Photosynthetic performance

Unlike cultures developed in the laboratory, where algae are subjected to controlled and regular conditions of light and photoperiod, cultures performed under environmental conditions are subjected to considerable variations in the luminous environment. Under these conditions, photoinhibition and photochemical damage without proper recovery have been known to occur in the middle of the day, i.e. chronic photoinhibition, when increased irradiances reach the cultivation systems and the amount of absorbed light is higher than the photosystem's capacity. In a practical way, photoinhibition has been detected by the determination of the maximum quantum yield of PSII (F_v/F_m) using PAM fluorometers (CRUCES et al., 2019; FIGUEROA et al., 2006, 2020; HANELT; NULTSCH, 1995). In the present study, we did not detect significant differences in the values of F_v/F_m determined at different times of the day for the two algae, suggesting the absence of photoinhibition. These

results differ from other studies carried out under similar conditions which observed a decrease in F_v/F_m at noon (CRUCES et al., 2019; FIGUEROA et al., 2020; MASOJÍDEK et al., 2021), and can be explained by special adaptations of *Ulva* spp. to light fluctuations. Some of the adaptive mechanisms described for *Ulva* spp. are the synthesis of UV-screening and antioxidant compounds (e.g. phenolic compounds), dissipation of energy as heat (xanthophyll cycle), and enzyme-based antioxidant activity (e.g. superoxide dismutase and ascorbate peroxidase) (BISCHOF et al., 2002; CRUCES et al., 2019). The regulation of internal physiological mechanisms of seaweeds to face photoinhibition and photodamage may be related to cultivation conditions, such as the supply of nutrients. Previous studies showed that photoinhibition caused by an increase in PAR was reduced under the increment of nutrient supply (CABELLO-PASINI et al., 2011; FIGUEROA et al., 2006; HENLEY et al., 1991). Since our culture systems contained sufficient nutrients, we can expect that such mechanisms were active for both species.

Contrasting with results obtained in other studies (eg. Cruces et al., 2019) that showed that ETR_{max} fluctuations along the day had an inverse relationship with PAR irradiances, our study does not identify a decrease in ETR_{situ} and ETR_{max} during irradiance peaks, but an increasing trend confirming the absence of photoinhibition. Similar results were obtained by Figueroa et al. (2020), which described increased ETR values and decreased F_v/F_m at noon. Our findings of a negative correlation between F_v/F_m and ETR_{situ} obtained from both *Ulva* species corroborate the aforementioned inverse correlation. These results reflect that while photosynthetic activity (ETR) tends to increase, the maximum quantum yield (F_v/F_m) tends to decrease as solar irradiance rises as a result of the photoprotection mechanisms presented by algae. Also, the negative correlation we detected between F_v/F_m and Ek is consistent with results reported by Figueroa et al. (2020), being related to the diurnal variations in irradiance. Finally, the photochemical efficiency (α_{ETR}) extracted from rapid light curves and F_v/F_m, despite being obtained from different methods, showed a positive correlation, reinforcing the reliability of PAM fluorometer data.

Photosynthesis-nitrate removal relationship

Nitrogen metabolism requires energy supplied directly from photosynthetic electron transport since the assimilation of inorganic nitrogen into amino acids demands carbon skeletons (ketoacids), energy in the form of ATP and reductants (HUPPE; TURPIN, 1994). As described by Huppe and Turpin (1994), inorganic nitrogen metabolism of seaweeds, regardless

of whether the original source is ammonium or nitrate, involves the incorporation of nitrogen into amino acids by the assimilation of ammonium through the glutamine synthetase (GS) and glutamine:2-oxoglutarate amino- transferase (GOGAT) pathway. For the maintenance of GOGAT activity, seaweed requires an adequate supply of carbon assimilated from photosynthetic activity. In this context, in the present study we present a mathematical relation between photosynthetic and biofiltration parameters. Spearman's correlation showed a positive relationship between α_{ETR} and NO_3^- uptake efficiency (NUE) for the two algal species. In addition, a linear model was obtained and reveals a positive relationship ($r^2 = 69.77\%$) between α_{ETR} and NUE, which is largely in line with the evidence that nitrate removal requires a coordination of the metabolic interactions between photosynthesis, respiration, and N assimilation (TURPIN et al., 1988). Moreover, NO_3^- assimilation demands larger quantities of carbon from the respiratory process and therefore we assume that the proposed model is valid only for nitrate as a source of nutrients, and does not include NH_4^+. The evidence for the integration of carbon and nitrogen assimilation has also been described in previous investigations with microalgae and seaweeds (FIGUEROA et al., 2009b; HUPPE; TURPIN, 1994; TURPIN, 1991). However, as far as we could verify, a mathematical model which correlated NO_3^- biofiltration and a photosynthetic parameter obtained with rapid measurements of *in vivo* chlorophyll *a* fluorescence has not yet been published.

Biomass productivity

Despite productivity values were relatively low compared to other studies, *U. pseudorotundata* and *U. rigida* were able to grow in effluent concentrations tested in this study and, considering that the experiments were performed in a system exposed to natural environmental conditions, it confirms the tolerance of both species to non-controlled changes in temperature and light. The best results were achieved for the *U. pseudorotundata* cultivation with system productivity values reaching 8.0 g DW m^{-2} d^{-1}. The feasibility of both *Ulva* species to keep growth even with temperature and light variations was in accordance with studies carried out with other *Ulva* species cultivated in mariculture effluent under open scale conditions. The maximum growth values obtained for *U. pseudorotundata* (4.8% ± 0.7) and *U. rigida* (2.4% ± 0.3) were lower than those previously obtained for *U. lactuca* (4-18% d^{-1}, Al-Hafedh et al., 2014; Shpigel et al., 2019) and *U. fasciata* (7.5-14.3% d^{-1}, Shahar et al., 2020). This may be related to the difference in the system's culture conditions such as nutrient source

(SHAHAR et al., 2020), biomass stocking densities (SHPIGEL et al., 2019), and effluent flow rate (AL-HAFEDH; ALAM; BUSCHMANN, 2014). Besides culture systems, environmental conditions directly influence biomass production. As verified by Friedlander et al., (1990), in land intensive seaweed cultivation not limited by nutrients, biomass productivity was influenced by changes in light and temperature as a result of season variability. In a study conducted in Portugal, Abreu et al., (2011) described the optimal relative growth rate and productivity for the red seaweed *Gracilaria vermiculophylla* during spring and summertime, with a decrease in growth rates and nutrient removal during autumn and winter months. In a 6-month study conducted with *U. ohnoi*, Mata et al. (2016) showed that biomass productivity had a temporal variation due to changes in temperature and light, and they also observed a positive relationship between light and biomass productivity. Those achievements indicate that a better understanding of cultivation conditions is essential to optimize system productivity.

Biochemical composition

Seaweed biomass is a source of bioactive compounds like pigments (chlorophyll and carotenoids), proteins, phenolic compounds, sulfated polysaccharides, which are known for their beneficial properties for human health (FARVIN; JACOBSEN, 2013; FLEURENCE; CHENARD; LUÇON, 1999; KALASARIYA et al., 2021; SCHNEIDER et al., 2020). Our results showed that *U. rigida* and *U. pseudorotundata* present similar protein content, ranging from 17.1 to 24.4% DW. These values are similar to those found in studies with *U. lactuca* (e.g. 10-25%, Shuuluka et al., 2013), *U. armoricana* (18%-24%, Fleurence et al., 1999), and *U. fenestrata* (20.79%, Steinhagen et al., 2022). In general, the protein content of *Ulva* species could vary between 10 and 47% DW (DOMINGUEZ; LORET, 2019). Higher values (up to 40%) were described for *U. fasciata* (30-38%, Shahar et al., 2020) and *U. lactuca* (24.9-41.1%, Shpigel et al., 2019) grown in nutrient-enriched seawater. In the present study, after cultivated in pure fish effluent, an increment in protein content of 5.1% was detected in both *Ulva* species. Since NH_4^+ concentrations were higher in pure effluent and complete removal of this nutrient was observed, it is plausible to assume that the higher uptake of N may be associated with a higher assimilation of N for amino acids and proteins. This result is in agreement with those reported by Shahar et al., (2020), which observed an increase in protein content in *Ulva* that was cultivated using only total ammonia nitrogen (TAN) rather than NO_3^- as a sole nitrogen source.

Chlorophylls and carotenoids are pigments of interest to the cosmetic and pharmaceutical areas mainly due to their antioxidant and anticancer capacity (BOOMINATHAN; MAHESH, 2015; KALASARIYA et al., 2021; PÉREZ-GÁLVEZ; VIERA; ROCA, 2020). When cultivated under conditions tested in our experiment, both *Ulva* species showed similar amounts of chlorophyll *a*, but not chlorophyll *b* and carotenoids. Moreover, although a variation in pigment composition was detected over the experimental time, it was less pronounced than that reported by Steinhagen et al., (2022), who observed a sharp decay in chlorophyll *a* and *b* and carotenoid content from *U. fenestrata* biomass grown in a sea based cultivation, under non-controlled conditions. So, the biomass of *Ulva* species used in this study remained with available pigments to be profitable in the above mentioned application, in a complementar alternative for biomass utilization.

6. CONCLUSIONS

Our study advanced toward biofiltration capacity, photosynthetic performance, productivity and biomass characteristics of *U. pseudorotundata* and *U. rigida* cultivated in effluents of *Chelon labrosus* ponds under natural environmental conditions of light and temperature. In conclusion, our findings show that *U. pseudorotundata* and *U. rigida* possess similar capabilities for removing inorganic nutrients from fish effluents. Both seaweed species, naturally found on the Spanish Mediterranean coast, presented equivalent photosynthetic performance and biomass composition. A linear regression model between NO_3^- uptake efficiency and photosynthetic efficiency (α_{ETR}) is presented. In addition, we highlighted the application of *U. pseudorotundata* and *U. rigida* as robust species for nutrient scrubbing of mariculture effluents, and their potential biomass composition as a sustainable source of raw material for the development of industrial products.

8. ACKNOWLEDGMENTS

We sincerely thank the Federal University of Santa Catarina (UFSC) and University of Malaga (UMA), especially the faculty members and technical staff of the Laboratory of Phycology (LAFIC - UFSC), Laboratory of Fotobiología y Biotecnología de Organismos acuáticos (FYBOA - UMA), research center Grice Hutchinson (UMA), and Servicios Centrales de Apoyo a la Investigación (SCAI - UMA) for providing space and resources for this work. We also thank Marta G. Sanchez, Cristina V. G. Fernández, Fabian Lopez, David Paniagua, Roberto Abdala, Nathalie K. Peinado, and Ellie Bergstrom for their support and assistance in carrying out experiments, data collection and manuscript revision. This study is part of the Doctoral

thesis of the first author to the UFSC Graduate Program in Biotechnology and Bioscience, Santa Catarina, Brazil.

Funding

Financial resources and scholarships were provided by: Andalusia Government (Spain) in the frame of the Project FACCO - UMA18-FEDER JA-162, Santa Catarina State Foundation for Research and Innovation Support (FAPESC process no 03/2017, Brazil), and Coordination for the Improvement of Higher Education Personnel (CAPES/PRINT process nos. 88887.470102/2019-00, Brazil). We also thanks the Conselho Nacional de Desenvolvimento Científico e Tecnológico (CNPq) financial support through research grants.

Data availability statement

The datasets generated during and/or analyzed during the current study are available from the corresponding author upon reasonable request.

Conflict of Interest

The authors declare that the research was conducted in the absence of any commercial or financial relationships that could be construed as a potential conflict of interest.

Author Contributions

TM: participated in the experimental design, experimental execution, water chemical analysis, statistical analysis, data interpretation, and original draft. VR and JV: participated in the experimental design and execution. BM and PCV: participated in the experimental execution. LPS: participated in the execution of statistical analysis and data interpretation. WO: provided the species phylogenetic analysis. AA: dedicated to water chemical analysis. JBB: participated in the experimental design and data interpretation. LR and FF: reviewed, edited the manuscript text, supervised and provided funding acquisition.

9. SUPPLEMENTARY MATERIAL

Abiotic parameter (pH, salinity, and oxygen) values obtained in experiments 1 and 2 are presented in table S1. In general, pH values in *Ulva* tanks ranged between 7.9 and 10.1 in experiment 1 and from 6.6 to 8.2 in experiment 2, considering all tanks of algae cultivation. The salinity ranged between 34 and 39 in experiment 1 and from 33 to 38 in experiment 2. Oxygen levels obtained in experiment 1 were 8.48 ± 0.84 mg L^{-1} and in experiment 2, were 8.26 ± 0.49 mg L^{-1}.

Table supplementary 1. Abiotic parameters: pH, salinity and oxygen (mg L^{-1}) profiles measured in the algal tanks cultivation throughout experiments 1 (50% fish effluent) and 2 (100% fish effluent). Values are mean ± SD, n = 3.

Time (experimental day)	*U. pseudorotundata*		*U. rigida*	
	AVG	SD	AVG	SD
Experiment 1: 50% effluent				
pH				
1	7.9	± 0.1	7.9	± 0.2
2	9.4	± 0.2	9.8	± 0.1
3	10.0	± 0.1	10.1	± 0.1
4	9.3	± 0.1	9.7	± 0.2
5	10.1	± 0.1	9.9	± 0.2
Salinity				
1	36	± 0.8	34	± 4.4
2	37	± 0.9	37	± 2.3
3	38	± 1.0	37	± 2.4
4	38	± 1.0	38	± 2.5
5	39	± 1.0	38	± 2.5
Oxygen (mg L^{-1})				
1	7.88	± 0.24	8.09	± 0.11
2	9.07	± 0.07	8.7	± 0.75
3	–	± –	–	± –
4	9.35	± 0.8	8.61	± 0.88
5	9.47	± 0.6	9.05	± 0.4
Experiment 2: 100% effluent				
pH				
1	7.1	± 0.0	7.0	± 0.1
2	6.7	± 0.2	6.6	± 0.0
3	7.4	± 0.5	8.0	± 0.0
4	7.9	± 0.0	8.2	± 0.1
Salinity				
1	36	± 0.9	33	± 4.1
2	37	± 1.1	35	± 2.8
3	38	± 0.8	36	± 2.1

4	38	± 1.0	36	± 1.2
Oxygen (mg L^{-1})				
1	7.62	± 0.12	7.66	± 0.34
2	8.22	± 0.25	8.23	± 0.12
3	8.59	± 0.30	8.06	± 0.33
4	8.73	± 0.40	9.00	± 0.28

Table supplementary 2. ANOVA analysis of nutrient concentration data (NO_3^-, NH_4^+, and PO_4^{3-}) from cultivation of *U. pseudorotundata* and *U. rigida* under two experimental conditions: (1) 50% fish effluent and (2) 100% fish effluent. Data are shown comparing experimental day, the hour of experiment, and the two species. *df:* degree of freedom; *R Sum Sq:* sum of squared deviations. Significant differences ($p < 0.05$) are shown in bold.

Nutrient source	Experiment (effluent concentration)				Experiment (effluent concentration)		
	1 (50% effluent)				2 (100% effluent)		
NO_3^-		*df*	R Sum Sq	*p-value*	*df*	R Sum Sq	*p-value*
	Day (1)	4	1854243.0	**0.000**	3	849860.0	**0.000**
	Hour (2)	4	137336.0	**0.000**	4	75427.0	**0.001**
	(1) x (2)	6	113681.0	**0.001**	4	2510	0.102
	Species (3)	1	6073.0	0.134	1	4840.0	0.332
	(1) x (3)	4	10564.0	0.548	3	28012.0	**0.019**
	(2) x (3)	4	15159.0	0.563	4	9704.0	0.526
	(1) x (2) x (3)	6	18297.0	0.727	4	13345.0	0.575
	Residuals	60	278000.0		48	141800.0	
NH_4^+							
	Day (1)	4	16375.0	**0.000**	3	170136.5	**0.000**
	Hour (2)	1	16061.0	**0.000**	1	102465.3	**0.000**
	Species (3)	1	27.0	0.922	1	39.1	0.413
	(1) x (3)	4	72.0	0.183	3	3305.7	**0.000**
	(2) x (3)	1	49.0	**0.031**	1	2381.2	**0.000**
	Residuals	24	225.0		20	1311.6	
PO_4^{3-}							
	Day (1)	4	1842.6	**0.004**	3	1974.8	**0.000**
	Hour (2)	1	50.0	0.380	1	9.8	0.667
	Species (3)	1	205.6	0.079	1	0.3	0.961
	(1) x (3)	4	105.6	0.877	3	6.4	0.868
	(2) x (3)	1	8.1	0.824	1	3.7	0.554

Residuals	24	1954.9	20	272.0	

Table supplementary 3. ANOVA analysis of nutrient uptake rate (NUR) and uptake efficiency (NUE) of *U. pseudorotundata* and *U. rigida* under two experimental conditions: (1) 50% fish effluent and (2) 100% fish effluent. Data are shown comparing experimental days and the two species. *df:* degree of freedom; *R Sum Sq:* sum of squared deviations. Significant differences ($p < 0.05$) are shown in bold.

Nutrient source	Experiment (effluent concentration)											
NUR NO_3^-		1 (50% effluent)			2 (100% effluent)			NUE NO_3^-	1 (50% effluent)			2 (100% effluent)		
		df	R Sum Sq	*p-value*	*df*	R Sum Sq	*p-value*		*df*	R Sum Sq	*p-value*	*df*	R Sum Sq	*p-value*
	Day (1)	4	30369.6	**0.000**	3	7444.1	**0.000**		4	13641.2	**0.000**	3	1867.9	**0.000**
	Species (2)	1	264.7	**0.000**	1	284.0	**0.001**		1	1006.8	**0.000**	1	138.5	**0.000**
	(1) x (2)	4	1323.3	**0.000**	3	198.0	**0.001**		4	544.5	**0.000**	3	59.1	**0.021**
	Residuals	20	129.1		16	82.3			20	326.1		16	70.4	
NUR NH_4^+								NUE NH_4^+						
	Day (1)	4	2862.4	**0.000**	3	15611.6	**0.000**		4	27.7	**0.007**	3	2006.0	**0.000**
	Species (2)	1	65.1	**0.001**	1	557.2	**0.000**		1	8.2	**0.023**	1	289.3	**0.001**
	(1) x (2)	4	161.3	**0.000**	3	1295.7	**0.000**		4	4.8	0.666	3	574.6	**0.001**
	Residuals	20	68.4		16	5.2			20	25.5		16	200.9	
NUR PO_4^{3-}								NUE PO_4^{3-}						
	Day (1)	4	22.987	**0.000**	3	0.239	**0.000**		4	2711.6	**0.000**	3	383	**0.000**
	Species (2)	1	0.019	0.155	1	0.034	**0.001**		1	215.3	**0.000**	1	18	**0.007**
	(1) x (2)	4	0.042	0.414	3	0.139	**0.000**		4	55.6	0.426	3	31	**0.002**
	Residuals	20	0.199		16	0.016			20	265.1		16	24	

Table supplementary 4. ANOVA analysis of photosynthetic parameters of *U. pseudorotundata* and *U. rigida* during cultivation under two experimental conditions: (1) 50% fish effluent and (2) 100% fish effluent. Data are shown comparing species, the time of day (hour) and day of the experiment. *df*: degree of freedom; *R Sum Sq:* sum of squared deviations. Significant differences ($p < 0.05$) are shown in bold.

Variable	Experiment (effluent concentration)						
	1 (50% effluent)				2 (100% effluent)		
F_v/F_m		*df*	R Sum Sq	*p-value*	*df*	R Sum Sq	*p-value*
	Species (1)	1	0.017	0.073	1	0.027	0.100
	Hour (2)	2	0.006	0.863	2	0.011	0.703
	(1) x (2)	2	0.018	0.183	2	0.001	1.000
	Day (3)	4	0.040	0.201	3	0.039	0.188
	(1) x (3)	4	0.046	0.135	3	0.003	0.975
	(2) x (3)	6	0.112	**0.014**	4	0.101	**0.029**
	(1) x (2) x (3)	6	0.030	0.669	4	0.001	1.000
	Residuals	52	0.342		40	0.364	
ETR_{situ}		*df*	R Sum Sq	*p-value*	*df*	R Sum Sq	*p-value*
	Species (1)	1	168.7	0.127	1	227.8	**0.006**
	Hour (2)	2	4767.0	**0.000**	2	80.8	0.480
	(1) x (2)	2	47.4	1.000	2	64.4	0.408
	Day (3)	4	56008.0	**0.000**	3	11157.2	**0.000**
	(1) x (3)	4	655.2	**0.038**	3	114.7	0.275
	(2) x (3)	6	23896.4	**0.000**	4	10827.2	**0.000**
	(1) x (2) x (3)	6	1400.8	**0.008**	4	90.6	0.698
	Residuals	52	3366.8		40	1508.1	
ETR_{max}		*df*	R Sum Sq	*p-value*	*df*	R Sum Sq	*p-value*
	Species (1)	1	303.3	0.146	1	169.8	0.073
	Hour (2)	2	431.2	0.203	2	155.1	0.351
	(1) x (2)	2	865.8	0.098	2	316.4	0.108
	Day (3)	4	754.1	0.513	3	604.3	0.053
	(1) x (3)	4	303.9	0.891	3	429.3	0.093
	(2) x (3)	6	1314.0	0.328	4	1733.7	**0.000**
	(1) x (2) x (3)	6	624.8	0.754	4	425.7	0.174
	Residuals	52	9358.9		40	2794.5	

Table supplementary 5. ANOVA analysis of growth rate (GR), productivity, and nitrogen uptake (N uptake) of *U. pseudorotundata* and *U. rigida* after being cultivated in two medium conditions: 50% fish effluent and 100% fish effluent. Data shown compare experiments and species. *df:* degree of freedom; *R Sum Sq:* sum of squared deviations. Significant differences ($p < 0.05$) are shown in bold.

Variable		GR		Productivity		N uptake	
Source	*df*	R Sum Sq	*p-value*	R Sum Sq	*p-value*	R Sum Sq	*p-value*
Experiment (1)	1	3.49	**0.015**	409.60	0.863	1.87	**0.000**
Species (2)	1	15.36	**0.000**	152240.38	**0.003**	0.16	**0.003**
(1) x (2)	1	0.03	0.745	658.51	0.725	0.07	**0.027**
Residuals	8	2.81		21415.69		0.07	

Table supplementary 6. ANOVA analysis of the elemental and biochemical composition of the dry biomass of *Ulva pseudorotundata* and *U. rigida* before and after cultivation in different sources of *Chelon labrosus* effluent: 50% and 100% effluent concentrations. Data are shown comparing experiment, species, and time. *df:* degree of freedom; *R Sum Sq:* sum of squared deviations. Significant differences ($p < 0.05$) are shown in bold.

Variable		%C		%H		%N		C:N		%Protein		Chl *a*		Chl *b*		Car.	
Source	*df*	R Sum Sq	*p-value*	R Sum Sq	*p-value*	R Sum Sq	*p-value*	R Sum Sq	*p-value*	R Sum Sq	*p-value*	R Sum Sq	*p-value*	R Sum Sq	*p-value*	R Sum Sq	*p-value*
Experiment (1)	1	1.641	0.548	1.641	0.615	0.021	0.804	0.087	0.444	0.619	0.667	0.863	**0.000**	0.119	**0.000**	0.023	**0.000**
Species (2)	1	47.455	**0.002**	47.455	**0.004**	0.021	0.615	2.755	**0.007**	0.622	0.686	0.665	**0.000**	0.103	**0.000**	0.025	**0.000**
(1) x(2)	1	0.507	0.804	0.507	0.706	0.001	0.922	0.007	0.941	0.034	0.961	0.006	0.314	0.048	**0.001**	0.026	**0.000**
Day (3)	1	0.233	0.843	0.233	0.706	1.516	**0.000**	8.313	**0.000**	45.021	**0.000**	0.156	**0.000**	0.002	0.408	0.001	0.408
(1) x (3)	1	21.135	**0.044**	21.135	0.063	1.131	**0.005**	1.933	**0.023**	33.609	**0.005**	0.314	**0.000**	0.035	**0.001**	0.005	**0.021**
(2) x (3)	1	0.404	0.765	0.404	0.980	0.179	0.144	0.852	0.183	5.308	0.103	0.316	**0.000**	0.001	0.505	0.000	0.516
(1) x (2) x (3)	1	8.987	0.191	8.987	0.175	0.320	0.085	0.376	0.335	9.507	0.079	0.049	**0.018**	0.001	0.706	0.001	0.223
Residuals	16	74.126		74.126		1.451		4.705		43.094		0.098		0.037		0.012	

CAPÍTULO 3

Manuscrito a ser submetido ao periódico *Marine Biotechnology*

Characterization, antioxidant and cytotoxicity activity of ulvan polysaccharide-rich fraction obtained from *Ulva pseudorotundata* and *Ulva rigida* and their potential for pharmaceutical application.

Massocato, T.*[1], Robles-Carnero, V.[2], Rodrigues, B.[1], Castro-Varela, P.[2], Bonomi-Barufi, J.[1], Abdala-Díaz, R.[2], Rörig, L.[1], Figueroa, F.[2]

[1]Pos-Graduate Program in Biotechnology and Biosciences, Phycology Laboratory, Department of Botany, Biological Sciences Center, Federal University of Santa Catarina, Florianópolis 88040-900, Santa Catarina, Brazil

[2] Malaga University, Andalusian Institute of Blue Biotechnology and Development (IBYDA), Experimental Centre Grice Hutchinson, Malaga University, Malaga 29004, Spain.

1. ABSTRACT

Seaweed from the genus *Ulva* (Ulvales, Chlorophyta) has worldwide distribution presenting a potential biomass source for biotechnological applications. In the present study we investigated ulvan polysaccharide-rich fraction (UPRF) isolated from two *Ulva* species (*U. rigida* and *U. pseudorotundata*), naturally occurring in the Spanish Mediterranean coast. Elemental and chemical characterization of UPRFs were performed in order to explore the polysaccharides composition. Biological assessment of UPRFs were compared by antioxidant activity and *in vitro* toxicity tests in human cell lines: HCT-116 (colon cancer), G-361 (malignant melanoma), U-937 (leukemia), and HACAT cells (immortalized keratinocytes). Chemical analysis revealed that both UPRFs presented rhamnose as the major sugar constituent (>50%) followed by glucose in *U. rigida* and xylose in *U. pseudorotundata* and also presenting glucuronic acid, galactose, ribose and mannose as the remaining monosaccharides. Similar antioxidant activity was obtained with increasing potential in response to the increment of polysaccharide concentrations. Both UPRFs presented moderate toxicity against HCT-116 cell lines and a selectivity index ≥3, suggesting a good potential for use in pharmaceutical products.

Keywords

Algal biotechnology, Antioxidant activity, *In vitro* cytotoxicity, *Ulva* spp., ulvan polysaccharides

2. INTRODUCTION

The search for sustainable sources to the development of industrial products has gained increasing attention in recent years. In this context, marine algae biomass has a huge potential as a source of promising biomolecules, being an emerging sector of the blue bioeconomy (ARAÚJO et al., 2021). Marine macroalgae, also known as seaweed, is a diverse group composed by more than 12,000 species including red (Rhodophyta), brown (Phaeophyceae), and green algae (Chlorophyta). Seaweed biomass can be a source for a wide range of applications such as food, agricultural, cosmetic and pharmaceutical industries since it is rich in primary (e.g. protein, peptides, carbohydrates, lipids) and secondary metabolites (e.g. pigments, polyphenols, phenolic compounds) (BUSCHMANN et al., 2017b). According to FAO (2020), the world production of seaweed has increased through the years, being used primarily for the food sector. Moreover, researchers have shown different potential applications for algal extracts and isolated compounds due to their bioactivity and *in vivo* effects on primary cells (KALASARIYA et al., 2021; MICHALAK; CHOJNACKA; SAEID, 2017; VEGA et al., 2021).

The diversity of compounds found in seaweed is associated to physiological adaptive mechanisms, which enable them to survive in constantly changing conditions like fluctuations in nutrient availability, light intensity, temperature, desiccation and the synthesis of chemical defenses against grazers (HURD et al., 2014). Throughout the synthesis of pigments (phycobilins, carotenoids, and chlorophylls) and other secondary metabolites, seaweeds can deal, for example, with increasing irradiances by developing photoprotection mechanisms such as the production of UV-screening and antioxidant compounds (e.g. mycosporine-like amino acids, phlorotannins, and phenolic compounds) (CRUCES et al., 2019; MENG et al., 2021; VEGA et al., 2021). Several studies demonstrated that molecules isolated from macroalgae have a range of applications in the pharmaceutical and cosmetic industries due to their antioxidant, anti-inflammatory, anticancer, antiviral, and photoprotective bioactivity (ÁLVAREZ-GÓMEZ et al., 2019; SCHNEIDER et al., 2020; VEGA et al., 2020b). Experiments conducted with polysaccharides isolated from the red algae *Hypnea spinella* and *Halopithys incurva* showed the capacity of these compounds to induce the synthesis of cytokines by murine macrophages (ABDALA-DÍAZ et al., 2011). Immunomodulatory and antioxidant activities of sulfated polysaccharides from *Laminaria ochroleuca*, *Porphyra umbilicalis*, and *Gelidium corneum* were also described by Abdala-Díaz et al. (2019). The

search for compounds of biotechnological interest becomes attractive especially for cultivable seaweed that present features like fast growing and robustness for large-scale cultivation, ensuring high quality biomass and the obtention of bioproducts with consistent composition.

The green macroalgae from the genus *Ulva* (Ulvales, Chlorophyta), commonly named as *sea lettuce*, have worldwide distribution and the ability to grow in a wide range of temperature and salinity (MANTRI et al., 2020). Moreover, *Ulva'*s species have a fast growth rate and high nutrient uptake efficiency (ASHKENAZI; ISRAEL; ABELSON, 2019; COHEN; NEORI, 1991; SHPIGEL et al., 2019). Those features enable *Ulva* spp. for commercial production, especially if linked to mariculture crops acting as a biofilter and as a source of high value biomass. Increasing attention has been given to the *Ulva*'s cell wall polysaccharides, ulvans. Ulvan is a water-soluble sulfated polysaccharide present in the cell wall which could vary from 9 to 36% of *Ulva* dry biomass and is mainly composed of the monosaccharides rhamnose, glucuronic acid, iduronic acid and xylose (LAHAYE; ROBIC, 2007; LAKSHMI et al., 2020; SUDHA; GOMATHI; KIM, 2020). Studies have described biological activities of ulvan as anticoagulant, immunomodulating, anticancer, antioxidant, anti-viral, antihyperlipidemic (KIDGELL et al., 2019b; QI et al., 2012; TZIVELEKA; IOANNOU; ROUSSIS, 2019b). The bioactivity of ulvan is linked to its ability to mimic naturally occurring cellular molecules in animal systems, such as glycosaminoglycans and proteoglycans, which are involved in distinct biological processes. The potential of ulvan as an anticancer molecule has been studied by the cytotoxicity against tumor cells. Ahmed and Ahmed (2014) demonstrated inhibition of cell proliferation of hepatoma (HepG2) and colon carcinoma (HCT116) cell lines with gradual increasing doses of ulvan, suggesting induction of apoptosis and cell cycle arrest of cancerous cells. However, structural features of ulvan, such as molecular weight, degree of sulfation, pattern of sulfation and constituent sugars, can impact its bioactivity performance (KIDGELL et al., 2019a). In this way, the composition of ulvan obtained from different species of *Ulva*, as well as their cultivation environment and previous ecophysiological conditions, could significantly influence ulvan's bioactivity.

The objective of the present study was to determine the structure and biological activities of an ulvan polysaccharide-rich fraction (UPRF) from two *Ulva* species: *U. rigida* and *U. pseudorotundata* collected in Southern Spain. To achieve these objectives the following procedures were performed: (1) extraction, characterization and identification of polysaccharides elemental constituents and molecular structure, (2) evaluation of

UPRFantioxidant capacity, and (3) determination of UPRF cytotoxicity against human cancer cell lines including HCT-116 (human colon cancer), G-361 (human malignant melanoma), U-937 (leukemia cell line). In order to determine the selectivity index of the UPRF, the cytotoxicity was also determined in HACAT cells (immortalized human keratinocytes). The results provide a background for the exploration of seaweeds as sources for medicinal and health products.

3. MATERIAL AND METHODS

Collection and cultivation of algal biomass

Ulva species used in the present studied were collected from two different places*: U. pseudorotudata* was collected from the salt marshes in the bay of Cádiz (36º30'N, 6º10'W) and, *U. rigida* was obtained from rocky intertidal shores of Málaga (36°42'43"N, 4°19'19"W), both situated at Andalusia (Spain). Algal biomass was transported and cultivated at Grice Hutchinson research center at Malaga University during the summer of 2020. Prior to cultivation, the biomass was cleaned to remove epiphytes, epibionts and sediments, than it was allocated in 500 L rectangular-shaped tanks containing artificial seawater and supplemented twice a day with 75 µmol L^{-1} of NH_4 NO_3, as nitrogen source, and 5 µmol L^{-1} of KH_2PO_4, as phosphorus source. Salinity and pH of the seawater were maintained at 35 and 8.0, respectively, and cultivation system was placed outdoor under ambient conditions of irradiance and temperature. When cultures reached sufficient fresh weight, the biomass was washed with Mili Q-water to remove salt and freeze-drying for further polysaccharides extraction.

Extraction of ulvan polysaccharide-rich fraction

Considering that ulvan is the mainly polysaccharide from *Ulva* sp. cell wall, all analysis were performed using an ulvan polysaccharide-rich fraction (both sulphated and non-sulphated), also identified in this paper as UPRF. To obtain the UPRFsfrom *U. pseudorotundata* and *U. rigida* the freeze-drying biomass was subjected to the following steps: pre-extraction, extraction, and precipitation process. The pre-extraction procedure consisted of removing and eliminating possible co-extraction of other compounds during the final extraction of the UPRFs (e.g. pigments). For pre-extraction, 10 g of freeze-dried tissue was homogenized in 200 mL absolute ethanol with constant stirring at room temperature for 2 hours and then centrifuged

(4000 rpm) for 15 min. The pellet was resuspended and re-extracted, as previously described, until a completely colorless supernatant was obtained. For polysaccharides extraction, the biomass was re-suspended in 200 mL of distilled water and warmed until reached 100°C. The solution was maintained for 2 hours at 100°C with constant stirring, and further centrifuged (4000 rpm) for 15 min. A second extraction was carried out with the precipitate resulted from the centrifugation. Polysaccharides were obtained by precipitation of the supernatant with 96% (v/v) ethanol 3:1 ratio during 48 h under 4°C. The solution was further centrifuged (4000 rpm for 10 min) and freeze-dryed to obtain the UPRFs.

Elemental analysis

Total carbon (C), hydrogen (H), nitrogen (N), and sulfur (S) were determined from the UPRFs by total combustion technique using LECO TruSppec Micro CHNSO-Elemental Analyzer. The complete and instantaneous oxidation of the sample was obtained by pure combustion with controlled oxygen at a temperature of up to 1050°C (C, H, N, S) and pyrolysis at 1300°C (O) for decomposition of O as CO and oxidation to CO_2. The resulting combustion products, CO_2, H_2O, SO_2, and N_2, were subsequently quantified by a selective IR absorption detector (C, H, S) and TCD differential thermal conductivity sensor (N). The result of each element (C, H, N, S) is expressed in % with respect to the weight of the sample.

Fourier Transform Infrared Spectroscopy

Fourier transform infrared (FTIR) spectra of the UPRFs from *U. pseudorotundata* and *U. rigida* were obtained by using self-supporting pressed disks of 16 mm in diameter of a mixture of polysaccharides and KBr (1% w/w) with a hydrostatic press at a force of 15.0 t cm^{-2} for 3 min. The FTIR spectra were obtained with a Thermo Nicolet Avatar 360 IR spectrophotometer (Thermo Electron Inc., USA) having a resolution of 4 cm^{-1} with a DTGS detector and using an OMNIC 7.2 software (bandwidth 50 cm^{-1}, enhancement factor 2.6) in the 400–4000 cm^{-1} region. Baseline adjustment was performed using the Thermo Nicolet OMNIC software to flatten the baseline of each spectrum. The OMNIC correlation algorithm was used to compare sample spectra with those of the spectral library (Thermo Fisher Scientific, USA).

Gas Chromatography–Mass Spectrometry (GC-MS)

Hydrolysis and derivatization of the UPRFs were performed by methanolysis and silylation reaction. For hydrolysis, 600 µL of HCl and MeOH 3N (Sigma Adrich) was added to 2 mg of polysaccharides samples. The resultant solution was kept at 80°C for 24 h. Next, samples were washed with methanol and dried under nitrogen gas flow at 50°C (Stuart Block Heater, SBH200D/3). For derivatization, a trimethylsilyl reaction was carried out with 300 µL of Tri-Sil (Pierce, Thermo) at 80°C for 1 h. The derivatized samples were cooled to room temperature and dried under a stream of nitrogen. The dry residue was extracted with 500 µL of hexane and centrifuged (15 min). The solution containing silylated monosaccharides was concentrated and reconstituted in 150 µL of hexane (LC-MS, Sigma), filtered and transferred to a GC-MS autosampler vial. Sample preparation and analyses were performed in duplicate. Polysaccharides samples and monosaccharides standards were treated using the same procedure.

The analyses GC-MSc were carried out using a gas chromatography Trace GC (Thermo Scientifics), autosampler TriPlus AS (Thermo Scientifics), and DSQ mass spectrometer quadrupole (Thermo Scientifics). The column was ZB-5 Zebron, Phenomenex (5% Phenyl, 95% Dimethylpolysiloxane) with dimensions of 30 m × 0.25 mm i.d. × 0.25 µm. The column temperature program started at 80°C (held 2 min) and underwent a gradient of 5°C min^{-1} to reach a final temperature of 230 °C. The carrier gas was helium (flow 1.2 mL min^{-1}). The injection volume was 1 µL in splitless mode at 250°C. The source and MS transfer line temperature were 230°C. The mass spectrometer was set for a Select Ion Monitoring (SIM) program in electron ionization mode (EI) at 70 eV. The TMS-derivatives were identified by characteristic retention times and mass spectrum compared to those of the standards that were used for the identification of monosaccharides (glucose, galactose, mannose, xylose, rhamnose, ribose, and glucouronic acid). The compounds were identified by comparing the mass spectra with those in the National Institute of Standards and Technology (NIST 2014) library.

Antioxidant capacity (ABTS) Free-Radical Method

The determination of the antioxidant capacity of UPRFs were verified by the ABTS method based on the protocol of Re et al. (1999), with modification. ABTS radical was obtained by the dissolution of 7mM ABTS (2,2'-azino-bis(3-ethylbenzothiazoline-6-sulphonic acid) with 2.45mM potassium persulfate for 16 hours in the dark at room temperature. After the incubation time for the formation of free-radicals, the solution was diluted to an absorbance of 0.75 at 727

nm with the phosphate buffer. The final concentrations of UPRFs were 2.5, 5.0, 7.5, 10.0, 15.0, and 20.0 mg.mL^{-1}. A total of 50 µL of these samples were mixed with 950 µL of ABTS solution. The resulting mixture was allowed to stand for 8 min at room temperature and absorbance was immediately recorded with a spectrophotometer at 427 nm. ABTS radical scavenging capacity was calculated according to the following equation:

$$AA\% = \left(\frac{Abs_{control} - Abs_{sample}}{Abs_{control}}\right) \times 100$$

where, $Abs_{control}$ is the absorbance of the ABTS radical in phosphate buffer at time 0 and Abs_{sample} is the absorbance of the ABTS radical solution mixed with the sample after 8 min.

Cell Cultures

Five cell lines were used: human colon cancer cell line (HCT-116, ATCC, USA), human malignant melanoma (G-361, ATCC, USA), leukemia cell line (U-937, ATCC, USA), and one human health cell lines related to the skin (immortalized human keratinocytes: HACAT, ATCC, USA). Cell lines HCT-116 and G-361 were routinely cultured in Dulbecco's modified Eagle's medium (DMEM) (Biowset, ref. L0103- 500) supplemented with 10% fetal bovine serum (Biowest ref. S1810-500), 1% penicillin–streptomycin solution 100x, (Biowest ref. L0022-020), and 0.5% of amphotericin B (Biowest ref. L0009-020). HACAT and U-937 were grown in RPMI-1640 medium (BioWhittaker, ref. BE12-167F) supplemented with 10% fetal bovine serum (Biowest ref. S1810-500), 1% penicillin–streptomycin solution 100×, and 0.5% of amphotericin B. All the cells were maintained sub-confluent at 37 °C in humidified air containing 5% CO_2. Cultured cells were collected by gentle scraping when confluence was reached 75% in the case of the HCT-116, HACAT, and G-361, as they are adherent cells. Scrapping of U-937 cells was not performed because these were cells in suspension. Thus, U-937 cells were collected by centrifugation at 1500 rpm for 5 min.

Cell Viability Assay

For cell viability assay, cells (6×10^3 cells well^{-1}) were incubated with different concentrations of UPRFs (5 to 9.7 x 10 $^{-3}$ mg.mL^{-1}) in serial dilutions. The experiment was conducted with each cell line in a 96-well microplate for 72 h at 37°C and 5% CO_2. Cell proliferation was estimated by the MTT (3-(4,5-dimethylthiazol-2-yl)-2,5- diphenyl

tetrazolium bromide) assay (ABDALA-DÍAZ et al., 2011). Briefly, a volume of 10 µL of the MTT solution (5 mg.mL^{-1} in phosphate buffered saline) was added to each well and the plates were incubated at 37 °C for 4h. The yellow tetrazolium salt of MTT is reduced by metabolically active cells due to the activity of the mitochondrial dehydrogenases resulting in insoluble purple formazan crystals. Formazan was dissolved by the addition of acid isopropanol (150 µL of 0.04 N HCl) and measured spectrophotometrically at 550 nm (BIO-TEK, FL600, INC. Winooski, VT, EUA). The relative cell viability was calculated with the follow equation:

$$\text{Cell viability}(\%) = \frac{\text{DO}_{\text{treatments}}}{\text{DO}_{\text{control}}} \times 100$$

where $DO_{treatments}$ is the absorbance of the treated cells, and $DO_{control}$ is the absorbance of the control cells (untreated cells). For the calculation of parameter EC_{50} we used the result obtained by cell viability (%) *versus* concentration (mg polysaccharide mL^{-1}). Four samples for each tested concentration were included in each experiment.

Determination of IC_{50} and selectivity index (SI)

The half maximal inhibitory concentrations (IC_{50}) of the UPRFs for each cell line was calculated by the linear part of the sigmoid curve of dose response relationship. To evaluate the cytotoxic selectivity of the UPRFs, we calculated the selectivity index (SI), defined as the ratio of the toxic concentration of a sample against its effective bioactive concentration (INDRAYANTO; PUTRA; SUHUD, 2020). The SI was calculated by the IC_{50} obtained from the normal cell line (HACAT) *vs* IC_{50} obtained from cancer cells lines according to the follow equation:

$$\text{SI} = \frac{IC_{50(\text{non-cancer cell})}}{IC_{50(\text{cancer cell})}}$$

Statistical Analysis

Antioxidant capacity and cell viability assay are presented as means ± standard deviations of experiments. Student's *t* test for paired comparisons were used to compare the effect of the UPRFs obtained from different *Ulva* species for antioxidant capacity and values

of IC_{50} obtained in all cell lines tested. Student's *t* test were also performed with the values obtained from selectivity index. Statistically significant differences were considered at $p < 0.05$.

4. RESULTS

Chemical Assessment

Elemental composition of Polysaccharides

The elemental composition of total carbon, hydrogen, nitrogen and sulfur content of UPRFs obtained from *U. rigida* and *U. pseudorotundata* are presented in Table 1. Carbon was the predominant element in both UPRF and similar values of sulfur were also observed.

Table. 1. Total carbon, hydrogen, nitrogen, and sufur content (%) in ulvan polysaccharide-rich fraction extracted from *Ulva rigida* and *Ulva pseudorotundada*.

	C	H	N	S
U. rigida	31.15	5.13	5.86	3.78
U. pseudorotundata	28.09	4.66	3.15	3.88

Fourier Transform Infrared Spectroscopy

The FT-IR spectroscopy of the UPRFs obtained from *U. rigida* and *U. pseudorotundata* exhibited the presence of several bands from 4.000 to 0.500 nm (Figure 1). Both FT-IR spectra revealed similar band patterns, however, UPRF from *U. rigida* presented stronger peaks for all bands. A strong and wide signal was localized between 3,000 and 3,600 cm^{-1} (A). Strong absorbances were also observed at approximately 1,650–1,700 (B) and 1,000–1,100 cm^{-1} (E). Peaks in the polysaccharides from both seaweeds were also observed at about 1,400 (C), 1,250, (D) 800-900 (F), and 600 cm^{-1} (G).

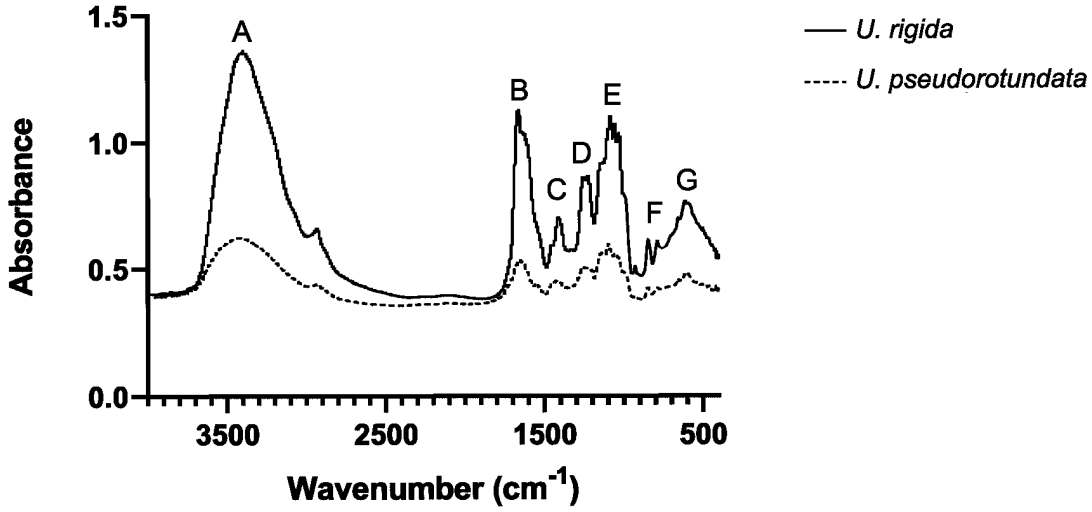

Fig. 1. Infrared spectrum of the ulvan polysaccharide-rich fractionisolated from *U. rigida* and *U. pseudorotundata*. Six bands (A, B, C, D, E, F and G) of greatest interest were identified according to their absorption bindings.

Gas Chromatography–Mass Spectrometry (GC-MS)

The gas chromatography-mass spectrometry (GC-MS) analysis (Figure 2) showed that chemical structure of the UPRF obtained from *U. rigida* (Figure 2A) are constituted by the monossacharides rhamnose (67.0%), glucose (23.8%), glucuronic acid (4.0%), xylose (3.0%), and galactose (2.0%). For *U. pseudorotundata*, rhamnose was also the main monosaccharide (about 51.2%), followed by xylose (24.1%), glucose (13.9%), glucuronic acid (4.8%), and galactose (2.8%). The presence of ribose and mannose were also detected representing only 1.6% and 1.2%, respectively.

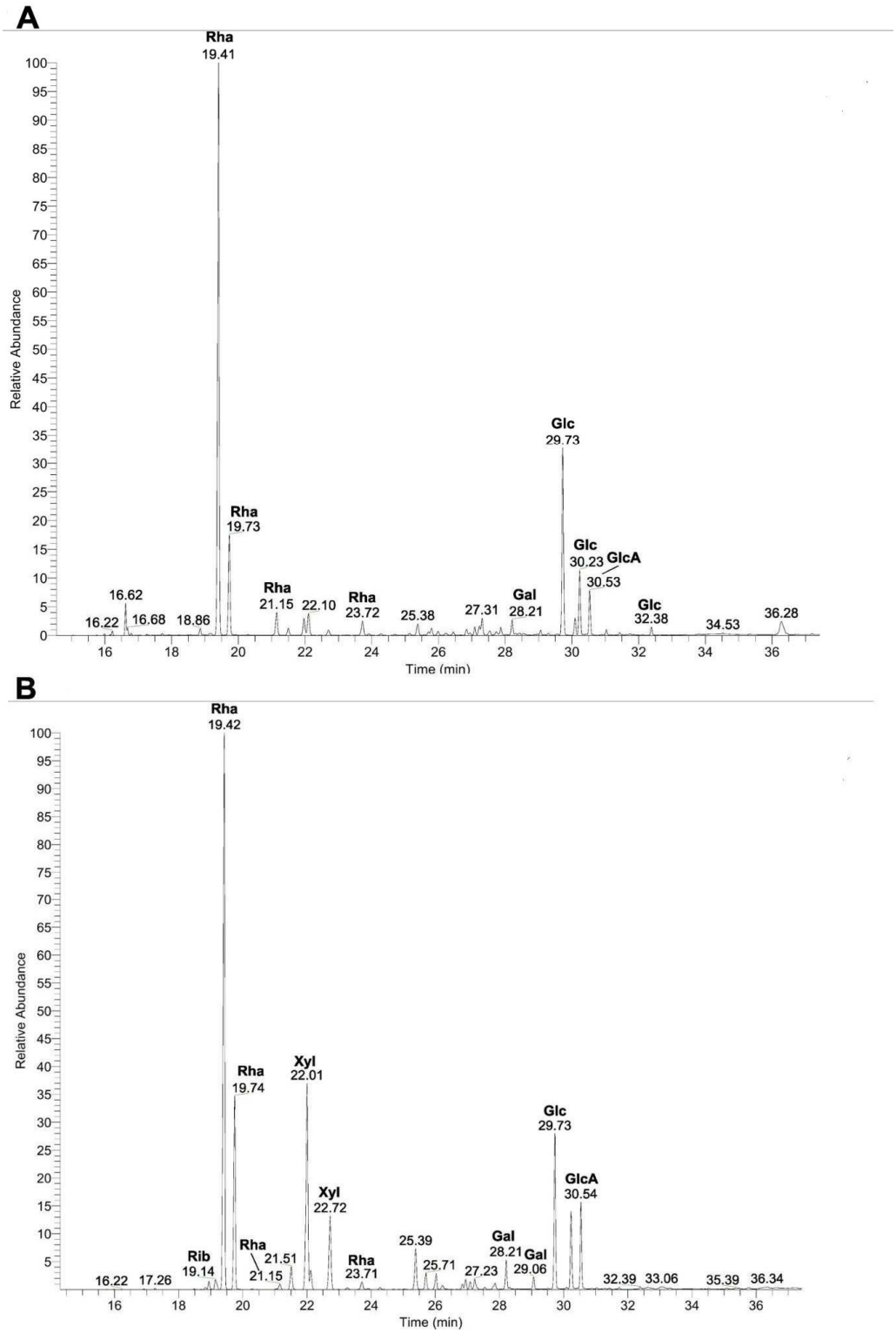

Fig. 2. Gas chromatography-mass spectrometry of the ulvan polysaccharide-rich fraction obtained from *U. rigida* (A) and *U. pseudorotundata* (B). The standards of monosaccharide composition identified: Rha: (rhamnose); Gal: (galactose); Glc: (glucose); GlcA: (glucouronic acid); Rib: (ribose); Xyl: (xylose).

Biological Assessment

Antioxidant Capacity

The antioxidant capacity of UPRFs obtained from *U. rigida* and *U. pseudorotundata* was measured using the radical $ABTS^{+}$. The antioxidant (reduction) potential of ABTS methodology is based on electron transfer. Figure 3 shows ABTS radical scavenging capacity of UPRFs from *U. rigida* and *U. pseudorotundata* and it was observed a dose-dependent radical scavenging capacity. The two UPRFs exhibited the same radical scavenging capacity at all tested concentrations except for the of 10 mg mL^{-1} where the UPRF extracted from *U. rigida* presented a higher antioxidant capacity than *U. pseudorotundata* (*t*-student, $t(4) = 4.468$, $p = 0.011$).

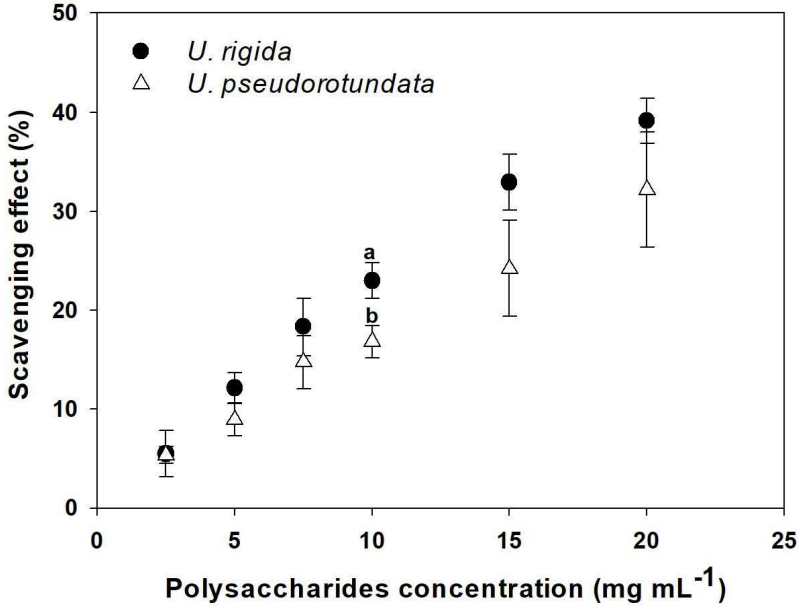

Fig. 3. Scavenging effects (%) of ulvan polysaccharide-rich fraction obtained from *U. rigida* and *U. pseudorotundata* on ABTS radical. Letters above the symbols indicate significant differences ($p < 0.05$, *t*-student test). Values are mean ± SD, n = 3.

Cell Viability Assay

The survival (%) of HCT-116, G-361, U-937, and HACAT cell lines were verified under different concentrations of UPRFs obtained from *U. rigida* and *U. pseudorotundata* (Fig. 4, Fig.5, Fig.6, Fig. 7, and Table 2). In regard to tumoral cell lines, the results obtained with the MMT assay indicated a lower IC_{50} values obtained to HCT-116 cells and no differences were

observed between both UPRFs with IC_{50} values of 0.31 ± 0.04 mg mL^{-1} for *U. rigida* and 0.32 ± 0.02 mg mL^{-1} for *U. pseudorotundata*. For G-361, no differences were observed in IC_{50} values comparing both UPRFs with IC_{50} value of 5.19 ± 0.40 mg mL^{-1} and 4.67 ± 0.72 mg mL^{-1} for *U. rigida* and *U. pseudorotundata*, respectively. Considering U-937 cell lines, UPRF isolated from *U. pseudorotundata* (IC_{50}: 2.47 ± 0.26 mg mL^{-1}) were more effective for inhibition of cell proliferation than UPRF obtained from *U. rigida* which presented an IC_{50} equivalent to 3.42 ± 0.18 mg mL^{-1}. In regard to the health cell line (HACAT), it was observed a higher IC_{50} for *U. rigida* (2.51 ± 0.75 mg mL^{-1}) than for *U. pseudorotundata* (1.3 ± 0.30 mg mL^{-1}) isolated UPRF. The selectivity index (SI) of UPRF's toxicity against HCT-116, G-361, U-937 are presented in Table 2. It was noticed that UPRFs extrated from both *Ulva* species presented the highest selectivity index against HCT-116 cell lines with values of 4.05 (±1.11) for *U. peseudorotundata* and 8.03 (± 1.48) for *U. rigida*.

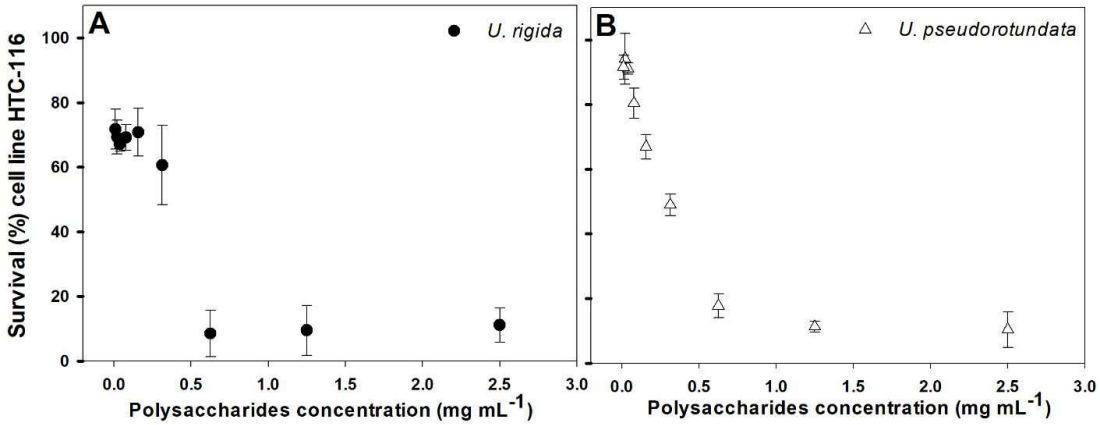

Fig. 4. Survival (%) of cell line HCT-116 exposed to different concentrations of ulvan polysaccharide-rich fraction obtained from *U. rigida* and *U. pseudorotundata*. Values are mean ± SD, n = 4.

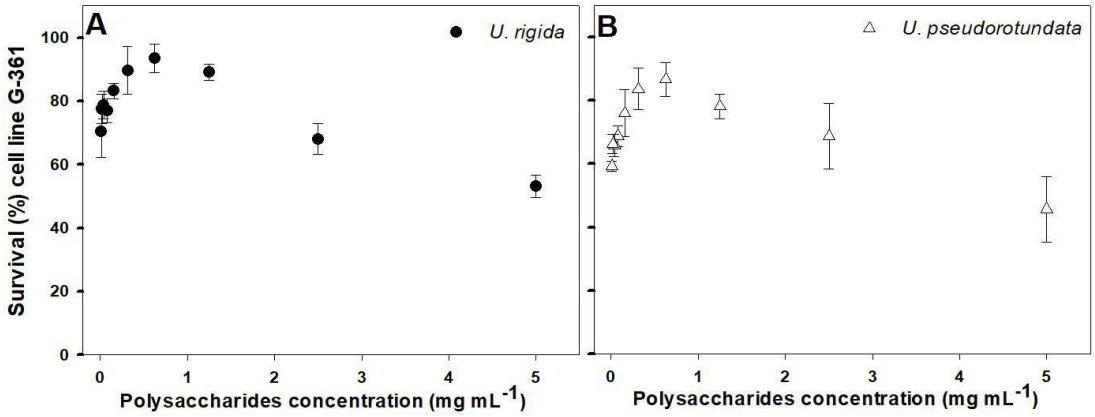

Fig. 5. Survival (%) of cell line G-361 exposed to different concentrations of ulvan polysaccharide-rich fraction obtained from *U. rigida* and *U. pseudorotundata*. Values are mean ± SD, n = 4.

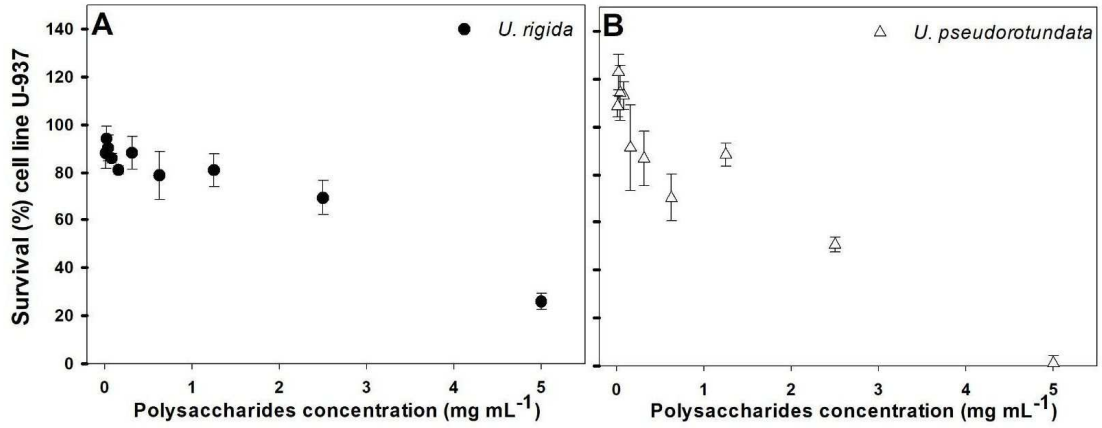

Fig. 6. Survival (%) of cell line U-937 exposed to different concentrations of ulvan polysaccharide-rich fraction obtained from *U. rigida* and *U. pseudorotundata*. Values are mean ± SD, n = 4.

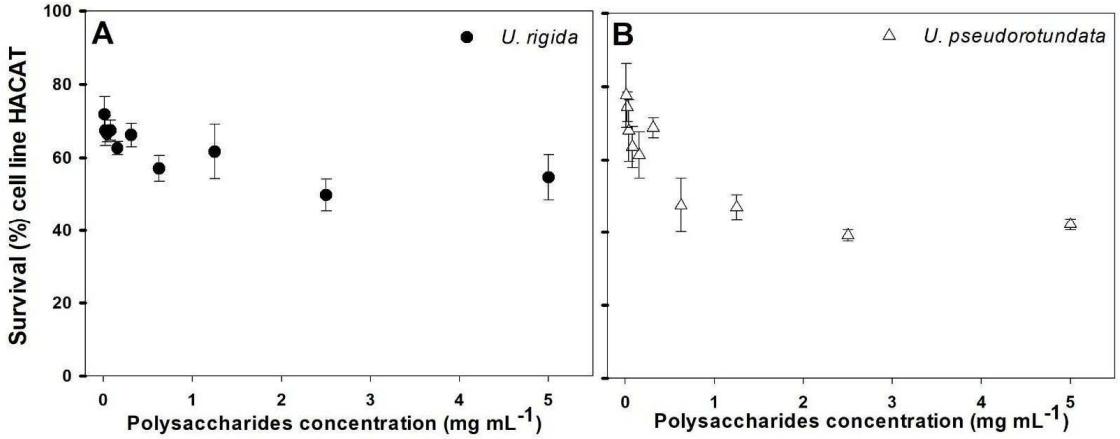

Fig. 7. Survival (%) of cell line HACAT exposed to different concentrations of ulvan polysaccharide-rich fraction obtained from *U. rigida* and *U. pseudorotundata*. Values are mean ± SD, n = 4.

Table. 2. Values of IC_{50} (mg mL^{-1}) obtained from the cell viability assay of HCT-116, G-361, U-937, and HACAT. Cell lines were treated with different ulvan polysaccharide-rich fraction concentrations obtained from *U. rigida* and *U. pseudorotundata*. The selectivity index (SI) of polysaccharides against HCT-116, G-361, U-937 are presented. Values are mean (± SD), n = 4. T-student test results are presented. *df*: degree of freedom; t-value: T-statistic. The significant differences in treatments ($p < 0.05$) are shown in bold.

	U. rigida	***U. pseudorotundata***	***df***	***t*-value**	***p***
IC_{50}					
HCT-116	0.31 ± 0.04	0.32 ± 0.02	6	0.72	0.50
G-361	5.19 ± 0.40	4.67 ± 0.72	6	-1.26	0.25
U-937	**3.42 ± 0.18**	**2.47 ± 0.26**	**6**	**-5.93**	**0.00**
HACAT	**2.51 ± 0.75**	**1.30 ± 0.30**	**6**	**-3.01**	**0.02**
SI					
HCT-116	**8.03 ± 1.48**	**4.05 ± 1.11**	**6**	**-4.31**	**0.01**
G-361	**0.49 ± 0.15**	**0.28 ± 0.02**	**6**	**-2.78**	**0.03**
U-937	0.74 ± 0.27	0.52 ± 0.11	6	-1.51	0.18

5. DISCUSSION

As bioeconomic development grows worldwide there is an increasing attention for the use of natural products as raw materials. In this context, seaweed biomass can be a source of a vast number of valuable compounds, which can be applied for biotechnological purposes. In the present study we characterized and obtained biological assessment of ulvan polysaccharide-rich fraction (UPRF) extracted from two *Ulva* species: *U. rigida* and *U. pseudorotundata*. Both UPRF presented similar chemical structure and composition. By the FT-IR spectroscopy we observed that UPRFs isolated from *U. rigida* and *U. pseudorotundata* revealed the presence of several functional groups: carboxylic, hydroxyl, and sulfonate groups. The spectra presented similar absorption peaks for both polysaccharides indicating the presence of the same functional groups in their composition. Moreover, absorbance peaks observed in the present work correspond to the typical infrared spectrum of ulvan already reported by Ray and Lahaye (1995) and Robic et al. (2009) characterized by high absorbances in the regions of 3,300-3,600, 1,650, 1,070, and 1,250 and smaller ones at about 1,400, 850, and 790 cm^{-1}. The broad and strong signal centered at around 3,000-3,600 can be related to hydroxyl (-OH) and amino (-NH) groups, typical of polysaccharides from seaweed (ABDALA-DÍAZ et al., 2019). Peaks in the regions of 1,650 and 1,400 correspond to carboxylate groups while the region of 1,070 could be related to the sugars rhamnose and glucuronic acid (C-O) (ROBIC et al., 2009). The presence of sulfate esters (S=O) are detected by the peak in the region of 1,250, which can be attributed

to the sulfate groups already described for sulfated polysaccharides in other different marine algae (ABDALA-DÍAZ et al., 2011, 2019). Bands located in 850 and 790 are related to sugar cycles (ROBIC et al., 2009).

As the composition of ulvans can vary depending on conditions prior to extraction (eg. species, location, cultivation conditions) and the following steps during extraction procedure (e.g. solvents, temperature, duration of extraction), the identification of ulvan's monosaccharides composition assumes a critical role in the study of biological properties. Monosaccharide composition analysis by GC-MS revealed that both UPRFs contained mainly rhamnose, which constituted over 50% of detected monosaccharides. This result is in agreement with previous data demonstrating the presence of rhamnose as a major sugar in ulvan (LAHAYE et al., 1999; MAO et al., 2006; RAY; LAHAYE, 1995). Although, in the present study, both species were previously acclimated under the same conditions and submitted to the same procedures for polysaccharides extraction, a variation was observed on the remaining monosaccharides composition. Besides rhamnose, UPRF extracted from *U. rigida* presented a higher quantity of glucose than *U. pseudorotundata*, which presented a higher concentration of xylose. According to Kidgell et al. (2019) ulvans obtained from *U. rigida* may present 1.6 to 46.1% glucose. In a study with ulvans obtained from various *Ulva* species, Lahaye et al. (1999) observed that the polysaccharide isolated from *U. rigida* tended to be mainly composed by rhamnose (50.9-58.3%) followed by glucuronic acid (19.0-30.4%) and presented glucose levels in a range between 6.3 and 12.0%. In the same study, *U. rotundata* (synonym of *U. pseudorotundata* - Guiry et al. 2014) exhibited predominantly rhamnose (46.7-54.0%) followed by glucuronic acid (17.8-28.9%) and xylose (5.4-23.8%). Those results demonstrated the variability of ulvan composition and chemical structure indicating the need of ulvan characterization prior to biological studies and potential applications.

In overall perspective, it should be noted that UPRF extracted from *U. rigida* and *U. pseudorotundata* presented similar antioxidant capacity, reaching between 32 and 39% of free radical scavenging. The antioxidant activity of ulvans has been verified in other *Ulva* species including *U. intestinalis* and *U. pertusa* (RAHIMI; TABARSA; REZAEI, 2016; ZHANG et al., 2010). Le et al. (2019) reported similar antioxidant capacity of ulvan extracted from *U. pertusa* however using a lower concentration of ulvan (0.8 mg mL^{-1}). The high antioxidant capacity presented by the previous work was obtained in an optimized ulvan extraction condition by microwave-assisted extraction technology under modulation of time, power, water-to-raw-

material ratio, and pH indicating that extraction processes do not affect antioxidant capacity of ulvans. According to Le et al. (2019) the antioxidant activity of ulvans depends on factors such as the presence of sulfate group, the content of hydroxyl and carboxyl groups of the monosaccharides as well as the hydrogen donation potential. Castro-Varela et al. (2022) reported significant antioxidant properties of sulfate polysaccharide and Phycoerythrin concentration from the red algae *Sarcopeltis skottsbergii* which were increased using ultrasound-assisted extraction (UAE) and high pressure homogenization (HPH) extraction techniques. In this context, we suggest that techniques employed for the ulvan extraction process e.g. microwaving, ultrasonication, and enzymatic reduction could enhance the availability of polysaccharides, releasing possible interaction sites that could promote greater antioxidant capacity.

Cell viability assay indicated that UPRFs obtained from both *Ulva* species exhibited anti-tumor activity against colon carcinoma (HCT-116) cell lines with an IC_{50} value lower than 0.33 mg mL^{-1}. In the case of tumor cell lines G-361 and U-937, the antiproliferative potential of both UPRFs were lower than that obtained from HTC-116 with IC_{50} higher than 4.6 and 2.4 mg mL^{-1}, respectively. In study with *U. lactuca,* Ahmed and Ahmed (2014) verified that ulvan had anti-tumor activity against HCT-116 and HepG2 (hepatoma) cell lines, exhibiting an IC_{50} 22.65 and 55.56 µg mL^{-1}, respectively. In comparison with polysaccharides extracted from other seaweed, the values obtained in the present work demonstrated that UPRF was more cytotoxic in HCT-116 cell line than sulfated polysaccharides isolated from the brown seaweed *Laminaria ochroleuca*, which exhibited a IC_{50} of 0.44 mg mL^{-1} (ABDALA-DÍAZ et al., 2019). According to Weerapreeyakul et al. (2012) an extract with IC_{50} value between 0.1 – 0.5 mg mL^{-1} could be considered as having moderate cytotoxicity, which was observed only for HTC-116 cell lines. As reported by Ahmed and Ahmed (2014), the anti-proliferative effect of ulvan against tumor cells line could be related to the upregulation of via pro-apoptotic and cell cycle arrest protein p53 but also by the down-regulation of Bcl-2 protein, responsible for promote cell viability. In this context, further studies with proteins and genes involved in the life of cancer cells should verify how ulvan is interfering in tumor suppressor mechanisms.

According to Indrayanto et al. (2020) the calculation of selectivity index should be obtained as part of the validation of in-vitro bioassay of an isolated compound. In this context, we evaluated whether the toxicity of our UPRFs against HCT-116 cell lines also affected normal cell lines (HACAT). As described by Weerapreeyakul et al. (2012), an isolated

compound with SI value ≥3 (IC_{50} 10 - 100 μg mL^{-1}) could be selected for further investigation. As the UPRFs obtained from *U. rigida* and *U. pseudorotundata* exhibited SI values greater than 3, we suggest that both polysaccharides should be considered in future evaluations regarding their potential anticancer bioactivity. Besides anti-cancer capacity, several works have been describing the potential of ulvan as an anti-coagulating, immunomodulating, and antiviral compound (CHIU et al., 2012; LEIRO et al., 2007; MAO et al., 2006). In work reported by Leiro et al. (2007), sulphated polysaccharides obtained from *U. rigida* demonstrated an *in vitro* immunomodulating activity by the stimulation of RAW264.7 macrophage cell lines. Anticoagulant potential of sulfated polysaccharides isolated from *U. conglobata* was described by the mediation of coagulation pathways as the inhibition of thrombin activity (MAO et al., 2006). In the study performed with sulfated polysaccharide obtained from *U. lactuca*, Chiu et al. (2012) reported the antiviral activity of the polysaccharide against Japanese encephalitis virus (JEV) due to mechanisms related to the reduction virus adsorption, inhibiting them to get into Vero cells. In this context the potential of ulvan for biomedical applications has been highlighted for nutraceutical and pharmaceutical product development.

In conclusion, our study suggested that ulvan polysaccharide-rich fraction isolated from *Ulva rigida* and *Ulva pseudorotundata*, native species from the Spanish Mediterranean coast, presented similar chemical and structure composition. Moreover, both UPRFs presented *in vitro* antioxidant capacity and selectivity cytotoxicity against HCT-116 cell line, which could be considered a potential valuable ingredient for the development of biotechnological products. We also suggest that further studies are needed to deeply understand the cellular and molecular mechanisms involved in the interaction of ulvan and cancer cells.

6. ACKNOWLEDGMENTS

We sincerely thank the Federal University of Santa Catarina (UFSC) and University of Malaga (UMA), especially the faculty members and technical staff of the Laboratory of Phycology (LAFIC - UFSC), Laboratory of Fotobiología y Biotecnología de Organismos acuáticos (FYBOA - UMA), and research center Grice Hutchinson (UMA). We also thank Dr. Luis Alemany and Dr. María de los Ángeles Vargas (Chemical Engineering Department, UMA) for their technical assistance in the FT-IR analysis and D. Augusto Martínez García, Technical Manager of the Chemical Analysis and Material Characterization Area: Elemental and Thermal Analysis Unit of the SCAI (Central Research Support Service) of the University of Malaga, for the technical assistance in the elementary analysis of the samples. This study is part of the Doctoral thesis of the first author to the UFSC Graduate Program in Biotechnology and Bioscience, Santa Catarina, Brazil.

Conflict of Interest
The authors declare they have no competing interests as defined by Springer, or other interests that might be perceived to influence the results and/or discussion reported in this paper.

Data availability statement
The datasets generated during and/or analyzed during the current study are available from the corresponding author upon reasonable request

Author Contributions
Massocato, T. dedicated to experimental design, algal cultivation, ulvan's extraction, statistical analysis, data interpretation, and original draft;
Robles-Carnero, V. responsible for algal cultivation and biomass provision;
Moreira, B. responsible for cells viability assay and data interpretation;
Castro-Varela, P. responsible for cells viability assay and ulvan's chemical assessment;
Bonomi-Barufi, J. reviewed and edited the manuscript text;
Abdala-Díaz, R. supervised polysaccharides extraction procedure, chemical assessment and cells viability assay;
Rörig, L. reviewed, edited the manuscript text, supervised and provided funding acquisition;
Figueroa, F.L. reviewed, edited the manuscript text, supervised and provided funding acquisition;

Funding
Financial resources and scholarships were provided by: Andalusia Government (Spain) in the frame of the Projects FACCO - UMA18-FEDER JA-162 and NAZCA (P20-00458), Santa Catarina State Foundation for Research and Innovation Support (FAPESC process no 03/2017, Brazil), and Coordination for the Improvement of Higher Education Personnel (CAPES/PRINT process nos. 88887.470102/2019-00, Brazil). We also thank the Conselho Nacional de Desenvolvimento Científico e Tecnológico (CNPq) financial support through research grants. P.C-V, thanks to Asociación Iberoamericana de Postgrado (AUIP) and Malaga University for PhD Scholarship.

CONSIDERAÇÕES FINAIS E CONCLUSÃO

O presente trabalho buscou entender aspectos de biofiltração de nutrientes presentes em efluentes advindos do cultivo de peixes utilizando macroalgas marinhas de duas espécies: *Ulva rigida* e *Ulva pseudorotundata*. Além do papel como organismos biofiltradores, também foi analisada a performance fisiológica dos cultivos algais através de medidas de fluorescência *in vivo* da clorofila-*a* para obtenção de parâmetros fotossintéticos. A biomassa gerada nos experimentos foi analisada em termos de composição elementar e bioquímica. Para avaliação da biomassa algal para aplicação biotecnológica foram extraídos polissacarídeos para posterior caracterização e ensaios de atividade anti-oxidante e citotoxidade celular.

No primeiro capítulo, foram utilizadas, de forma isoladas, 3 diferentes concentrações de duas fontes de nitrogênio inorgânico (NH_4^+ e NO_3^-) simulando nutrientes presentes no efluente de peixes. Os experimentos realizados em condições não controladas de luz e temperatura nos permitiram analisar a performance dos cultivos em condições próximas de escala piloto de produção comercial de algas. Os dados obtidos nos possibilitam observar que, em 24 horas de experimento, as biomassas de algas utilizadas foram suficientes para remoção total dos nutrientes nas concentrações testadas. No entanto, observamos que a remoção de NH_4^+ foi mais rápida que a remoção NO_3^-. Tal aspecto condiz com dados obtidos por outros trabalhos também realizados com algas do gênero *Ulva*, sob condições *indoor* e *outdoor* de experimentos, o que é explicado pela preferência de *Ulva* em assimilar NH_4^+ que NO_3^-. A rápida remoção de NH_4^+ em relação a NO_3^- está ligada aos mecanismos de absorção e incorporação dessas duas diferentes fontes de nitrogênio, envolvendo maior gasto energético de NO_3^-. Ao analisar os dados de forma integrada observamos que os maiores valores dos parâmetros de ETR_{max} (taxa máxima de transporte de elétrons) obtidos das curvas rápidas de luz (RLC), estão agrupados próximos aos que correspondem à remoção de NO_3^-, o que indica o maior custo energético para absorção e assimilação dessa fonte de nutriente. No âmbito de composição elementar e bioquímica da biomassa não foi verificada diferenças significativas em decorrência dos nutrientes usados.

Os dados apresentados no segundo capítulo nos mostram que as espécies de *U. rigida* e *U. pseudorotundata*, apesar de coletadas em locais ambientalmente distintos em termos de variação de luz, temperatura, dessecação e disponibilidade de nutrientes, apresentaram aspectos similares de remoção de nutrientes e performance fotossintética. Neste capítulo foi utilizado efluentes advindos dos cultivos de *Chelon labrosus* em que estavam presentes as duas fontes

de nutrientes usadas no capítulo 1. Ambas as espécies removeram mais rapidamente NH_4^+ que NO_3^-, o que condiz com os dados obtidos no capítulo 1. Dessa forma, concluímos que quando as duas fontes de nutrientes estiverem disponíveis no meio, os cultivos de *Ulva* removerão preferencialmente NH_4^+ que NO_3^-. Os dados obtidos através dos parâmetros fotossintéticos mostraram que, mesmo expostas às condições ambientais de irradiância, os cultivos não apresentaram fotoinibição nos períodos do dia de maior incidência de luz, o que pode estar atrelado à condição de nutriente suficiente fornecida aos cultivos, permitindo mecanismos de fotoproteção das algas. Nesse sentido, podemos inferir que a disponibilidade suficiente de nitrogênio no meio permite a redução dos efeitos inibitórios comuns de estresse a curto prazo, como o aumento da irradiância, na fotossíntese. Os dados obtidos ao longo do período experimental correspondentes à eficiência de biofiltração de NO_3^- (NUE) e eficiência fotossintética das algas (α_{ETR}) permitiram a obtenção de um modelo de regressão linear evidenciando correlação positiva entre fotossíntese e remoção de NO_3^-. Dados de biomassa mostraram que as taxas de crescimento das algas cultivadas em 100% efluente foram maiores do que aquelas obtidas em 50% efluente. Além disso, quando cultivadas na concentração de 100% de efluente, foi detectado um incremento significativo no teor de proteína em ambas as espécies de *Ulva*.

Como possível destino da biomassa de *Ulva* foram realizadas extração, caracterização elementar e química dos polissacarídeos. Concluímos que os polissacarídeos, compostos majoritariamente por ulvanos, apresentaram capacidade antioxidante em função do aumento das concentrações utilizadas dos mesmos. Em ensaios *in vitro* com cultivos celulares de diferentes linhagens celulares verificamos que os polissacarídeos de ambas as algas apresentaram maior toxicidade para linhagens celulares de câncer de cólon (HTC-116). O índice de seletividade (*selectivity index*) nos permitiu verificar que apesar de apresentarem toxicidade às células cancerígenas (HTC-116) estes compostos não são potencialmente tóxicos para células de linhagens não cancerígenas (queratinócitos – HACAT) o que indica a potencial utilização dos polissacarídeos para formulação de componentes farmacológicos.

Como sugestões para trabalhos futuros destacamos a realização de experimentos com cultivos acoplados de algas e peixes. Também se propõe a elaboração de sistemas de cultivo que poderiam potencializar o papel biofiltrador das algas, como por exemplo, a alternância da entrada de efluentes entre diferentes cultivos algais, permitindo que os cultivos passem por um período de *starvation* o que poderia manter máxima capacidade de remoção dos nutrientes

advindos dos efluentes. Também sugerimos que experimentos realizados especialmente com o nutriente NH_4^+ tenham o monitoramento contínuo do pH do meio afim de compreender se os cultivos algais atuam na remoção indireta de nitrogênio através da atividade fotossintética.

Com respeito à exploração da biomassa para diferentes destinos comerciais, sugere-se a realização de ensaios com a biomassa remanescente da extração de polissacarídeos, como por exemplo, para a utilização como fertilizantes na agricultura.

Os dados obtidos na presente tese permitem verificar a aplicabilidade na utilização de cultivos de espécies de *Ulva* coletadas na costa mediterrânea da Espanha para depuração de nutrientes de efluentes da maricultura gerando potencial biomassa como fonte sustentável de matéria-prima para o desenvolvimento de produtos industriais. No entanto, é importante destacar que no litoral brasileiro, até o atual momento, já foram descritas a ocorrência de 15 espécies de algas deste gênero (CARNEIRO, 2021) evidenciando a potencialidade do Brasil como país promissor para cultivos de *Ulva* em sistemas multitróficos integrados e posterior exploração da biomassa algal.

REFERÊNCIAS

ABDALA-DÍAZ, R. T. et al. Characterization of polysaccharides from Hypnea spinella (Gigartinales) and Halopithys incurva (Ceramiales) and their effect on RAW 264.7 macrophage activity. **Journal of Applied Phycology**, v. 23, n. 3, p. 523–528, jun. 2011.

ABDALA-DÍAZ, R. T. et al. Immunomodulatory and Antioxidant Activities of Sulfated Polysaccharides from Laminaria ochroleuca, Porphyra umbilicalis, and Gelidium corneum. **Marine Biotechnology**, v. 21, n. 4, p. 577–587, 15 ago. 2019.

ABREU, M. H. et al. IMTA with Gracilaria vermiculophylla: Productivity and nutrient removal performance of the seaweed in a land-based pilot scale system. **Aquaculture**, v. 312, n. 1–4, p. 77–87, 2011a.

ABREU, M. H. et al. Nitrogen uptake responses of Gracilaria vermiculophylla (Ohmi) Papenfuss under combined and single addition of nitrate and ammonium. **Journal of Experimental Marine Biology and Ecology**, v. 407, n. 2, p. 190–199, 2011b.

AHMED, O. M.; AHMED, R. R. Anti-proliferative and apoptotic efficacies of ulvan polysaccharides against different types of carcinoma cells in vitro and in vivo. **Journal of Cancer Science and Therapy**, v. 6, n. 6, p. 202–208, 2014.

AL-HAFEDH, Y. S.; ALAM, A.; BUSCHMANN, A. H. Bioremediation potential, growth and biomass yield of the green seaweed, Ulva lactuca in an integrated marine aquaculture system at the Red Sea coast of Saudi Arabia at different stocking densities and effluent flow rates. **Reviews in Aquaculture**, v. 7, p. 1–11, 2014.

ALE, M. T.; MIKKELSEN, J. D.; MEYER, A. S. Differential growth response of Ulva lactuca to ammonium and nitrate assimilation. p. 345–351, 2011.

ÁLVAREZ-GÓMEZ, F. et al. UV photoprotection, cytotoxicity and immunology capacity of red algae extracts. **Molecules**, v. 24, n. 2, 18 jan. 2019.

ANDERSEN, R. A. **Algal Culturing Techniques**. [s.l.] Elsevier Academic Press, 2005.

ARAÚJO, R. et al. Current Status of the Algae Production Industry in Europe: An Emerging Sector of the Blue Bioeconomy. **Frontiers in Marine Science**, v. 7, n. January, p. 1–24, 2021.

ASHKENAZI, D. Y.; ISRAEL, A.; ABELSON, A. A novel two-stage seaweed integrated multi-trophic aquaculture. **Reviews in Aquaculture**, v. 11, n. 1, p. 246–262, 2019.

BARCELÓ-VILLALOBOS, M. et al. Production of Mycosporine-Like Amino Acids from Gracilaria vermiculophylla (Rhodophyta) Cultured Through One Year in an Integrated Multi-trophic Aquaculture (IMTA) System. **Marine Biology Research**, v. 19, p. 246–254, 2017.

BARROSO, C. B.; PEREIRA, G. T.; NAHAS, E. Solubilization of CAHPO4 and ALPO4 by Aspergillus niger in culture media with different carbon and nitrogen sources. **Brazilian Journal of Microbiology**, v. 37, n. 4, p. 434–438, 2006.

BEN-ARI, T. et al. Management of Ulva lactuca as a biofilter of mariculture effluents in IMTA system. **Aquaculture**, v. 434, p. 493–498, 2014.

BENJAMA, O.; MASNIYOM, P. Nutritional composition and physicochemical properties of two green seaweeds (Ulva pertusa and U. intestinalis) from the Pattani Bay in Southern Thailand. **Songklanakarin J. Sci. Technol.**, v. 33, n. 5, p. 575–583, 2011.

BERMEJO, R. et al. Spatial and temporal variability of biomass and composition of green tides in Ireland. **Harmful Algae**, v. 81, n. November 2018, p. 94–105, 2019.

BIKKER, P. et al. Biorefinery of the green seaweed Ulva lactuca to produce animal feed, chemicals and biofuels. **Journal of Applied Phycology**, v. 28, n. 6, p. 3511–3525, 2016.

BISCHOF, K. et al. Solar ultraviolet radiation affects the activity of ribulose-1,5-bisphosphate carboxylase-oxygenase and the composition of photosynthetic and xanthophyll cycle pigments in the intertidal green alga Ulva lactuca L. **Planta**, v. 215, n. 3, p. 502–509, 2002.

BOOMINATHAN, M.; MAHESH, A. Seaweed carotenoids for cancer therapeutics. In: KIM, S.-K. (Ed.). . **Handbook of Anticancer Drugs from Marine Origin**. [s.l.] Springer International Publishing Switzerland, 2015. p. 185–203.

BUSCHMANN, A. H. et al. Seaweed production: overview of the global state of exploitation, farming and emerging research activity. **European Journal of Phycology**, v. 52, n. 4, p. 391–406, 2017a.

BUSCHMANN, A. H. et al. Seaweed production : overview of the global state of exploitation , farming and emerging research activity. **European Journal of Phycology**, v. 52, n. 4, p. 391–406, 2017b.

BUSCHMANN, A. H.; TROELL, M.; KAUTSKY, N. Integrated algal farming: A review. **Cahiers de Biologie Marine**, v. 42, n. 1–2, p. 83–90, 2001.

CABELLO-PASINI, A. et al. Effect of nitrate concentration and UVR on photosynthesis, respiration, nitrate reductase activity, and phenolic compounds in Ulva rigida (Chlorophyta). **Journal of Applied Phycology**, v. 23, n. 3, p. 363–369, 2011.

CABELLO-PASINI, A.; FIGUEROA, F. L. Effect of nitrate concentration on the relationship between photosynthetic oxygen evolution and electron transport rate in Ulva rigida (Chlorophyta). **Journal of Phycology**, v. 41, n. 6, p. 1169–1177, 2005.

CARNEIRO, M. A. A.; FREIRE, F. A. D. M.; MARINHO-SORIANO, E. Study on biofiltration capacity and kinetics of nutrient uptake by Gracilaria cervicornis (Turner) J . Agardh (Rhodophyta ,. n. 3, p. 329–333, 2011.

CARNEIRO, V. A. R. **Estudos moleculares e morfológicos do gênero Ulva L. (Ulvales, Chlorophyta) no sudeste do Brasil**. [s.l.] Universidade de São Paulo, 2021.

CASTRO-GONZÁLEZ, M. I. et al. Composición química de alga verde Ulva lactuca. **Ciencias Marinas**, v. 22, n. 2, p. 205–213, 1996.

CASTRO-VARELA, P. et al. Highly Efficient Water-Based Extraction of Biliprotein R-Phycoerythrin From Marine the Red-Macroalga Sarcopeltis skottsbergii by Ultrasound and High-Pressure Homogenization Methods. **Frontiers in Marine Science**, v. 9, n. June, p. 1–14, 2022.

CELIS-PLÁ, P. S. M. et al. A new approach for cultivating the cyanobacterium Nostoc calcicola (MACC-612) to produce biomass and bioactive compounds using a thin-layer raceway pond. **Algal Research**, v. 59, n. July, p. 102421, 2021.

CHIU, Y. H. et al. Inhibition of Japanese Encephalitis Virus Infection by the Sulfated Polysaccharide Extracts from Ulva lactuca. **Marine Biotechnology**, v. 14, n. 4, p. 468–478, 2012.

CHOPIN, T. et al. Integrating Seaweeds into Marine Aquaculture Systems: a Key Toward Sustainability. **Journal of Phycology**, v. 37, p. 975–986, 2001.

COHEN, I.; NEORI, A. Ulva lactuca Biofilters for Marine Fishpond Effluents. I. Ammonia Uptake Kinetics and Nitrogen Content. **Botanica Marina**, 1991.

COLLOS, Y.; HARRISON, P. J. Acclimation and toxicity of high ammonium concentrations to unicellular algae. **Marine Pollution Bulletin**, v. 80, n. 1–2, p. 8–23, 2014.

COPERTINO, M. D. S.; TORMENA, T.; SEELIGER, U. Biofiltering efficiency,

uptake and assimilation rates of Ulva clathrata (Roth) J. Agardh (Clorophyceae) cultivated in shrimp aquaculture waste water. **Journal of Applied Phycology**, v. 21, n. 1, p. 31–45, fev. 2009.

CRUCES, E. et al. Interaction of Photoprotective and Acclimation Mechanisms in Ulva rigida (Chlorophyta) in Response to Diurnal Changes in Solar Radiation in Southern Chile. **Journal of Phycology**, v. 55, n. 5, p. 1011–1027, 2019.

DEL RÍO, MI. J.; RAMAZANOV, Z.; GARCÍA-REINA, G. Ulva rigida (Ulvales, Chlorophyta) tank culture as biofilters for dissolved inorganic nitrogen from fishpond effluents. v. 66, n. November, p. 61–66, 1996.

DIAZ, R. J.; ROSENBERG, R. Spreading dead zones and consequences for marine ecosystems. **Science**, v. 321, n. 5891, p. 926–929, 2008.

DOMINGUEZ, H.; LORET, E. P. Ulva lactuca, A Source of Troubles and Potential Riches. **Marine Drugs**, v. 17, n. 6, 2019.

DUBOIS, M. et al. A colorimetric method for determination of sugars and related substances. **Analytical chemistry**, v. 28, p. 350–356, 1956.

EILERS, P. H. C.; PEETERS, J. C. H. A model for the relationship between light intensity and the rate of photosynthesis in phytoplankton. **Ecological Modelling**, v. 42, n. 3–4, p. 199–215, 1988.

ERICKSON, R. J. An evaluation of mathematical models for the effects of pH and temperature on ammonia toxicity to aquatic organisms. **Water Research**, v. 19, n. 8, p. 1047–1058, 1985.

FAN, X. et al. The effect of nutrient concentrations, nutrient ratios and temperature on photosynthesis and nutrient uptake by Ulva prolifera: Implications for the explosion in green tides. **Journal of Applied Phycology**, v. 26, n. 1, p. 537–544, 2014.

FAO. **The State of World Fisheries and Aquaculture 2016. Contributing to food security and nutrition for all.** Rome: [s.n.].

FAO. **The State of World Fisheries and Aquaculture 2020. Sustainability in Action**. Rome: [s.n.]. Disponível em: <https://doi.org/10.4060/ca9229en>.

FARVIN, K. H. S.; JACOBSEN, C. Phenolic compounds and antioxidant activities of selected species of seaweeds from Danish coast. **Food Chemistry**, v. 138, n. 2–3, p. 1670–1681, 2013.

FELSENSTEIN, J. Confidence Limits on Phylogenies: An Approach Using the Bootstrap. **Evolution**, v. 39, n. 4, p. 783, 1985.

FERDOUSE, F. et al. The global status of seaweed production, trade and utilization. **FAO Globefish Research Programme**, v. 124, 2018.

FIGUEROA, F.; CONDE-ALVAREZ, R.; GOMEZ, I. Relations between electrion transport rates determined by pulse amplitude modulated chlorophyll fluorescence and oxygen evolution in macroalgae under different light conditions. **Photosynthesis Research**, v. 75, p. 259–275, 2003.

FIGUEROA, F. L. et al. The use of chlorophyll fluorescence for monitoring photosynthetic condition of two tank-cultivated red macroalgae using fishpond effluents. **Botanica Marina**, v. 49, n. 4, p. 275–282, 2006.

FIGUEROA, F. L. et al. Accumulation of Mycosporine-like Amino Acids in Asparagopsis armata Grown in Tanks with Fishpond Effluents of Gilthead Sea. **Journal of the World Aquaculture Society**, v. 39, n. 5, p. 692–699, 2008.

FIGUEROA, F. L. et al. Effects of nutrient supply on photosynthesis and pigmentation in Ulva lactuca (Chlorophyta): Responses to short-term stress. **Aquatic Biology**, v. 7, n. 1–2,

p. 173–183, 2009a.

FIGUEROA, F. L. et al. Effects of nutrient supply on photosynthesis and pigmentation in Ulva lactuca (Chlorophyta): responses to short-term stress. v. 7, n. November, p. 173–183, 2009b.

FIGUEROA, F. L. et al. Biofiltration of fishpond effluents and accumulation of N-compounds (phycobiliproteins and mycosporine-like amino acids) versus C-compounds (polysaccharides) in Hydropuntia cornea (Rhodophyta). v. 64, p. 310–318, 2012.

FIGUEROA, F. L. et al. Short-term effects of increased CO2, nitrate and temperature on photosynthetic activity in Ulva rigida (Chlorophyta) estimated by different pulse amplitude modulated fluorometers and oxygen evolution. **Journal of Experimental Botany**, v. 72, n. 2, p. 491–509, 2020.

FINKL, C. W. Coastal Zones : Solutions for the 21st Century. **Journal of Coastal Research**, v. 32, n. 6, p. 1508–1509, 2016.

FLEURENCE, J.; CHENARD, E.; LUÇON, M. Determination of the nutritional value of proteins obtained from Ulva armoricana. **Journal of Applied Phycology**, v. 11, n. 3, p. 231–239, 1999.

FRIEDLANDER, M.; GALAI, N.; FARBSTEIN, H. A model of seaweed growth in an outdoor culture in Israel. **Hydrobiologia**, v. 204, p. 367–373, 1990.

FROEHLICH, H. E. et al. Blue Growth Potential to Mitigate Climate Change through Seaweed Offsetting. **Current Biology**, v. 29, n. 18, p. 3087- 3093.e3, 2019.

GENTY, B.; BRIANTAIS, J.-M.; BAKER, N. R. electron transport and quenching of chlorophyll fluorescence. **BBA - General Subjects**, v. 990, n. 1, p. 87–92, 1989.

GEVAERT, F.; BARR, N. G.; REES, T. A. V. Diurnal cycle and kinetics of ammonium assimilation in the green alga Ulva pertusa. **Marine Biology**, v. 151, n. 4, p. 1517–1524, 2007.

GORDILLO, F. J. L.; FIGUEROA, F. L.; NIELL, F. X. Photon- and carbon-use efficiency in Ulva rigida at different CO 2 and N levels. **Planta**, v. 218, n. 2, p. 315–322, 2003.

GRANADA, L. et al. Modelling integrated multi-trophic aquaculture : Optimizing a three trophic level system. **Aquaculture**, v. 495, p. 90–97, 2018.

GRASSHOFF, K.; KREMLING, K.; EHRHARDT, M. **Methods of Seawater Analysis**. 3nd. ed. [s.l.] WILEY-VCH,Weinheim, 1999.

GRZYMSKI, J.; JOHNSEN, G.; SAKSHAUG, E. The significance of intracellular self-shading on the bio optical properties of brown, red and green macroalgae. **Journal of Phycology**, v. 33, p. 408–414, 1997.

GUIRY, M. D. et al. AlgaeBase: An on-line resource for algae. **Cryptogamie, Algologie**, v. 35, n. 2, p. 105–115, 2014.

GUTTMAN, L. et al. Combinations of Ulva and periphyton as biofilters for both ammonia and nitrate in mariculture fishpond effluents. **Algal Research**, v. 34, n. July, p. 235–243, 2018.

GUTTMAN, L. et al. An integrated Ulva-periphyton biofilter for mariculture effluents: Multiple nitrogen removal kinetics. **Algal Research**, v. 42, n. May, p. 101586, 2019.

HÄDER, D. P.; HELBLING, W.; VILLAFA, V. E. **Anthropogenic Pollution of Aquatic Ecosystems**. [s.l: s.n.].

HAMMER, O.; HARPER, D. A. T.; RYAN, P. D. Paleontological statistics software package for education and data analysis. **Palaeontologia Electronica**, v. 4, n. 1, p. 9, 2001.

HAN, Q.; LIU, D. Macroalgae blooms and their effects on seagrass ecosystems. **Journal of Ocean University of China**, v. 13, n. 5, p. 791–798, 2014.

HANELT, D.; NULTSCH, W. Field Studies of Photoinhibition Show Non-Correlationsbetween Oxygen and Fluorescence Measurements in the Arctic Red Alga Palmaria palmata. **Journal of Plant Physiology**, v. 145, n. 1–2, p. 31–38, 1995.

HARRISON, P. J.; HURD, C. L. Nutrient physiology of seaweeds: Application of concepts to aquaculture. **Cahiers de Biologie Marine**, v. 42, p. 71–82, 2001.

HEESCH, S. et al. Ulva, Umbraulva and Gemina: Genetic survey of New Zealand taxa reveals diversity and introduced species. **European Journal of Phycology**, v. 44, n. 2, p. 143–154, 2009.

HENLEY, W. J. et al. Photoacclimation and photoinhibition in Ulva rotundata as influenced by nitrogen availability. **Planta**, v. 184, n. 2, p. 235–243, 1991.

HERATH, S. S.; SATOH, S. Environmental impact of phosphorus and nitrogen from aquaculture. **Feed and Feeding Practices in Aquaculture**, p. 369–386, 2015.

HUOVINEN, P. et al. The role of ammonium in photoprotection against high irradiance in the red alga Grateloupia lanceola. **Aquatic Botany**, v. 84, n. 4, p. 308–316, 2006.

HUPPE, H. C.; TURPIN, D. H. Integration of carbon and nitrogen metabolism in plant and algal cells. **Annual review of plant biology**, v. 45, n. 3, p. 577–607, 1994.

HURD, C. L. et al. **Seaweed Ecology and Physiology**. [s.l: s.n.].

IBGE. **Instituto Brasileiro de Geografia e EstatísticaRegiões metropolitanas, aglomerações urbanas e regiões integradas de desenvolvimento 2010-2019.** [s.l: s.n.]. Disponível em: <https://www.ibge.gov.br/geociencias-novoportal/organizacao-do-territorio/estrutura-territorial/18354-regioes-metropolitanas-aglomeracoes-urbanas-e-regioes-integradas-de-desenvolvimento.html>.

INDRAYANTO, G.; PUTRA, G. S.; SUHUD, F. **Validation of in-vitro bioassay methods : Application in herbal drug research**. 1. ed. [s.l.] Elsevier Inc., 2020.

JEREZ, C. G. et al. Chlorella fusca (Chlorophyta) grown in thin-layer cascades: Estimation of biomass productivity by in-vivo chlorophyll a fluorescence monitoring. **Algal Research**, v. 17, p. 21–30, 2016.

JONES, M.; PINN, E. The impact of a macroalgal mat on benthic biodiversity in Poole Harbour. **Marine Pollution Bulletin**, v. 53, n. 1, p. 63–71, 2006.

JUSADI, D. et al. Potential of Underutilized Marine Organisms for Aquaculture Feeds. **Frontiers in Marine Science**, v. 7, n. February, 2021.

KALASARIYA, H. S. et al. Seaweed-based molecules and their potential biological activities: An eco-sustainable cosmetics. **Molecules**, v. 26, n. 17, p. 1–22, 2021.

KANG, Y. H. et al. A preliminary study of the bioremediation potential of Codium fragile applied to seaweed integrated multi-trophic aquaculture (IMTA) during the summer. **Journal of Applied Phycology**, v. 20, n. 2, p. 183–190, 2008a.

KANG, Y. H. et al. A preliminary study of the bioremediation potential of Codium fragile applied to seaweed integrated multi-trophic aquaculture (IMTA) during the summer. **Journal of Applied Phycology**, v. 20, n. 2, p. 183–190, abr. 2008b.

KHAN, M.; MOHAMMAD, F. **Eutrophication: Challanges and Solutions**. Dordrecht: Springer, 2014.

KIDGELL, J. T. et al. Ulvan: A systematic review of extraction, composition and function. **Algal Research**, v. 39, n. March, p. 101422, 2019a.

KIDGELL, J. T. et al. **Ulvan: A systematic review of extraction, composition and functionAlgal Research**Elsevier B.V., , 1 maio 2019b.

KIMURA, M. A simple method for estimating evolutionary rates of base substitutions through comparative studies of nucleotide sequences. **Journal of Molecular Evolution**, v. 16,

n. 2, p. 111–120, 1980.

KORBEE, N. et al. Availability of ammonium influences photosynthesis and the accumulation of mycosporine-like amino acids in two Porphyra species (Bangiales, Rhodophyta). **Marine Biology**, v. 146, n. 4, p. 645–654, 2005.

LAHAYE, M. et al. Chemical composition and 13C NMR spectroscopic characterisation of ulvans from Ulva (Ulvales, Chlorophyta). **Journal of Applied Phycology**, v. 11, n. 1, p. 1–7, 1999.

LAHAYE, M.; ROBIC, A. Structure and Functional Properties of Ulvan, a Polysaccharide from Green Seaweeds. v. 8, n. 6, p. 24–30, 2007.

LAKSHMI, D. S. et al. A short review on the valorization of green seaweeds and ulvan: Feedstock for chemicals and biomaterials. **Biomolecules**, v. 10, n. 7, p. 1–20, 2020.

LE, B. et al. Optimization of microwave-assisted extraction of polysaccharides from ulva pertusa and evaluation of their antioxidant activity. **Antioxidants**, v. 8, n. 5, 2019.

LE MOAL, M. et al. Eutrophication: A new wine in an old bottle? **Science of the Total Environment**, v. 651, p. 1–11, 2019.

LEIRO, J. M. et al. Immunomodulating activities of acidic sulphated polysaccharides obtained from the seaweed Ulva rigida C. Agardh. **International Immunopharmacology**, v. 7, n. 7, p. 879–888, 2007.

LIGNELL, A.; PEDERSÉN, M. Agar composition as a function of morphology and growth rate. Studies on some morphological strains of Graciliaria secundata and Graciliaria verrucosa (Rhodophyta). **Botanica Marina**, v. 32, n. 3, p. 219–227, 1989.

LIU, D. et al. The world's largest macroalgal bloom in the Yellow Sea, China: Formation and implications. **Estuarine, Coastal and Shelf Science**, v. 129, p. 2–10, 2013.

LOTZE, H. K. et al. Depletion, degradation, and recovery potential of estuaries and coastal seas. **Science (New York, N.Y.)**, v. 312, n. 5781, p. 1806–9, jun. 2006.

LOUGHNANE, C. J. et al. Morphology, rbcL phylogeny and distribution of distromatic Ulva (Ulvophyceae, Chlorophyta) in Ireland and southern Britain. **Phycologia**, v. 47, n. 4, p. 416–429, 2008.

MACCHIAVELLO, J.; BULBOA, C. Nutrient uptake efficiency of Gracilaria chilensis and Ulva lactuca in an IMTA system with the red abalone Haliotis rufescens. **Latin American Journal of Aquatic Research**, v. 42, n. 3, p. 523–533, 2014.

MANTRI, V. A. et al. Concise review of green algal genus Ulva Linnaeus. **Journal of Applied Phycology**, v. 32, n. 5, p. 2725–2741, 2020.

MAO, W. et al. Sulfated polysaccharides from marine green algae Ulva conglobata and their anticoagulant activity. **Journal of Applied Phycology**, v. 18, n. 1, p. 9–14, 2006.

MAO, Y. et al. Potential of the seaweed Gracilaria lemaneiformis for integrated multi-trophic aquaculture with scallop Chlamys farreri in North China. **Journal of Applied Phycology**, v. 21, n. 6, p. 649–656, 2009.

MASOJÍDEK, J. et al. Productivity correlated to photobiochemical performance of Chlorella mass cultures grown outdoors in thin-layer cascades. **Journal of Industrial Microbiology and Biotechnology**, v. 38, n. 2, p. 307–317, 2011.

MASOJÍDEK, J. et al. Changes in photosynthesis, growth and biomass composition in outdoor Chlorella g120 culture during the metabolic shift from heterotrophic to phototrophic cultivation regime. **Algal Research**, v. 56, n. December 2020, 2021.

MASSOCATO, T. F. et al. Growth, biofiltration and photosynthetic performance of Ulva spp. cultivated in fishpond effluents: An outdoor study. **Frontiers in Marine Science**, v. 9, n. September, p. 1–19, 2022.

MATA, L. et al. **Cultivation of Ulva rotundata (Ulvales, Chlorophyta) in raceways using semi-intensive fishpond effluents: yield and biofiltration.** Proceedings of the 17th International Seaweed Symposium (28 January-2 February 2001). **Anais**...Cape Town, South Africa: Oxford University Press, 2003. Disponível em: <http://www.cabdirect.org/abstracts/20033183342.html;jsessionid=913580A26234A2B1E97F538D9D5BD6AE>

MATA, L. et al. The effects of light and temperature on the photosynthesis of the Asparagopsis armata tetrasporophyte (Falkenbergia rufolanosa), cultivated in tanks. **Aquaculture**, v. 252, n. 1, p. 12–19, 2006.

MATA, L. et al. The intensive land-based production of the green seaweeds Derbesia tenuissima and Ulva ohnoi : biomass and bioproducts. **Journal of Applied Phycology**, v. 1, p. 365–375, 2016.

MATA, L.; SCHUENHOFF, A.; SANTOS, R. A direct comparison of the performance of the seaweed biofilters, Asparagopsis armata and Ulva rigida. **Journal of Applied Phycology**, v. 22, n. 5, p. 639–644, 2010.

MAXWELL, K.; JOHNSON, G. N. Chlorophyll fluorescence - A practical guide. **Journal of Experimental Botany**, v. 51, n. 345, p. 659–668, 2000.

MAXWELL1, K.; JOHNSON2, G. N. **Chlorophyll fluorescence-a practical guideJournal of Experimental Botany**. [s.l: s.n.].

MENG, W. et al. Phlorotannins: A review of extraction methods, structural characteristics, bioactivities, bioavailability, and future trends. **Algal Research**, v. 60, n. May, p. 102484, 2021.

MICHALAK, I.; CHOJNACKA, K.; SAEID, A. Plant Growth Biostimulants, Dietary Feed Supplements and Cosmetics Formulated with Supercritical CO2 Algal Extracts. **Molecules**, n. October 2016, p. 1–17, 2017.

NARDELLI, A. E. et al. Integrated multi-trophic farming system between the green seaweed Ulva lactuca, mussel, and fish: a production and bioremediation solution. **Journal of Applied Phycology**, v. 31, n. 2, p. 847–856, 2019.

NAYLOR, R. L. et al. A 20-year retrospective review of global aquaculture. **Nature**, v. 591, n. 7851, p. 551–563, 2021.

NEORI, A. et al. A novel three-stage seaweed (Ulva lactuca) biofilter design for integrated mariculture A novel three-stage seaweed (Ulva lactuca) biofilter design for integrated mariculture. **Journal of Applied Phycology**, v. 15, p. 543–553, 2003.

NEORI, A. et al. Integrated aquaculture : rationale , evolution and state of the art emphasizing seaweed biofiltration in modern mariculture. v. 231, p. 361–391, 2004.

NEORI, A.; COHEN, I.; GORDIN, H. Ulva lactuca Biofilters for Marine Fishpond Effluents I. Ammonia Uptake Kinetics and Nitrogen Content. **Botanica Marina**, v. 34, n. 1, p. 475–482, 1991.

OSMOND, C. B. et al. Fluorescence quenching during photosynthesis and photoinhibition of Ulva rotundata blid. **Planta**, v. 190, n. 1, p. 97–106, 1993.

PARSONS, T. R.; STRICKLAND, J. D. H. Marine-plant Pigments, with Revised Equations far Ascertaining Chlorophylls and Carotenoids. **Journal of Marine Research**, v. 21, n. 3, p. 155–163, 1963.

PEDERSEN, M. F. Transient ammonium uptake in the macroalga Ulva lactuca (Chlorophyta): Nature, regulation, and the consequences for choice of measuring technique. **Journal of Phycology**, v. 30, n. 6, p. 980–986, 1994.

PERALTA, E.; JEREZ, C. G.; FIGUEROA, F. L. Centrate grown Chlorella fusca (

Chlorophyta): Potential for biomass production and centrate bioremediation. **Algal Research**, v. 39, n. February, p. 101458, 2019.

PÉREZ-GÁLVEZ, A.; VIERA, I.; ROCA, M. Carotenoids and chlorophylls as antioxidants. **Antioxidants**, v. 9, n. 6, p. 1–39, 2020.

PINCHETTI, J. L. G. et al. Nitrogen availability influences the biochemical composition and photosynthesis of tank-cultivated Ulva rigida (Chlorophyta). **Journal of Applied Phycology**, v. 10, n. 4, p. 383–389, 1998.

PRITCHARD, D. W. et al. Restricted use of nitrate and a strong preference for ammonium reflects the nitrogen ecophysiology of a light-limited red alga. **Journal of Phycology**, v. 51, n. 2, p. 277–287, 2015.

PROVASOLI, L.; MCLAUGHLIN, J. J. A.; DROOP, M. R. **The Development of Artificial Media for Marine Algae**. [s.l: s.n.].

QI, H. et al. Antihyperlipidemic activity of high sulfate content derivative of polysaccharide extracted from Ulva pertusa (Chlorophyta). **Carbohydrate Polymers**, v. 87, n. 2, p. 1637–1640, 2012.

RAHIMI, F.; TABARSA, M.; REZAEI, M. Ulvan from green algae Ulva intestinalis: optimization of ultrasound-assisted extraction and antioxidant activity. **Journal of Applied Phycology**, v. 28, n. 5, p. 2979–2990, 2016.

RAVEN, J. A.; SMITH, F. A. Nitrogen assimilation and transport in vascular land plants in relation to intracelular pH regulation. **New Phytologist**, v. 76, n. 3, p. 415–431, 1976.

RAY, B.; LAHAYE, M. Cell-wall polysaccharides from the marine green alga Ulva "rigida" (Ulvales, Chlorophyta). Chemical structure of ulvan. **Carbohydrate Research**, v. 274, n. C, p. 313–318, 1995.

RE, R. et al. Antioxidant activity applying an improved ABTS radical cation decolorization assay. **Free Radical Biology & Medicine**, v. 26, p. 1231–1237, 1999.

REARTE, T. A. et al. Photosynthetic performance of Chlorella vulgaris R117 mass culture is moderated by diurnal oxygen gradients in an outdoor thin layer cascade. **Algal Research**, v. 54, n. December 2020, 2021.

REIS, M. A.; BAUER, W.; MARTINS, R. M. BluEco Net – Workshop sobre Aquicultura Multitrófica Integrada e o futuro da aquicultura sustentável no Brasil. **Aquaculture Brasil**, p. 45–47, volume: 17, 2019.

RITCHIE, R. J. Consistent sets of spectrophotometric chlorophyll equations for acetone, methanol and ethanol solvents. **Photosynthesis Research**, v. 89, n. 1, p. 27–41, 2006.

ROBIC, A. et al. Determination of the chemical composition of ulvan, a cell wall polysaccharide from Ulva spp. (Ulvales, Chlorophyta) by FT-IR and chemometrics. **Journal of Applied Phycology**, v. 21, n. 4, p. 451–456, 2009.

ROLEDA, M. Y.; HURD, C. L. Seaweed nutrient physiology: application of concepts to aquaculture and bioremediation. **Phycologia**, v. 58, n. 5, p. 552–562, 2019.

SALVI, K. P. et al. A new model of Algal Turf Scrubber for bioremediation and biomass production using seaweed aquaculture principles. **Journal of Applied Phycology**, v. 33, n. 4, p. 2577–2586, 2021.

SCHNEIDER, G. et al. Photoprotection properties of marine photosynthetic organisms grown in high ultraviolet exposure areas: Cosmeceutical applications. **Algal Research**, v. 49, n. July 2019, p. 101956, 2020.

SHAHAR, B. et al. Changes in metabolism, growth and nutrient uptake of Ulva fasciata (Chlorophyta) in response to nitrogen source. **Algal Research**, v. 46, n. July 2019, p. 101781, 2020.

SHPIGEL, M. et al. A proposed model for " environmentally clean " land-based culture of fish , bivalves and seaweeds. **Aquaculture**, v. 117, p. 115–128, 1993.

SHPIGEL, M. et al. Ulva lactuca from an Integrated Multi-Trophic Aquaculture (IMTA) biofilter system as a protein supplement in gilthead seabream (Sparus aurata) diet. **Aquaculture**, v. 481, n. August, p. 112–118, 2017.

SHPIGEL, M. et al. Ulva lactuca biofilter from a land-based integrated multi trophic aquaculture (IMTA) system as a sole food source for the tropical sea urchin Tripneustes gratilla elatensis. **Aquaculture**, v. 496, n. June, p. 221–231, 2018.

SHPIGEL, M. et al. Is Ulva sp. able to be an efficient biofilter for mariculture effluents? **Journal of Applied Phycology**, v. 31, n. 4, p. 2449–2459, 2019.

SHUULUKA, D.; BOLTON, J. J.; ANDERSON, R. J. Protein content , amino acid composition and nitrogen-to-protein conversion factors of Ulva rigida and Ulva capensis from natural populations and Ulva lactuca from an aquaculture system , in South Africa. v. 25, p. 677–685, 2013.

SISTEMA NACIONAL DE INFORMAÇÕES SOBRE SANEAMENTO. Diagnóstico Temático Serviços de Água e Esgoto - Visão Geral Ano de Referência 2020. **Sistema Nacional de Informações sobre Saneamento - SNIS**, p. 1–91, 2021.

SMETACEK, V.; ZINGONE, A. Green and golden seaweed tides on the rise. **Nature**, v. 504, n. 7478, p. 84–88, 2013.

SMITH, V. H.; TILMAN, G. D.; NEKOLA, J. C. Eutrophication : impacts of excess nutrient inputs on freshwater , marine , and terrestrial ecosystems. **Environmental Pollution**, v. 100, p. 179–196, 1999.

STEINHAGEN, S. et al. Harvest Time Can Affect the Optimal Yield and Quality of Sea Lettuce (Ulva fenestrata) in a Sustainable Sea-Based Cultivation. **Frontiers in Marine Science**, v. 9, 2022.

SUDHA, P. N.; GOMATHI, T.; KIM, S. Ulvan in Tissue Engineering. **Encyclopedia of Marine Biotechnology**, p. 1335–1350, 2020.

TAMURA, K.; STECHER, G.; KUMAR, S. MEGA11: Molecular Evolutionary Genetics Analysis Version 11. **Molecular Biology and Evolution**, v. 38, n. 7, p. 3022–3027, 2021.

TAYLOR, M. W.; REES, T. A. V. Kinetics of ammonium assimilation in two seaweeds, Enteromorpha sp. (Chlorophyceae) and Osmundaria colensoi (Rhodophyceae). **Journal of Phycology**, v. 35, n. 4, p. 740–746, 1999.

TROELL, M. et al. **Integrated mariculture: Asking the right questions**. Aquaculture. **Anais**...2003.

TURPIN, D. H. et al. Interactions between photosynthesis, respiration, and nitrogen assimilation in microalgae. **Canadian Journal of Botany**, v. 66, n. 10, p. 2083–2097, 1988.

TURPIN, D. H. **Effects of Inorganic N Availability on Algal Photosynthesis and Carbon MetabolismJournal of Phycology**, 1991.

TZIVELEKA, L. A.; IOANNOU, E.; ROUSSIS, V. Ulvan, a bioactive marine sulphated polysaccharide as a key constituent of hybrid biomaterials: A review. **Carbohydrate Polymers**, v. 218, n. March, p. 355–370, 2019a.

TZIVELEKA, L. A.; IOANNOU, E.; ROUSSIS, V. Ulvan, a bioactive marine sulphated polysaccharide as a key constituent of hybrid biomaterials: A review. **Carbohydrate Polymers**, v. 218, p. 355–370, 2019b.

UNESCO. **The United Nations Decade of Ocean Science for Sustainable Development, 2021-2030**. The United Nations Decade of Ocean Science for Sustainable

Development, 2021-2030. **Anais**...Paris, France: 2018. Disponível em: <http://en.unesco.org/ocean-decade>

VALIELA, I. et al. Macroalgal blooms in shallow estuaries: Controls and ecophysiological and ecosystem consequences. **Limnology and Oceanography**, v. 42, n. 5 II, p. 1105–1118, 1997.

VEGA, J. et al. Antioxidant activity of extracts from marine macroalgae, wild-collected and cultivated, in an integrated multi-trophic aquaculture system. **Aquaculture**, v. 522, n. February, 2020a.

VEGA, J. et al. Antioxidant activity of extracts from marine macroalgae, wild-collected and cultivated, in an integrated multi-trophic aquaculture system. **Aquaculture**, v. 522, n. February, p. 735088, 2020b.

VEGA, J. et al. Mycosporine-like amino acids from red macroalgae: Uv-photoprotectors with potential cosmeceutical applications. **Applied Sciences (Switzerland)**, v. 11, n. 11, 2021.

VIAROLI, P. et al. Growth of the seaweed Ulva rigida C. Agardh in relation to biomass densities, internal nutrient pools and external nutrient supply in the Sacca di Goro lagoon (Northern Italy). **Hydrobiologia**, v. 329, n. 1–3, p. 93–103, 1996.

VITOUSEK, P. M. Human Domination of Earth's Ecosystems. **Science**, v. 277, n. 5325, p. 494–499, jul. 1997.

WAN, A. H. L. et al. Assessment and characterisation of Ireland's green tides (Ulva species). **PLoS ONE**, v. 12, n. 1, 2017.

WEERAPREEYAKUL, N. et al. Evaluation of the anticancer potential of six herbs against a hepatoma cell line. **Chinese Medicine (United Kingdom)**, v. 7, p. 1–7, 2012.

WU, R. S. S. The environmental impact of marine fish culture: Towards a sustainable future. **Marine Pollution Bulletin**, v. 31, n. 4–12, p. 159–166, 1995.

YE, N. HAO et al. "Green tides" are overwhelming the coastline of our blue planet: Taking the world's largest example. **Ecological Research**, v. 26, n. 3, p. 477–485, 2011.

ZHANG, Z. et al. Extraction of the polysaccharides from five algae and their potential antioxidant activity in vitro. **Carbohydrate Polymers**, v. 82, n. 1, p. 118–121, 2010.

APÊNDICE A

O sequenciamento obtido das identificações moleculares das algas estudadas neste trabalho: *Ulva rigida* e *Ulva pseudorotundata*, através de marcadores do gene RbcL, foram depositados no banco de dados GenBank - National Center for Biotechnology Information (NCBI), Números de acesso: OP020918.1 (*U. rigida*) and OP020919.1 (*U. pseudorotundata*). Os dados presentes nesse anexo complementam a árvore filogenética apresentada no capítulo 2 desta tese.

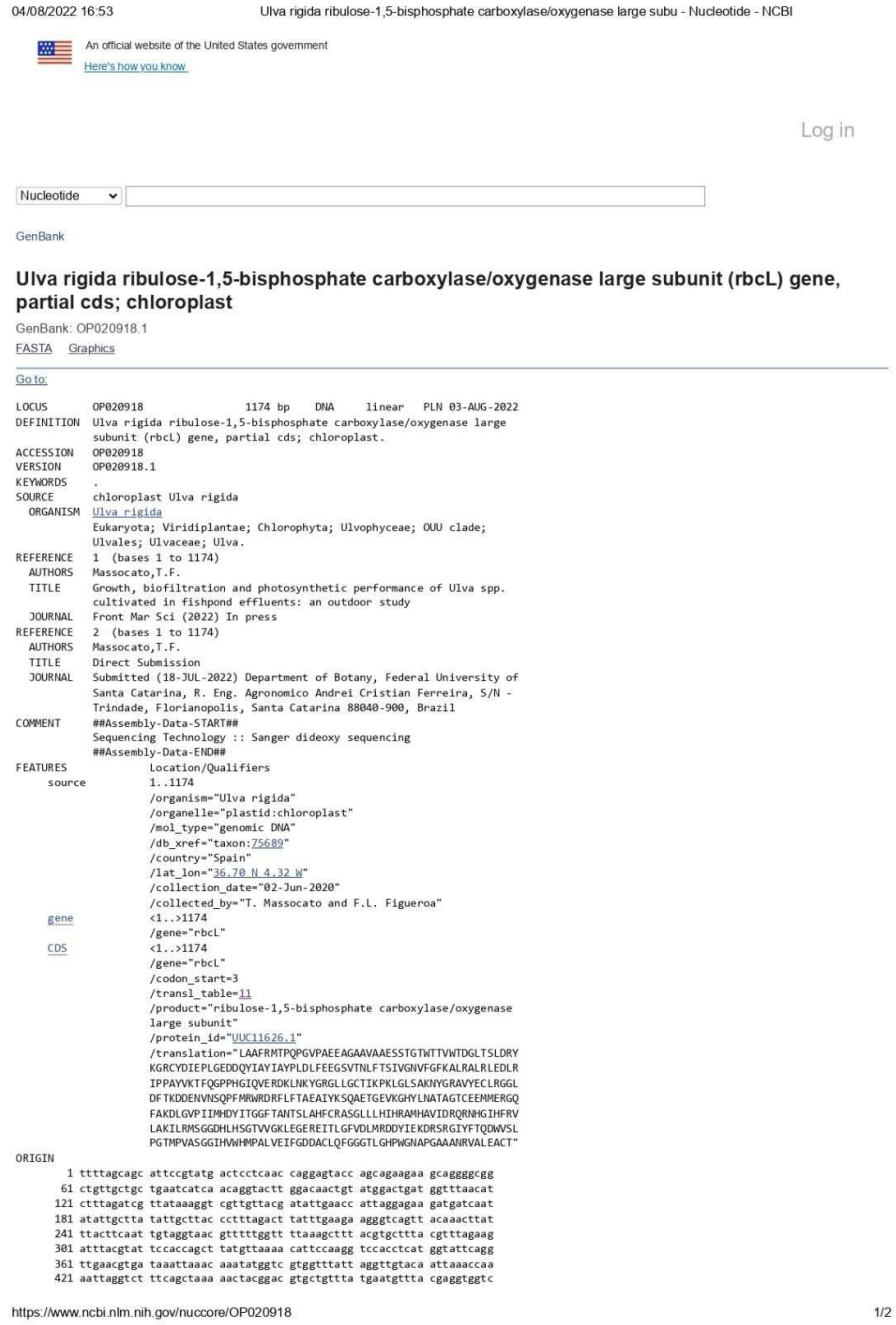

04/08/2022 16:53 Ulva rigida ribulose-1,5-bisphosphate carboxylase/oxygenase large subu - Nucleotide - NCBI

An official website of the United States government

Here's how you know

Log in

Nucleotide

GenBank

Ulva rigida ribulose-1,5-bisphosphate carboxylase/oxygenase large subunit (rbcL) gene, partial cds; chloroplast

GenBank: OP020918.1

FASTA Graphics

Go to:

```
LOCUS       OP020918               1174 bp    DNA     linear   PLN 03-AUG-2022
DEFINITION  Ulva rigida ribulose-1,5-bisphosphate carboxylase/oxygenase large
            subunit (rbcL) gene, partial cds; chloroplast.
ACCESSION   OP020918
VERSION     OP020918.1
KEYWORDS    .
SOURCE      chloroplast Ulva rigida
  ORGANISM  Ulva rigida
            Eukaryota; Viridiplantae; Chlorophyta; Ulvophyceae; OUU clade;
            Ulvales; Ulvaceae; Ulva.
REFERENCE   1  (bases 1 to 1174)
  AUTHORS   Massocato,T.F.
  TITLE     Growth, biofiltration and photosynthetic performance of Ulva spp.
            cultivated in fishpond effluents: an outdoor study
  JOURNAL   Front Mar Sci (2022) In press
REFERENCE   2  (bases 1 to 1174)
  AUTHORS   Massocato,T.F.
  TITLE     Direct Submission
  JOURNAL   Submitted (18-JUL-2022) Department of Botany, Federal University of
            Santa Catarina, R. Eng. Agronomico Andrei Cristian Ferreira, S/N -
            Trindade, Florianopolis, Santa Catarina 88040-900, Brazil
COMMENT     ##Assembly-Data-START##
            Sequencing Technology :: Sanger dideoxy sequencing
            ##Assembly-Data-END##
FEATURES             Location/Qualifiers
     source          1..1174
                     /organism="Ulva rigida"
                     /organelle="plastid:chloroplast"
                     /mol_type="genomic DNA"
                     /db_xref="taxon:75689"
                     /country="Spain"
                     /lat_lon="36.70 N 4.32 W"
                     /collection_date="02-Jun-2020"
                     /collected_by="T. Massocato and F.L. Figueroa"
     gene            <1..>1174
                     /gene="rbcL"
     CDS             <1..>1174
                     /gene="rbcL"
                     /codon_start=3
                     /transl_table=11
                     /product="ribulose-1,5-bisphosphate carboxylase/oxygenase
                     large subunit"
                     /protein_id="UUC11626.1"
                     /translation="LAAFRMTPQPGVPAEEAGAAVAAESSTGTWTTVWTDGLTSLDRY
                     KGRCYDIEPLGEDDQYIAYIAYPLDLFEEGSVTNLFTSIVGNVFGFKALRALRLEDLR
                     IPPAYVKTFQGPPHGIQVERDKLNKYGRGLLGCTIKPKLGLSAKNYGRAVYECLRGGL
                     DFTKDDENVNSQPFMRWRDRFLFTAEAIYKSQAETGEVKGHYLNATAGTCEEMMERGQ
                     FAKDLGVPIIMHDYITGGFTANTSLAHFCRASGLLLHIHRAMHAVIDRQRNHGIHFRV
                     LAKILRMSGGDHLHSGTVVGKLEGEREITLGFVDLMRDDYIEKDRSRGIYFTQDWVSL
                     PGTMPVASGGIHVWHMPALVEIFGDDACLQFGGGTLGHPWGNAPGAAANRVALEACT"
ORIGIN
        1 ttttagcagc attccgtatg actcctcaac caggagtacc agcagaagaa gcaggggcgg
       61 ctgttgctgc tgaatcatca acaggtactt ggacaactgt atggactgat ggtttaacat
      121 ctttagatcg ttataaaggt cgttgttacg atattgaacc attaggagaa gatgatcaat
      181 atattgctta tattgcttac cctttagact tatttgaaga agggtcagtt acaaacttat
      241 ttacttcaat tgtaggtaac gtttttggtt ttaaagcttt acgtgcttta cgtttagaag
      301 atttacgtat tccaccagct tatgttaaaa cattccaagg tccacctcat ggtattcagg
      361 ttgaacgtga taaattaaac aaatatggtc gtggtttatt aggttgtaca attaaaccaa
      421 aattaggtct ttcagctaaa aactacggac gtgctgttta tgaatgttta cgaggtggtc
```

https://www.ncbi.nlm.nih.gov/nuccore/OP020918 1/2

```
      481 ttgattttac aaaagatgat gaaaacgtaa actcacaacc tttcatgcgt tggcgtgacc
      541 gtttcttatt tactgctgaa gcaatttata aatctcaagc tgaaactggt gaggttaaag
      601 gtcattactt aaatgcaaca gcaggtacat gtgaagaaat gatggaacgt ggtcaatttg
      661 ctaaagattt aggtgttcca attattatgc atgactatat tactggtggt tttacagcta
      721 acacttcatt agctcatttc tgtcgtgcta gtggattatt attacatatt caccgtgcta
      781 tgcacgctgt tattgatcgt caacgtaatc acggtattca cttccgagta ttagcgaaaa
      841 ttttacgtat gtcaggtggt gaccacttac attcaggaac agtagtaggt aaattagaag
      901 gtgaacgtga aattacttta ggtttcgttg atttaatgcg tgatgactac attgaaaaag
      961 atcgtagtcg tggtatctac tttacacaag attgggttag tttaccaggt acaatgcctg
     1021 tagcttcagg tggtattcac gtttggcata tgcccgcatt agttgaaatt tttggtgatg
     1081 atgcatgttt acaattcggt ggtggtacat taggacaccc ttggggtaat gctccaggag
     1141 ccgctgcaaa ccgtgttgct ttagaagctt gtac
//
```


Ulva pseudorotundata ribulose-1,5-bisphosphate carboxylase/oxygenase large subunit (rbcL) gene, partial cds; chloroplast

GenBank: OP020919.1

FASTA Graphics

Go to:

```
LOCUS       OP020919                611 bp    DNA     linear   PLN 03-AUG-2022
DEFINITION  Ulva pseudorotundata ribulose-1,5-bisphosphate
            carboxylase/oxygenase large subunit (rbcL) gene, partial cds;
            chloroplast.
ACCESSION   OP020919
VERSION     OP020919.1
KEYWORDS    .
SOURCE      chloroplast Ulva pseudorotundata
  ORGANISM  Ulva pseudorotundata
            Eukaryota; Viridiplantae; Chlorophyta; Ulvophyceae; OUU clade;
            Ulvales; Ulvaceae; Ulva.
REFERENCE   1  (bases 1 to 611)
  AUTHORS   Massocato,T.F.
  TITLE     Growth, biofiltration and photosynthetic performance of Ulva spp.
            cultivated in fishpond effluents: an outdoor study
  JOURNAL   Front Mar Sci (2022) In press
REFERENCE   2  (bases 1 to 611)
  AUTHORS   Massocato,T.F.
  TITLE     Direct Submission
  JOURNAL   Submitted (18-JUL-2022) Department of Botany, Federal University of
            Santa Catarina, R. Eng. Agronomico Andrei Cristian Ferreira, S/N -
            Trindade, Florianopolis, Santa Catarina 88040-900, Brazil
COMMENT     ##Assembly-Data-START##
            Sequencing Technology :: Sanger dideoxy sequencing
            ##Assembly-Data-END##
FEATURES             Location/Qualifiers
     source          1..611
                     /organism="Ulva pseudorotundata"
                     /organelle="plastid:chloroplast"
                     /mol_type="genomic DNA"
                     /db_xref="taxon:523339"
                     /country="Spain"
                     /lat_lon="36.50 N 6.17 W"
                     /collection_date="30-Jun-2020"
                     /collected_by="T. Massocato and F.L. Figueroa"
     gene            <1..>611
                     /gene="rbcL"
     CDS             <1..>611
                     /gene="rbcL"
                     /codon_start=3
                     /transl_table=11
                     /product="ribulose-1,5-bisphosphate carboxylase/oxygenase
                     large subunit"
                     /protein_id="UUC11627.1"
                     /translation="TLTNLFTSIVGXVFGFKALRALRLEDLRIPPAYVKTFQGPPHGI
                     QVERDKLNKYGRGLLGCTIKPKLGLSAKNYGRAVYECLRGGLDFTKDDENVNSQPFMR
                     WRDRFLFVAEAIYKSQAETGEVKGHYLNATAGTCEAMMERGQFAKDLGVPIVMHDYIT
                     GGFTANTSLAHFCHASGLLLHIHRAMHAVIDRQRNHGIHFRVL"
ORIGIN
        1 gaacactgac aaacttattt acttcaattg taggtagngt ttttggtttt aaagctttac
       61 gtgctttacg tttagaagat ttacgtattc caccagctta tgttaaaaca ttccaaggtc
      121 caccgcatgg tattcaggtt gaacgtgata aattaaataa atacggtcgt ggtttattag
      181 gttgtacaat taaaccaaaa ttaggtcttt cagctaaaaa ctatggacgt gctgtttatg
      241 aatgtttacg aggtggtctt gattttacaa aagatgatga aaacgtaaac tcacaacctt
      301 tcatgcgttg gcgtgaccgt ttcttatttg ttgctgaagc aatttataaa tctcaagctg
      361 aaactggtga agttaaagga cattacttaa atgcaacagc gggtacatgt gaagcaatga
      421 tggaacgtgg tcaatttgct aaagatttag gtgttccaat tgttatgcat gactatatta
      481 ctggtggttt tacagctaac acttcattag ctcatttctg tcatgctagt ggattattat
      541 tacacattca ccgtgctatg cacgctgtta ttgaccgtca acgtaatcac ggtattcact
```

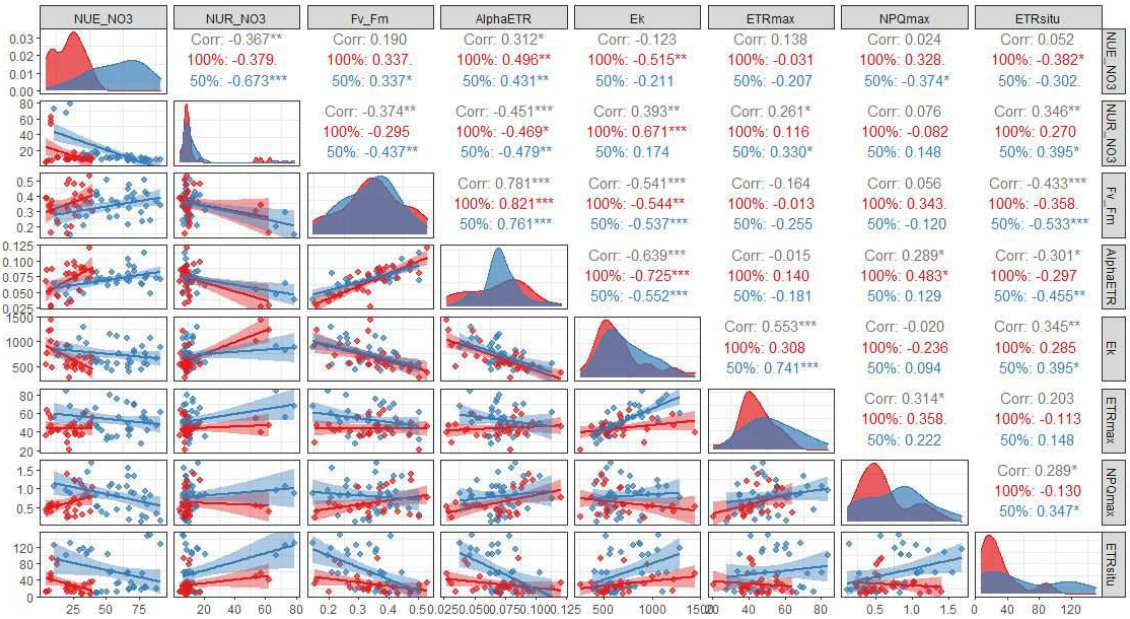

Anexo 1. Spearman correlation values between nitrate biofiltration parameters and photosynthetic parameters obtained from *U. pseudorotundata* cultivation under two experimental conditions: (1) 50% fish effluent and (2) 100% fish effluent. Symbols indicate significance level: *$p < 0.05$, **$p < 0.01$, ***$p < 0.001$.

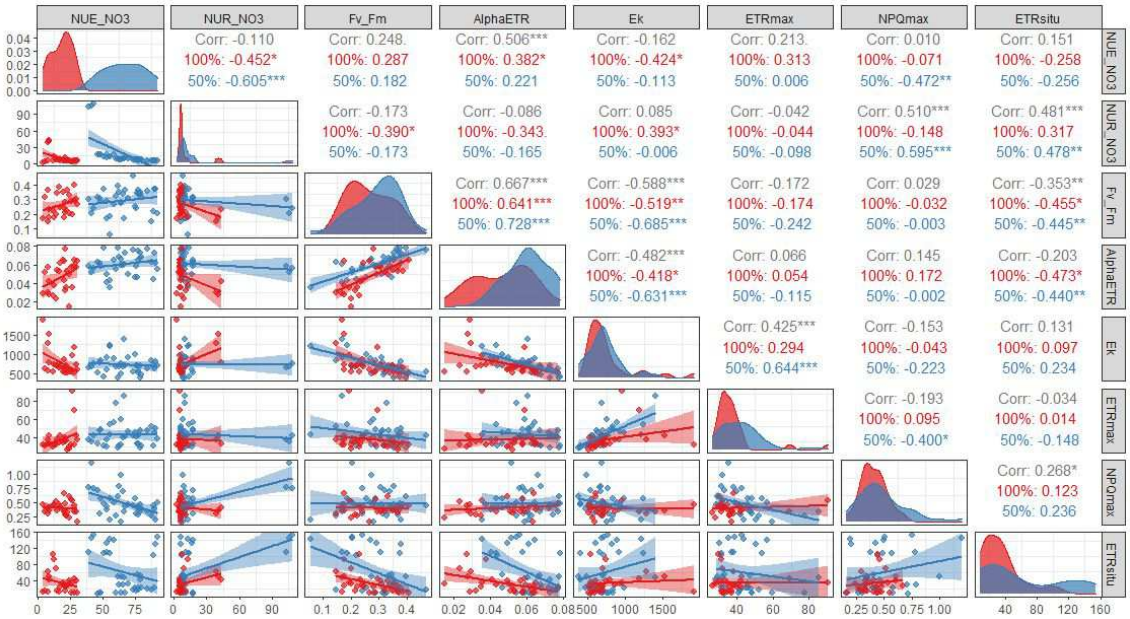

Anexo 2. Spearman correlation values between nitrate biofiltration parameters and photosynthetic parameters obtained from *U. rigida* cultivation under two experimental conditions: (1) 50% fish effluent and (2) 100% fish effluent. Symbols indicate significance level: *$p < 0.05$, **$p < 0.01$, ***$p < 0.001$.

ANEXO A

A seguir estão apresentadas equações de conversão:

$$NH_4\ (mg/L) = NH_4\ (\mu mol)\ .\ 0{,}018$$

$$NO_3\ (mg/L) = NO_3\ (\mu mol)\ .\ 0{,}062$$

$$PO_4\ (mg/L) = PO_4\ (\mu mol)\ .\ 0{,}094$$